The Research Department of Neuroscience, Physiology and Pharmacology

The Division of Biosciences

University College London

Gower Street

London

WC1E 6BT

EXPRESSION AND FUNCTION OF

Kv7/M-CHANNELS WITHIN THE PERIPHERAL NOCICEPTIVE PATHWAY

by

Joanne Margaret Reilly BSc, MSc (*Otago, New Zealand*)

2012

A thesis submitted for the degree of

Doctor of Philosophy

University College London

DECLARATION

I, Joanne Margaret Reilly confirm that the work presented in this thesis is my own. Where information has been derived from other sources, I confirm that this has been indicated in the thesis.

_____

Joanne Margaret Reilly

For Mum, Dad and Symon

ABSTRACT

Novel targets for the treatment of pain are continually being sought. These new targets may lie within the pain pathway, which facilitates the detection, transmission and perception of pain and include ion channels which control neuronal excitability such as Kv7/M-channels, which have been implicated in the control of neuronal excitability in peripheral neurons. The aim of this work was to determine the expression of Kv7/M-channels in the peripheral components of the nociceptive sensory pathway and to investigate aspects of their functional significance. Immunohistochemical techniques to determine the localisation of the channel were completed using antibodies to the Kv7.2 subunit of the channel and to various neuronal makers. Immunoreactivity to Kv7.2 was detected in a variety of DRG sensory neurons and peripheral sensory nerve fibres; including small nociceptive neurons. Immunoreactivity to Kv7.2 was also detected diffusely along unmyelinated fibres within the vagus nerve. Electrophysiological measurement found that these fibres could be hyperpolarised in a XE991 sensitive manner by retigabine. The Kv7/M-channel was also identified in keratinocytes by immunoreactivity for Kv7.2, RT-PCR, electrophysiological recordings and a potentiated induced release of ATP by retigabine was observed, this effect was blocked by XE991. These new neuroanatomical locations for M-channel are helpful in the interpretation of functional studies on the role of M-channels in regulating peripheral nociception. The localisation of the channel in presumably non-nociceptive fibres raises additional possibilities regarding their role in other forms of sensation. The functional studies also expand potential roles for M-channels to the regulation of C-fibre activity and also to aspects of keratinocyte function. These results also raise the question of how far the effects of retigabine (and other M-channel enhancers) observed in other studies are due to peripheral actions.

PREFACE

The work described in this thesis was completed in fulfilment of a part-time postgraduate (PhD) degree, whilst undertaking work as a research technician in Professor D.A. Brown's laboratory. My duties in this capacity ranged very widely in support of a large research group, and the work described in this thesis reflects only one component of this, plus work undertaken independently "out of hours". This experimental work started in 2006. Much of the work was undertaken to complement the studies of Dr. G.M. Passmore on the functional role of M-channels in nociceptive sensory transduction and transmission. However, Dr. Passmore's work is not included in this thesis and all of the work described and illustrated was undertaken solely on my own unless otherwise indicated. Because of the prolonged duration of a part-time postgraduate course, some results of the originally initiated work overlaps with subsequently-published information from other labs. Notwithstanding, this latter work is included in the Introduction (where most relevant) and discussed elsewhere in the thesis as appropriate.

A preliminary report of some of this work was communicated to the Federation of European Neuroscience Societies (FENS) Forum in 2008 (reference 1 below) and published in Passmore et al, 2012 (reference 2)

REFERENCES

(1). Reilly, JM, Passmore, GM and Brown, DA (2008). M-/Kv7 channel localisation and function in peripheral afferent fibres of isolated rat skin. 6th FENS Forum Abstracts 078.23.

(2). Passmore GM, Reilly JM, Thakur M, Keasberry VN, Marsh SJ, Dickenson AH and Brown DA (2012) Functional significance of M-type potassium channels in nociceptive cutaneous sensory endings. Front. Mol. Neurosci. 5:63.

ACKNOWLEDGMENTS

I would like to extend my gratitude to those that have supported and encouraged me throughout the completion of this thesis.

Firstly, I would like to thank Professor David Brown, for providing me with the opportunity to complete PhD and whose unsurpassable knowledge has been invaluable. I would also like to thank him for providing an amazing group of people to work with. I can only hope in my future that I get to work in a group where such a special environment of support and encouragement exists.

I would like to express my thanks Dr Steve Marsh for his patience, guidance, technical and scientific advice and constant support throughout the research and the writing of this thesis and who to paraphrase Feynman, taught me the 'difference between knowing the name of something and knowing something'.

I am also indebted Dr Gayle Passmore, for her editorial support with the writing and also for her kindness and encouragement throughout my PhD.

I would like to thank all the other past and present members of the Brown group, I would especially like to thank Dr Olga Stelmashenko and Dr Alexander Filippov for all the friendship and support that they have shown me over the years. I would like to express my thanks to all those that have supported me and contributed to the success of this study within UCL. I would especially like to thank Professor Steve Hunt and Dr Martin Stocker and the members of their laboratories for technical support with experiments

I would like to thank all my friends for pretending to be interested in subject of my thesis and cheering me up when I needed it most. Mostly I would like to thank my family especially my Mum, Dad, Husband and brother to whom this thesis is dedicated and whose unconditional support and love keep me in perspective of what is really important in life.

TABLE OF CONTENTS

LIST OF FIGURES

LIST OF TABLES

LIST OF ABBREVIATIONS

2-APB: 2-Aminoethoxydiphenyl borate

5HT-3: 5-hydroxytryptamine receptor 3

5HT-4: 5-hydroxytryptamine receptor 4

aa: amino acid

ACh: Acetylcholine

Ag/AgCl: Silver/silver chloride

AKAP: A-kinase anchoring protein

AMPA: (2-amino-3-(3-hydroxy-5-methyl-isoxazol-4-yl)propanoic acid) receptor

ATP: Adenosine triphosphate

BSA: Bovine serum albumin

BK: Bradykinin

BFNC: benign familial neonatal convulsions

CAP: Compound action potential

$CaCl_2$: Calcium chloride

CGRP: Calcitonin gene related peptide

CHO: Chinese hamster ovaries cells

CNS: Central nervous system

CO_2: Carbon dioxide

COX: cyclooxygenase

dH_20: Distilled water

DNA: Deoxyribonucleic acid

DAG: Diacylglycerol

DRG: Dorsal root ganglia

DMSO: Dimethyl sulphonic acid

EDTA: Ethylenediaminetetraacetic acid

EGTA: Ethylene glycol tetraacetic acid

ER: Endoplasmic reticulum

FBS: Foetal Bovine Serum

GABA: Gama-aminobutyric acid

GDNF: Glial cell-derived neurotrophic factor

GPCR: G-protein coupled receptors

HBSS: Hank's Balanced Salt Solution

HEPES: 4-(2-hydroxyethyl)-1-piperazineethanesulfonic acid

IB4: Isolectin IB4

IP3: Inositol (1,4,5)P3 or Inositol trisphosphate

KCl: Potassium chloride

KCNQ: gene the encodes Kv7 subunits

Kv7: Potassium voltage-gated channel, KQT-like subfamily

$LaCl_3$: Lanthanum chloride

M1: Muscarinic acetylcholine receptor 1

M3: Muscarinic acetylcholine receptor 3

MAPK: Mitogen-activated protein kinases

$MgCl_2$: Magnesium chloride

M-MLV: Moloney Murine Leukemia Virus

MrgD: MAS-related G-protein Coupled Receptor

mRNA: Messenger Ribonucleic acid

N52: clone 52 from C-terminal segment of pig neurofilament 200

NaCl : Sodium chloride

NMDA: (N-Methyl-D-aspartic acid) receptor

NaOH: Sodium hydroxide

NF 200: Neurofilament 200

NGF: Nerve growth factor

NK1: Neurokinin 1receptor

P2Y receptor: Purinergic type 2 ATP receptor;G-protein-coupled receptors

P2X receptor: Purinergic type 2 ATP receptor;Ligand gated ion channel

PCR: Polymerase chain reaction

PI4K: Phosphatidylinositol 4-kinase

$PI(4,5)P_2$, PIP_2: Phosphatidylinositol 4,5-bisphosphate

PKC: Protein kinase C

PBS: Phosphate buffered saline

PFA: Paraformaldehyde

PLC: Phospholipase C

PKC: Protein kinase C

RNA: Ribonucleic acid

RTG: Retigabine

RT-PCR: Reverse transcription polymerase chain reaction

SCG: Superior cervical ganglia

SEM: Standard error of the mean

SFM: Serum free media

TrkA: Tropomyosin receptor kinase A

TRP: Transient receptor potential channel

TRPV1: transient receptor potential cation channel member 1

TRPV3: Transient receptor potential cation channel member 3

TTX: Tetrodotoxin

UTP: Uridine 5'-triphosphate

UV: Ultraviolet light

WDR: wide dynamic range neuron

XE991: 10,10-*bis*(4-Pyridinylmethyl)-9(10*H*)–anthracenone dihydrochloride

CHAPTER 1.

GENERAL

INTRODUCTION

The aim of this thesis is to further elucidate the location of Kv7/M-channels within neurons that make up the cutaneous component of the peripheral nociceptive pathway and some aspects of their function therein. The following chapter provides a general overview of the peripheral nociceptive pathway, Kv7/M-channels and what is currently known about their role within this pathway.

1.1 PAIN

"Pain is an unpleasant sensory and emotional experience associated with actual or potential tissue damage, or described in terms of such damage"
The International Association for the Study of Pain (Loeser, 1994)

Pain is an essential adaptive process that under normal conditions allows the body to detect noxious stimuli or tissue damage and thereby respond accordingly to limit any further damage. The quality of life of the individual suffering pain, especially long-term pain, can be severely impaired, and the cost to society is immense. The American Pain Society estimates the cost of pain in the U.S.A to be "between $560 billion to 630 billion in direct medical costs and lost productivity" (Fillingim, 2012). Pain can be categorised into two main types, acute and chronic pain, and there are numerous diseases and injuries that can induce both. Acute pain abates when the injury that initiated the pain has healed. Chronic pain on the other hand remains after the injury has healed and is usually caused by an aberration within the nerves or tissues, leading to inflammatory or neuropathic pain. This is often induced by sensitisation of the nerve from either posttranslational modification or a change in the level of expression of the proteins involved in nociceptive transmission, leading to hypersensitivity to painful (hyperalgesia) and non-painful (allodynia) stimuli. It is worth noting that pain has a psychological as well as a physiological component. The psychological component of pain will not be discussed as the as subject matter of thesis relates to the physiological causes of pain.

1.2 THE PAIN PATHWAY

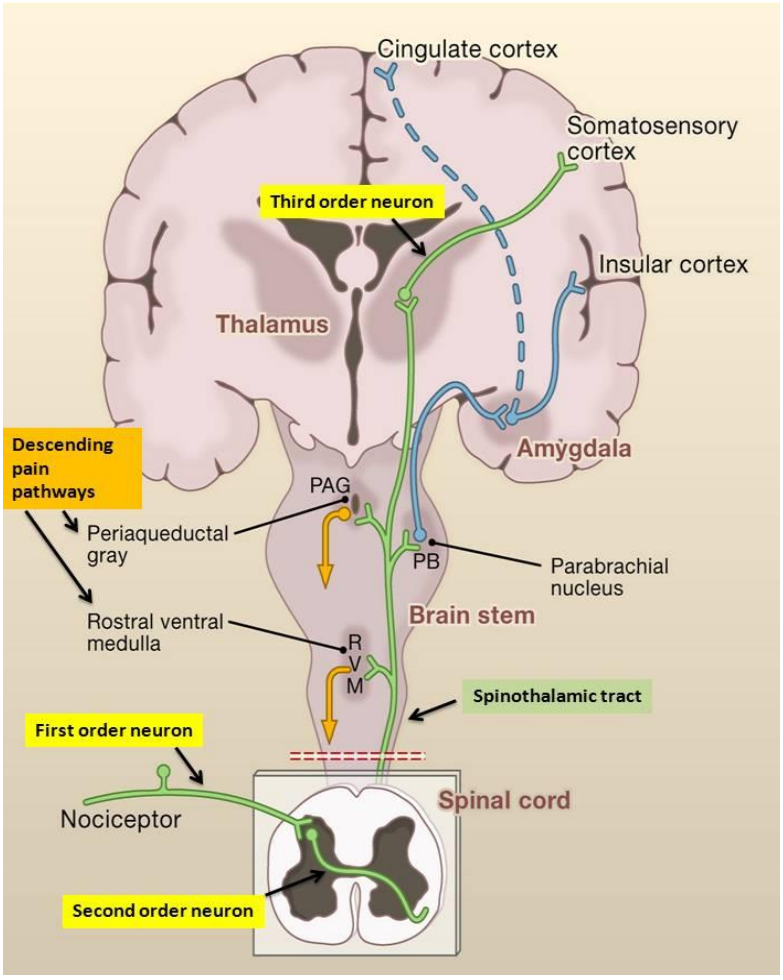

Figure 1.1: Anatomy of the pain pathway of peripheral nociceptive fibres . *(taken from Basbaum et al.,(2009)).*

The pain pathway (figure 1.1) transmits noxious stimuli originating from peripheral nerve terminals to the central nervous system and ultimately to the higher centers of the brain. The subject matter of this thesis is the peripheral nociceptive pathway specifically the cutaneous nerves that transmit noxious signals to the spinal cord. It is important however to provide a brief overview of the main features of the entire pain pathway and the drugs that are commonly used to modulate this pathway.

1.2.1 Periphery to spinal cord

Initially noxious stimuli are detected by ion channels (either directly or via other receptive proteins) present on the peripheral terminals of specialised nerve fibres capable of detecting nociceptive signals called nociceptors (first order neurons; detailed further in section 1.4). If the noxious stimulus is of sufficient intensity, an action potential is generated at the nerve terminal and is transmitted along the nociceptor's axons to the spinal cord. The axon either directly enters the and synapses in the dorsal horn of the spinal cord or it may move up or down a segment or two of spinal cord in Lissauer's tract before synapsing in the dorsal horn.

1.2.2 Processing in spinal cord

The nociceptive axon synapses onto second order neurons in the outer laminas (substantia gelatinosa) of the dorsal horn. Neurotransmitters including glutamate or substance P are released across the synaptic cleft where they bind to receptors, respectively AMPA (2-amino-3-(3-hydroxy-5-methyl-isoxazol-4-yl) propanoic acid) and Neurokinin 1 (NK-1) generating an action potential within the postsynaptic (second order) neuron. The axons of the second order neurons cross the midline of the spinal cord and then ascend the via the lateral spinothalamic tract.

Whether an action potential is transmitted to the second order neuron can be controlled by inhibitory interneurons within the spinal cord, which can modulate the transmission of nociceptive signals and explain why increasing somatosensory input e.g. rubbing injury, reduces the pain perceived. These interneurons underlie what is termed 'gate-control theory of pain' (Melzack and Wall, 1965). Normal somatosensation from large diameter fibres activates the inhibitory interneuron, closing the gate to ascending transmission of stimuli from small fibres. Conversely, when the majority of input onto the inhibitory interneuron is from small fibres the inhibitory interneuron is inactivated and nociceptive stimuli can project to the brain.

1.2.3 Spinal cord to brain

The action potential is transmitted along the second order neuron to the thalamus (specifically the ventral posterior lateral nucleus) where it synapses with a third order neuron. The third order neurons then relay the nociceptive signal to various areas in the somatosensory cortex where the perception of pain occurs.

1.2.4 Descending control of pain- endogenous analgesia

Pain is not only detected via the pain pathway but can be modulated by the brain via the descending control of pain pathway. Serotonergic neurons projecting from the nucleus raphe magnus in the midbrain, (via a pathway originating in the somatosensory cortex and hypothalamus descending from the periaqueductal grey (PAG)) and adrenergic neurons projecting from the Locus ceruleus in the pons synapse on enkephalin (endogenous opioid) releasing interneurons within the spinal cord. This induces the release of enkephalin on the synapse between the first and second order neurons which can then act locally on opioid receptors effectively shutting down the synapse by reducing Ca^{2+} entry, inhibiting neurotransmitter (substance P, glutamate) release and hyperpolarising the post-synaptic membrane.

1.3 PAIN TREATMENTS

Conventional pain treatment involves the use of drugs that modulate the transmission of the nociceptive signal at various points within the pain pathway. The search for new pain treatments continues and there has also been an increase in the use of drugs that were originally designed for use in other conditions but now have been successfully used in the treatment of pain. The next section provides a brief overview on the drugs involved in the clinical management of pain.

1.3.1 Local anaesthetics

Local anaesthetics (e.g. benzocaine and lignocaine) acutely shut down action potentials and are utilised in the management of acute, cancer and chronic pain and also diagnostically as nerve blocks which can aid in the localisation of the source of pain. They can be administered in a variety of ways most commonly regionally (in combination with a vasoconstrictors) at the site of pain or via epidural (block of nerve roots in the spinal cord). Due to numbness and risk of nerve damage these drugs tend to be less frequently utilised in chronic pain conditions.

1.3.2 Non-steroidal anti-inflammatory drugs (NSAIDs)- cyclooxygenase inhibitors

Non-steroidal anti-inflammatory drugs (NSAIDs) act primarily at the periphery by inhibiting the enzymes called cyclooxygenases (COX-1 and/or COX-2) responsible for the synthesis of inflammatory mediators called prostaglandins; lipid mediators, which are produced from thromboxane and arachidonic acid in response to tissue damage and inflammation which sensitise nociceptors to fire under conditions in which they normally wouldn't. Commonly used NSAIDS include aspirin, ibuprofen and diclofenac these are effective in acute pain and the main side effects form NSADS include allergic reaction, renal failure, coagulation problems, altered healing processes and other effects associated with homeostatic functions of the COX enzymes, particularly the COX-1 enzyme and which has a role in the maintenance of gut mucosa. COX-2 specific inhibitors have been developed to counter adverse gastrointestinal effects observed with conventional NSAIDs but increased cardiovascular side effects have reported.

Paracetamol is also an analgesic that works by inhibiting cyclooxygenases, however due to weak anti-inflammatory action it is therefore not classified as a NSAID. Paracetamol exhibits limited effects on coagulation, gastric mucosa compared to most NSAIDs but metabolites of paracetamol can cause significant hepatotoxicity therefore long term use should be monitored.

1.3.3 Opioid analgesics

Opioid analgesics, most famously morphine and its analogs are derived from the opium poppy and are often referred to as the 'gold-standard' analgesic; the one to which all other analgesics are compared. Opioids act on endogenous opioid receptors present in neurons within the central nervous system. Most opiods available including morphine act on the mu opioid receptor but drugs with greater specificity for the delta opioid receptor are associated with fewer side effects. As with endogenous opioids (enkephalins; see 1.2.4), opiates inhibit synaptic transmission of the nociceptive signal by inhibiting neurotransmitter release and hyperpolarising the post synaptic membrane. Although opioids have proven efficacy in persistent nociceptive and neuropathic pain, they are only beneficial in a small subpopulation of chronic pain sufferers and adverse effect of opioid use include: nausea, vomiting, constipation, sedation, tolerance and physical dependence and addiction in prone individuals

1.3.4 Antidepressants as analgesics:

Tricyclic antidepressants (e.g amitriptyline) were original used to treat the depression associated with chronic pain in patients but they have been shown to have an analgesic effect independent of the antidepressant action and to relieve chronic pain including neuropathic pain. These drugs can utilise the pathways modulated in the descending control of pain; increase the levels of noradrenaline and serotonin in the spinal cord and brain leading to endogenous enkephalin release from interneurons. Tricyclic antidepressants are often used in combination with other analgesics and side effects most commonly include drowsiness, decreased gut motility, impairment of cognitive function and a dry mouth.

1.3.5 NMDA receptor antagonists

NMDA (N-Methyl-D-aspartic acid) receptor antagonists are utilised in analgesia as they can prevent excitatory transmission via glutamate which leads to ‘wind-up’; an increased response to repetitive stimuli in the spinal cord (in a mechanism similar to that of long term potentiation), resulting in increased

perception of pain. Most notable of the NMDA receptor antagonists used in analgesia is ketamine, a dissociative anaesthetic more commonly used in general anaesthesia which has been shown to be an effective analgesic for chronic pain conditions at low doses. Low doses are crucial to minimise the drugs' side effects which can include hallucinations and paranoid delusions.

1.3.6 Anticonvulsants as analgesics

Anticonvulsants are typically used to treat disorders of excitability primarily epilepsy, but there has been an increase in the use of these drugs in pain, particularly chronic pain. There are 3 main pathways through these drugs typically can decrease the excitability of neurons and subsequently decrease pain transmission. Some anticonvulsants act by increasing gamma amino butyric acid (GABA) induced inhibition in the CNS either directly or indirectly (e.g. gabapentin) or by decreasing glutamate excitation (e.g. Topiramate). Other anticonvulsants act on voltage-activated ion channels, including flupirtine an opener of Kv7 voltage gated potassium channels which has is approved for the treatment of acute and chronic pain within Europe.

1.4 NOCICEPTORS

Peripheral nociceptors are sensory neurons whose cell bodies lie within trigeminal ganglion in the case of facial peripheral nociceptors or the dorsal root ganglion in the case of peripheral nociceptors. The dorsal root ganglion is comprised of three major types of neuron based on the degree of myelination of their axons, which correlates with the size of the soma of the cells. These DRG types are Aβ-type neurons with heavily myelinated axons, Aδ-type neurons with lightly myelinated axons and C –type neurons with unmyelinated axons, see table 1.1.

DRG type neuron	Threshold	Function	Average diameter of cell body (μm)	Conduction velocity (m/s)
Aβ	Low	Mechanoreceptor	38	>14
Aδ	Low and High	Mechanoreceptor Nociceptor	30	2.2-8
C	Low	Mechanoreceptor Nociceptor Thermoreceptor	24	< 2

Table 1.1: Dorsal root ganglion neuronal types. *(table derived from (Harper and Lawson, 1985))*

The DRG neuronal types Aδ and C are believed to be responsible for nociceptive transmission (Basbaum et al., 2009). These neurons can be subdivided in various ways. Aδ nociceptors can be divided electrophysiologically into two main classes Type I Aδ nociceptors which can respond to chemical, high threshold mechanical, and high temperature (>50°C) stimuli but are also capable of responding to lower temperature stimuli if the stimulus is prolonged and Type II Aδ nociceptors which are also high mechanical threshold nociceptors but have a lower heat threshold (Basbaum et al., 2009). C-type nociceptors are comprised of a mixed population of neurons that are sensitive to heat, chemical or mechanical stimulation or in some cases to both. C-type nociceptors are sensitive to a lower threshold stimuli than seen with Aδ-type nociceptors (Perl, 2007). These properties led to the conclusion that Aδ-type nociceptors and their axons are likely to be involved in transmitting acute sharp pain and C-type nociceptors and their axons in transmitting dull, aching pain. Interestingly, C- type nociceptors previously insensitive to stimuli, so called 'silent' can become sensitised following injury (Schmidt et al., 1995).

C-type nociceptors can also be categorised by their neurochemistry (Julius and Basbaum, 2001). These categories are based on the distinct repertoire of proteins they express and the different neurotrophins to which they respond. They are referred to as peptidergic or nonpeptidergic nociceptors. Peptidergic nociceptors express tropomyosin receptor kinase A (TrkA) neurotrophin

receptor which binds nerve growth factor (NGF). They also express substance P and calcitonin-gene related peptide (CGRP). The nonpeptidergic nociceptors express the tyrosine kinase receptor, c-Ret whose ligand is the neurotrophin glial-derived neurotrophic factor (GDNF). They also express the MrgD family of G-protein coupled receptors, the ATP receptor P2X3, and are capable of binding the plant lectin IB4. These markers provide a way to classify DRG into subtypes.

The different categories of nociceptors also project to different laminae within the dorsal horn of the spinal cord. Aδ- type nociceptors project to laminae I and V, nonpeptidergic C-type nociceptors project to the inner part of lamina II and peptidergic C -type nociceptors project to lamina I (Basbaum et al., 2009). Nociceptors are capable of differentiating numerous painful stimuli. This ability is conferred by the expression of different ion channels that can detect mechanical, chemical and thermal stimuli. The search for the channels responsible for the transduction of mechanical stimuli in mammals is still ongoing but possible candidate channels include members of the acid-sensing ion channels (ASICs), some members of the transient receptor protein (TRP) channel family members and recently discovered members of the Piezo protein family (Delmas et al., 2011). Chemical stimuli are detected by a variety of receptors that are specific for each stimulus i.e. change in pH, hormones, cytokines, neurotransmitters, growth factors, inflammatory mediators, and opioids (Costigan and Woolf, 2000). Thermal stimuli are largely detected through members of a family of cation channel receptors called the transient receptor potential (TRP) group of ion channels (Ramsey et al., 2006). TRP channels are very diverse which enables them to differentiate between many different thermal stimuli. TRP channels can also be activated by certain chemicals which, electrophysiologically and perceptively, can give rise to similar responses as that of the temperature profiles specific to whichever TRP channel family member they stimulate, for example TRPV1 is activated at temperature noxious temperature (>42°C) and also by capsaicin the compound responsible for the 'hot' sensation of chillies (Patapoutian et al., 2003).

The influx of cations through the channels described above can induce a depolarisation in the cell membrane which, if large enough, can lead to the generation of action potentials. Action potentials are generated by the opening of voltage-gated sodium channels. Sodium channels that have a particular role in nociception include NaV1.7 NaV1.8 and NaV1.9: these determine the magnitude and frequency of nociceptor action potentials (Momin and Wood, 2008). The frequency of action potentials is also important as this is correlated with the degree of pain perceived; therefore ion channels that regulate excitability in neuron are likely to be important in nociception. A channel that has been implicated in the control of excitability in peripheral neurons is the *'M-channel'*, which is composed of Kv7 potassium channel subunits, discussed further in the next section.

1.5 Kv7/M-CHANNEL

Kv7/M-channels are voltage gated potassium channels which are capable of modulating excitability. This is ability is conferred by the kinetics of the channel: they are open at sub-threshold potentials, activate slowly, and do not inactivate (Delmas & Brown, 2005). This makes the Kv7/M-channel a protein of interest in studying diseases associated with hyper excitability such as epilepsy, or (in the case of the subject matter of this thesis) the transmission of painful stimuli. The following section provides a brief description of the current knowledge regarding the genetics, expression and function of Kv7/M-channel with particular emphasis on neuronal Kv7/M-channels.

1.5.1 Kv7/M-CHANNEL GENETICS

The M-channel was first identified by cholinergic stimulation of muscarinic receptors in bullfrog and rat sympathetic ganglion in the early 1980s (Brown and Adams, 1980;Constanti and Brown, 1981). About twenty years later the molecular identity of the M-channel was deciphered as being composed of the members of the KQT-like voltage-gated potassium channel subfamily encoded

by the *KCNQ* genes. There are 5 known members of the *KCNQ* gene family, *KCNQ1* to *KCNQ5* respectively, which encode the proteins Kv7.1 to Kv7.5 (Jentsch, 2000;Robbins, 2001). *KCNQ* genes are of clinical importance as mutations in *KCNQ* genes have been linked to disorders in neuronal excitability; KCNQ1: long QT syndrome (Wang et al., 1996) KCNQ2 and KCNQ3: benign familial neonatal convulsions (BFNC) (Biervert et al., 1998;Singh et al., 1998;Dedek et al., 2001);KCNQ2: myokymia (Dedek et al., 2001); KCNQ4: congenital deafness (Kubisch et al., 1999;Kharkovets et al., 2000)

1.5.2 Kv7/M-CHANNEL EXPRESSION

The Kv7 proteins have differential tissue expression patterns. Kv7.1 is expressed in cardiac tissue where it is responsible for long QT syndrome (Wang et al., 1996) and it is also widely expressed in various epithelial tissues (Demolombe et al., 2001). Kv7.4 is expressed in the inner ear (Kubisch et al., 1999;Kharkovets et al., 2000), in neurons associated with the auditory pathway in the brain (Kharkovets et al., 2000) and has been recently reported in mechanically sensitive peripheral neurons (Heidenreich et al., 2012). Kv7.2, Kv7.3 and Kv7.5 expression is largely confined to central and peripheral neurons (Schroeder et al., 1998;Yang et al., 1998;Wang et al., 1998;Lerche et al., 2000;Cooper et al., 2000;Schroeder et al., 2000;Cooper et al., 2001;Shah et al., 2002) although there is evidence for Kv7.5 expression in smooth muscle (Schroeder et al., 2000;Greenwood and Ohya, 2009). The neuronal expression of the Kv7 proteins can alter with development: for example, an increase in Kv7.3 expression was observed in rat sympathetic ganglion with increasing age (Hadley et al., 2003).

1.5.3 Kv7/M-CHANNEL STRUCTURE AND FUNCTION

The structure of the Kv7 subunits is similar to that of other voltage gated potassium channels (see figure 1.2). They comprise 6 transmembrane domains (S1- S6) with an intracellular carboxy-tail, which is particularly long compared to that of other voltage gated potassium channels. A highly conserved pore

region or P-loop forms between the transmembrane domains S5 and S6. Transmembrane domains S1- S4 make up the voltage-sensing domain of the Kv7 subunit protein; S4 is believed to form the voltage sensor and as contained within this domain is a sequence of positively charged amino acids. There are a number of domains within the carboxy terminus of the Kv7 subunits that are capable of binding regulatory elements such as calmodulin, A-kinase anchoring protein (AKAP79/150 human/rat), phosphatidylinositol-4,5-bisphosphate (PtdIns (4,5)P_2 or PIP2) and a sequence of serines capable of phosphorylation by protein kinase C (PKC); see figure 1.2.

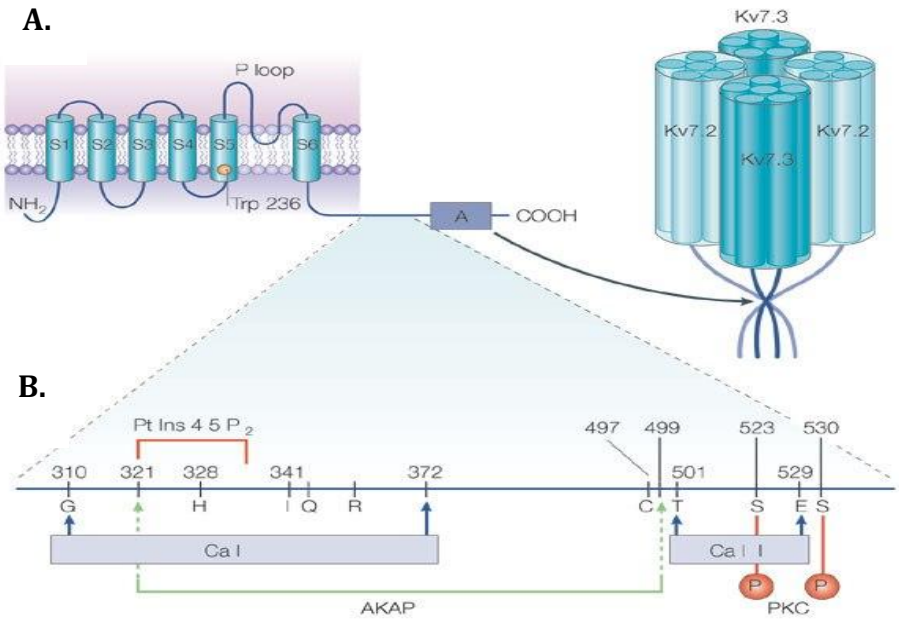

Figure 1.2: Kv7/M-channel structure. *The channel is composed of 6 transmembrane domains (S1–S6) with a single pore (P)-loop that forms the selectivity filter of the pore, a positively-charged fourth transmembrane domain (S4) that acts as a voltage sensor and a long intracellular carboxy-terminal tail. Four subunits make up a functional Kv7 channel. (Delmas and Brown, 2005)*

All of the Kv7 protein subunits (Kv7.1-Kv7.5) are capable of forming a tetrameric channel comprised of either homomeric subunits or certain heteromeric combinations of subunits, usually (Jentsch, 2000) but not necessarily (Bal et al., 2008b) incorporating Kv7.3. The specificity of the

assembly of the subunits is denoted by a conserved domain (A domain) within the carboxy tail (Schwake et al., 2003). When the Kv7 subunits are expressed homomerically in cell lines or oocytes all subunits produce an M-like current. It is the Kv7.2/Kv7.3 heteromeric tetramer that is believed to form the majority of M-channels in mammalian peripheral neurons (see figure 1.3), as the kinetic and pharmacological profile of this combination of Kv7 subunit proteins most closely mimics that observed with endogenous M-channel (Wang et al., 1998;Hadley et al., 2003).

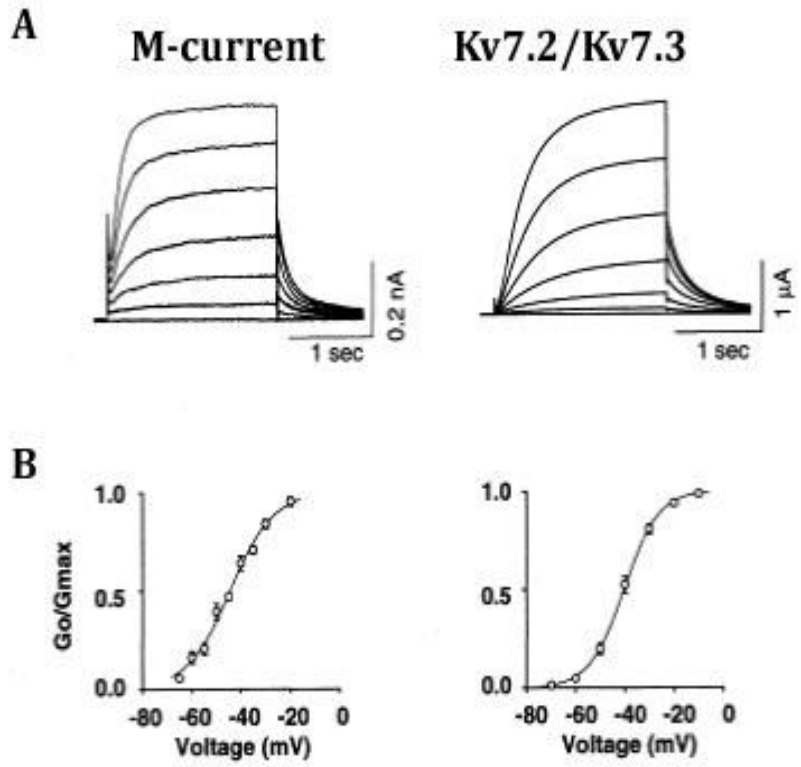

Figure 1.3: Comparison of the kinetic properties of native M current in rat SCG neurons with KCNQ2+KCNQ3 heteromultimers expressed in Xenopus oocytes. *(A) Activation curve from a holding potential of −60 mV in 5 mV increments. (B) Voltage dependence of activation (from (Wang et al., 1998a) via (Brown and Yu, 2000))*

The physiological function of the Kv7/M-channel is to inhibit repetitive firing which can underlie conditions such as epilepsy and chronic pain. As the cell depolarises more channels open, which in turn inhibits further depolarisation, effectively forming a 'voltage clamp' to stop action potential firing; if this clamp

is removed then the cell can fire tonically (Wang et al., 1998;Basbaum et al., 2009).

1.5.4 PHYSIOLOGICAL MODULATION OF Kv7/M-CHANNEL FUNCTION

Kv7/M channels are voltage gated but the physiological activation and inhibition of Kv7/M-channel is dependent on the interaction of PIP2 with the channel (Gamper and Shapiro, 2007;Hughes et al., 2007) physiologically the M-channel requires PIP2 in order to open. The binding of PIP2 has been shown to directly lead to increased opening of the Kv7/M- channel (Gamper and Shapiro, 2003;Zaika et al., 2006;Gamper and Shapiro, 2007;Hernandez et al., 2008;Bal et al., 2008a;Bal et al., 2008b;Zaika et al., 2011a;Zaika et al., 2011b); (Telezhkin et al., 2012). The amount of PIP2 in the membrane is dependent on the availability of ATP and the action of kinases by processes which either increase PIP2 synthesis or inhibit PIP2 hydrolysis.

The channels are inhibited physiologically by neurotransmitters and chemical messengers that activate G protein-coupled receptors (GPCRs) which couple to the G protein $G_{q/11}$ (Caulfield et al., 1994). Some of these (e.g., acetylcholine (ACh), acting on M1 (or M3) muscarinic receptors) inhibit the channels by stimulating the hydrolysis of PIP2 and reducing the amount of PIP2 in the membrane. Others (e.g., bradykinin (BK) acting on B2 receptors) also induce PIP2 hydrolysis but inhibit the channels primarily through the downstream release of intracellular calcium. These two proposed modalities of GPCR-induced inhibition are illustrated in figure 1.4.

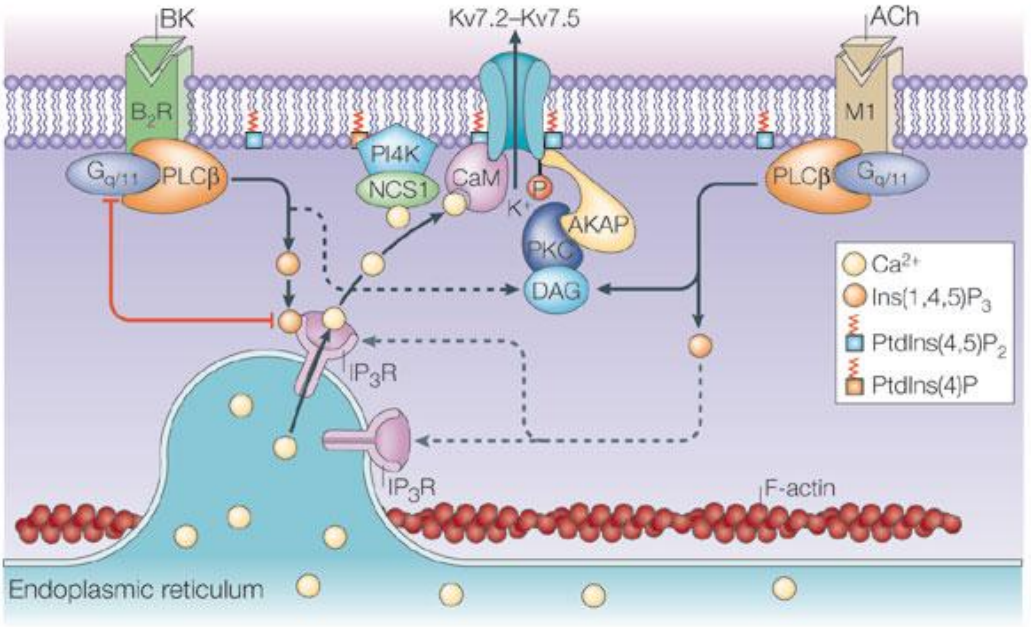

Figure 1.4: The mechanisms of inhibition of Kv7/M-channels via G-proteins *(from(Delmas and Brown, 2005))*

In both modalities the initial step is the binding of an agonist leading to the dissociation of the GPCR complex and activation of phospholipase C (PLC). PLC then hydrolyses PIP2 into diacylglycerol (DAG) and inositol triphosphate (IP3). If the GPCR is in close proximity to the endoplasmic reticulum (ER) in what is termed a microdomain, as in the case of the bradykinin receptor (Delmas et al., 2002) the diffused IP3 can induce calcium release from the ER. The released calcium can in turn activate calmodulin which can bind to the c-terminus of the Kv7/M-channel channel (Gamper and Shapiro, 2003;Bal et al., 2008a) leading to inhibition of the Kv7/M-channel. The calcium released from the ER can also activate phosphatidylinositol 4-kinase PI4K (probably via the calcium-binding protein NCS1), thereby maintaining PIP2 synthesis (Gamper et al., 2004;Winks et al., 2005;Hughes et al., 2007;Zaika et al., 2011a).

Muscarinic stimulation can also activate the GPCR pathway and lead to the inhibition of the Kv7/M-channel via PIP2 hydrolysis alone. However, this also

leads to DAG production which in turn can activate PKC which is associated to the M-channel via AKAP. The activation of PKC leads to phosphorylation of the channel and increases its sensitivity to PIP2 depletion (Higashida et al., 2005).

1.5.5 PHARMACOLOGICAL MODULATION OF THE Kv7/M-CHANNEL FUNCTION

Kv7/M-channels can be modulated by various compounds that act on the GPCR signalling pathway and direct pharmacological modulators of the channel have been discovered enabling a greater understanding of the channel as these allow specific modulation of the channel.

1.5.5.1 Kv7/M-channel activators

There are many compounds known to act as activators of Kv7/M-channel directly including zinc pyrithione (Xiong et al., 2007), a type of acrylamide (*S*)-*N*-[1-(3-morpholin-4-yl-phenyl)-ethyl]-3-phenyl-acrylamide [(S)-1] (Bentzen et al., 2006;Xiong et al., 2007), the compound BMS-204352 (Schroder et al., 2001) the compound ICA-27243 (N-(6-chloro-pyridin-3-yl)-3,4-difluoro-benzamide) (Padilla et al., 2009) and the structurally similar compounds flupirtine (Martire et al., 2004) and retigabine (Main et al., 2000;Wickenden et al., 2000;Tatulian et al., 2001)

1.5.5.2 Retigabine

Retigabine is a pharmacological activator of Kv7/M-channels which induces a leftward shift of the voltage dependent curve of the Kv7/M-channel, see figure 1.5 (B) (Wickenden et al., 2000;Rundfeldt and Netzer, 2000a). Retigabine is capable of activating Kv7.2-Kv7.5 but not the cardiac expressed Kv7.1 (Wickenden et al., 2001;Tatulian et al., 2001). This selectivity makes retigabine an interesting compound for the possible treatment of neuronal disorders related to increased excitability. Although retigabine can increase the current through $GABA_A$ receptors (Rundfeldt and Netzer, 2000b) the concentration range which retigabine is used for Kv7/M-channel activation (0.1 – 10 μM) is

much less than that which is required for GABA receptors. Retigabine has been demonstrated to decrease excitability in sympathetic, central and peripheral neurons, see example in figure 1.5 (C).

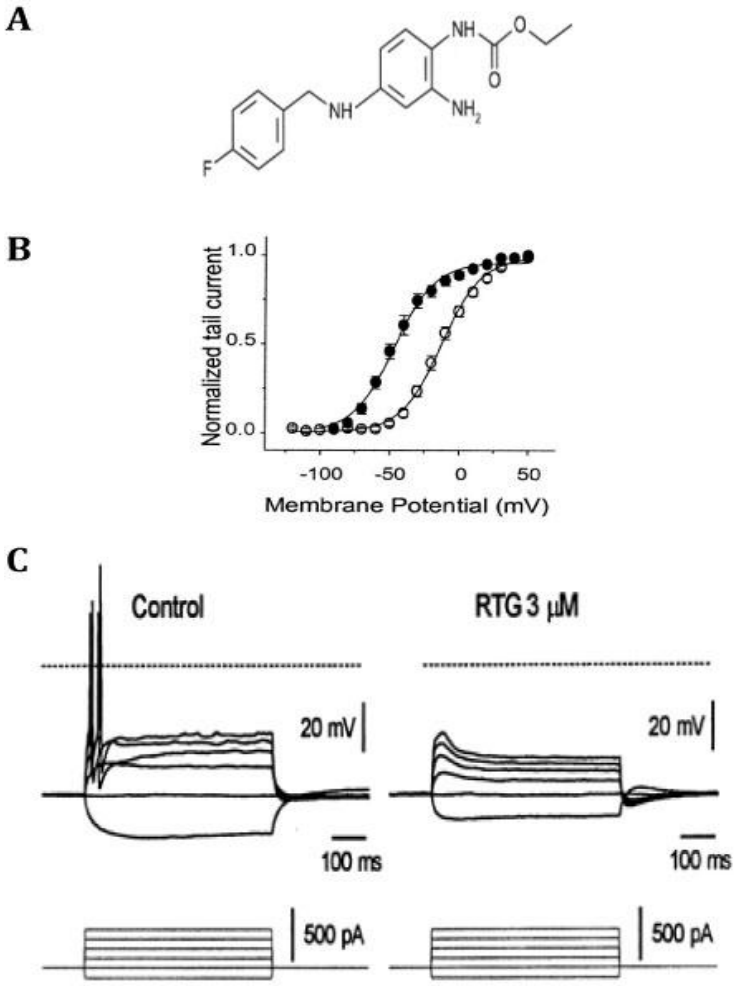

Figure 1.5: Retigabine and its effect on the M-current. *(A) The chemical structure of retigabine (N-(2-amino-4-(4-fluorobenzylamino)-phenyl) carbamic acid ethyl ester)(Rundfeldt, 1997). (B) Retigabine shifts the M-current activation curve to the left (absence (○) and presence (●) of retigabine in Kv7.2/Kv7.3 stably transfected CHO cells) (C) Retigabine (RTG) reduces the excitability of SCG neurons. (B) and (C) from (Rundfeldt, 1997;Tatulian et al., 2001)*

Mutational analysis of The Kv7/M-channel revealed that site of action of retigabine is within the pore region specifically amino acid residues Trp236 and Gly301 in the trans membrane domains S5 and S6. Retigabine binding to the channel at these positions holds the pore in a position that is more energetically favourable to the open position (Wuttke et al., 2005).

1.5.5.3 Kv7/M-channel blockers XE991 and Linopirdine

The drugs XE991 (10,10-*bis*(4-Pyridinylmethyl)-9(10*H*)-anthracenone dihydrochloride) (Hughes et al., 2007) and linopirdine (1,3-Dihydro-1-phenyl-3,3-*bis*(4-pyridinylmethyl)-2*H*-indol-2-one dihydrochloride) are structurally similar (figure 1.6 (A)) selective blockers of the Kv7/M-channel in neurons (Brown and Passmore, 2009). Blocking the Kv7/M-current with XE991 leads to both a reduction in the current produced and the excitability of neurons, see figure 1.6 (B) and (C). Both drugs act by block the pore directly. XE991 is more potent that linopirdine with an IC_{50} = 0.6 - 0.98 μM compared to linopirdine IC_{50} = 4 - 7 μM.

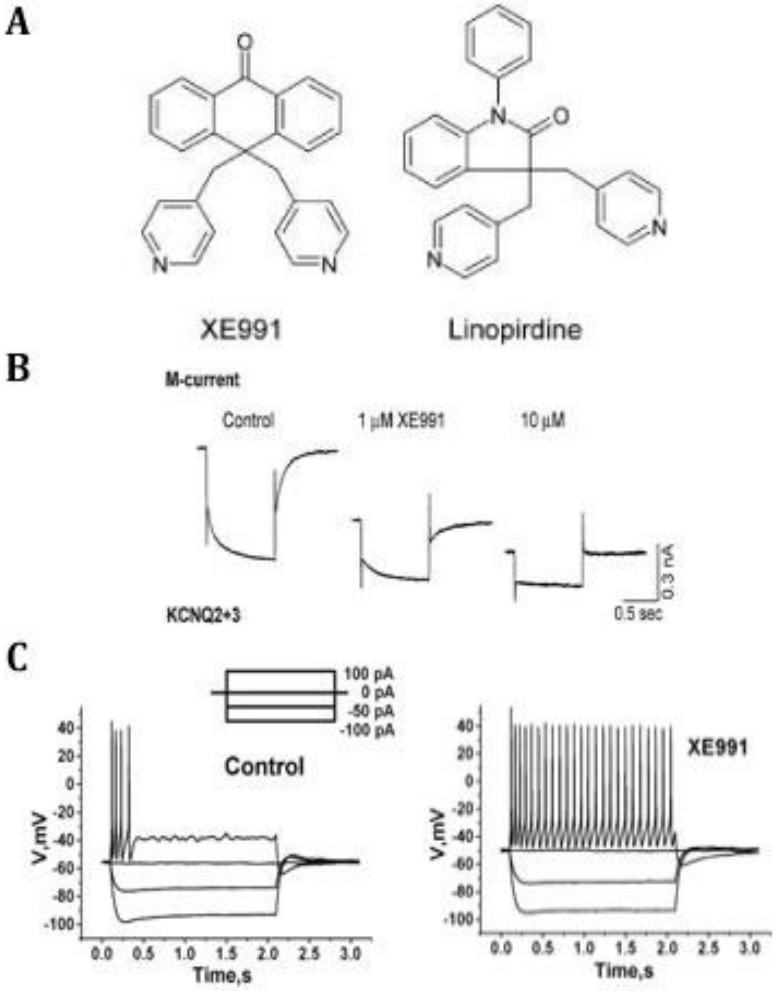

Figure 1.6: Kv7/M-channel blockers XE991 and linopirdine and the effect of XE991 on M-current. *(A)The chemical structure XE991 and linopirdine ester (from (Yeung and Greenwood, 2005). (B) Blockade of M-current in SCG neurons by XE991.(Wang et al., 1998). (C) XE991 increases the excitability of SCG neurons (from (Zaika et al., 2006)*

1.5.6 Kv7/ M-CHANNELS AND PAIN

The pain pathway requires the transduction and transmission of an excitatory signal to the CNS. Kv7/M-channels are important in controlling excitation in many tissues and there is evidence of the contribution of these channels to the transmission of pain. Thus, M-currents have been identified biophysically and pharmacologically in neurons isolated from rat dorsal root ganglia (DRG), including those sensitive to capsaicin (and hence presumably nociceptive)(Passmore et al., 2003; Crozier et al, 2007; Linley et al, 2008;(Liu et al., 2010)), and also in DRG neurons *in situ* (Rose et al., 2011). Further, DRG neuron M-currents can be inhibited by inflammatory/nocifensive mediators such as β-alanine (via MrgD receptors: Crozier et al, 2007), activators of the protease-activated receptor PAR-2 (Linley et al., 2008) and bradykinin (Liu et al., 2010), with an accompanying increase in excitability.

Evidence that Kv7/M-channels may play an important in controlling pain has been reported. Linley et al (2008) observed increased nocifensive behaviour in rats following intraplantar injection of the channel blocker XE991 similarly in a study by Passmore et al (2003) retigabine also inhibited responses to intraplantar application of carrageenan in a rat model of chronic pain, the effects were reversed by XE991.

Conversely, the M-channel enhancer retigabine has been shown to significantly attenuate pain responses in the chronic constriction injury and spared nerve models animal models of pain, which were reversed with the application of XE991 (Blackburn-Munro and Jensen, 2003); and post-surgical application of the homologous M-channel enhancer, flupirtine, led to a reduction in the pain threshold of rats (Rose *et al.*, 2011). These and other observations have led to suggestions that Kv7 channel enhancers maybe effective in the treatment of pain (Wickenden & McNaughton-Smith, 2009).

1.5.7 Kv7/M-CHANNEL LOCALISATION IN PAIN PATHWAY

Kv7 subunits and functional M-channels have been detected within various parts of the somatosensory pathway. Thus, in addition to functional M-currents, mRNAs for Kv7.2, 7.3, 7.4 and 7.5 were detected in whole dorsal root ganglia, and both mRNAs and immunolabelled Kv7.2, Kv7.3 and Kv7.5 were found in individual cultured DRG neurons, including TRPV1-positive neurons, inferred to be nociceptive (Passmore et al., 2003). Kv7.2 immunolabelling of dorsal root ganglion cells *in situ*, co-localising variably with TRPV1, IB4 and NF200, has been subsequently reported, together with localisation within the rat sciatic nerve (Rose et al., 2011). There is also experimental evidence for M-channels within the dorsal horn since the M-channel opener retigabine decreased the excitability of dorsal root afferents (Rivera-Arconada and Lopez-Garcia, 2006) and was also shown to reduce evoked responses within dorsal horn neurons (Passmore et al., 2003). Passmore et al. (2003) demonstrated that application of retigabine, to the dorsal spinal cord could inhibit evoked C and Aδ fiber-mediated responses and importantly a reduction in "windup" due to repetitive stimulation in normal and injured rats. Kv7.2, Kv7.3 and Kv7.5 immunoreactivity, together with functional M-channels, have also been reported in nodose visceral sensory neurons (Wladyka and Kunze, 2006) and have been shown to play a functional role in regulating arterial baroceptor responses to intra-arterial pressure (Wladyka et al., 2008).

Kv7/M-channels have been detected within peripheral axons. (Schwarz et al., 2006) detected Kv7.2 and functional Kv7/M-channels, as defined by retigabine sensitivity, at nodes of Ranvier within the sciatic nerve. (Schwarz et al., 2006) also found Kv7.3 protein within the nerve but the expression of this appeared more diffuse along the axon. Recently, (King and Scherer, 2012) have localised immunoreactivity for Kv7.5 in unmyelinated fibre bundles in the rat sciatic nerve, with Kv7.2 confined to nodes of Ranvier as previously reported.

The Kv7/M-channel enhancer modulator retigabine increases the membrane potential of unmyelinated fibres of isolated human sural nerves in an XE991-antagonisable manner (Lang et al., 2008), and the M-channel enhancer flupirtine has been reported to have a similar effect on myelinated fibres in isolated rat sural nerves (Sittl et al., 2010).

Interestingly, in an experiment involving the axotomy of mouse saphenous nerves Kv7.2 protein showed increased co-localisation with sodium channels in areas proximal to the neuroma but the not in distal areas suggesting a role Kv7/M-channels in compensating for over excitability in injured tissue (Roza et al., 2011). Further evidence of expression of Kv7/M-channels at distal axons comes from the staining for Kv7.4 protein within neuronal structures associated with somatosensation within the skin (Heidenreich et al., 2012).

Recently, experiments using the intact *in vitro* skin nerve preparation revealed that the Kv7/M-channels may have a role in action potential generation at the peripheral nerve terminals in the skin, since the number of action potentials induced in Aδ-type afferent nociceptor fibres by noxious heat was increased by blockade of Kv7/M-channel and conversely decreased by the enhancing the channel's activity (Passmore et al., 2012); illustrated in figure 1.7 (B).

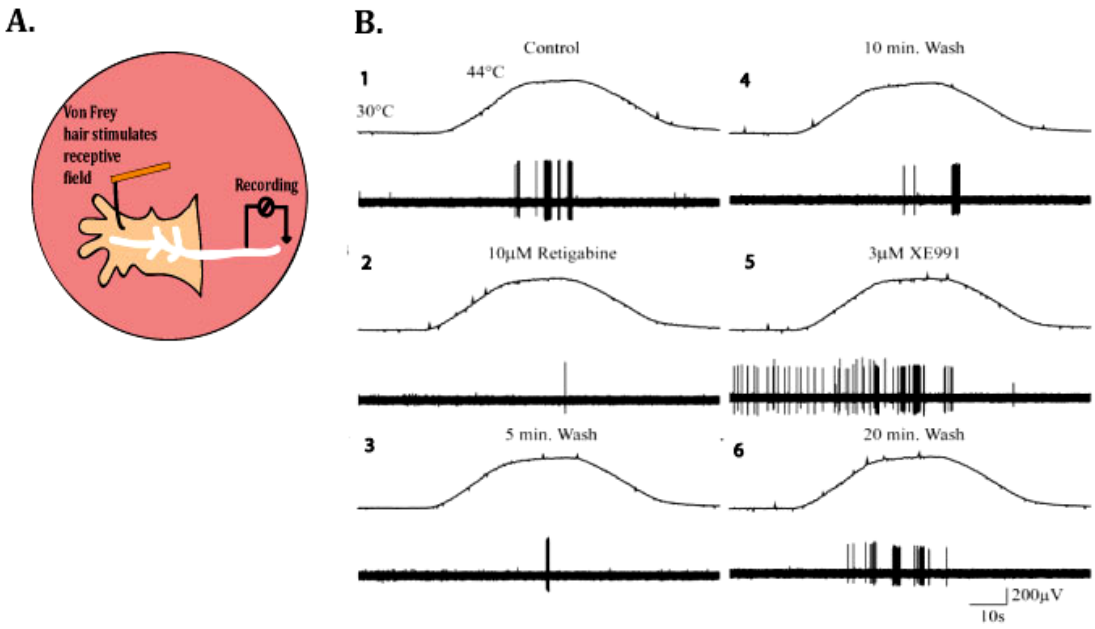

Figure 1.7 Skin nerve recording of an Aδ axon response to noxious heat. *(A) Cartoon of the skin nerve recording set up. (B) Recording of an Aδ axon response to noxious heat experiment carried out in numerical order as illustrated. (Image courtesy of G. Passmore: see Passmore et al, (2012), for details)*

1.6 AIMS OF THIS PROJECT

The overall aim of this work was to determine the expression of Kv7/M-channels in the peripheral components of the nociceptive sensory pathway (in association with functional studies by Dr. G.M.Passmore), and to assess aspects of their functional significance.

Specific aims were:

1. To further define the expression of Kv7.2 M-channel subunits within the different types of neuron within the rat dorsal root ganglion, by immunofluorescence. Kv7.2 was selected for study because it probably constitutes the most abundant subunit of the functional M-channel in these neurons, whether expressed heteromerically with Kv7.3 or homomerically (Passmore et al., 2003)

2. To determine the expression of Kv7.2 subunits in the peripheral nerves within the skin of the rat's paw. These experiments were undertaken in association with the functional studies of Dr. G.M. Passmore on the role of M-channels in regulating nociceptive sensory discharges in afferents from the rat paw skin (see figure 1.6).

3. To find out if Kv7/M-channels were functionally active in unmyelinated peripheral sensory nerve fibres, using the isolated rat vagus nerve.

4. Following on from observations in (2) above, to determine the expression of Kv7.2 in non-neural elements within the rat paw skin, and assess their possible functional consequences.

CHAPTER 2.

METHODS AND MATERIALS

2.1 TISSUE CULTURE

All of the procedures undertaken in this study were performed in accordance with the Animals (Scientific Procedures) Act 1986. Animals, (Sprague Dawley rats) were either killed by asphyxiation using a rising gradient of CO_2 followed by decapitation for rats older than 10 days, or dislocation of the neck for younger rats. Aseptic techniques were applied throughout the tissue culture procedures to minimise the risk of possible contamination from microorganisms.

2.1.1 CULTURE OF SUPERIOR CERVICAL GANGLION (SCG) AND DORSAL ROOT GANGLION (DRG) NEURONS

The methods for the culture of superior cervical ganglia (SCG) and dorsal root ganglia (DRG) neurones were based on those previously described by (Owen et al., 1990). SCGs and DRGs were isolated from Sprague Dawley rats 17 days postnatal or older. In each case the whole ganglion was dissected from the adjoining tissue and placed into L-15 media (Sigma, UK). The epineurium that surrounds the ganglion was carefully removed using microdissecting tweezers (Swiss pattern no.1, Harvard Apparatus, UK).

The dissociation of the ganglia into isolated cells involved enzymatic digestion. Two incisions were made in the ganglia. The ganglia were then incubated for 20 minutes at 37°C at 5% CO_2 in collagenase (type IA from *Clostridium histolyticum*; 400 U/ml), bovine serum albumin (BSA) (essentially globulin free; 6 mg/ml) dissolved in Hanks Balanced Salt Solution (Ca^{2+} and Mg^{2+} free ((HBSS; Invitrogen, UK) with 10mM HEPES. The collagenase was removed and the ganglia were washed (x3) with HBSS. The ganglia were then incubated in trypsin solution (1 mg/ml trypsin type XII S; 6 mg/ml BSA in HBSS dissolved in 10 mM HEPES) for 30 minutes at 37°C with 5% CO_2.

Following the enzymatic digestion the ganglia were placed in 2 ml of SCG/DRG growth media containing; L-15 (Sigma, UK), 24 mM $NaHCO_3$ (Invitrogen, UK), 10% Foetal Bovine Serum (FBS) (Invitrogen, UK), 0.6% w/v Glucose; 2mM L-Glutamine (Invitrogen, UK), 100 U/ml of penicillin/streptomycin (Invitrogen, UK), 50 ng/ml NGF 7S (Sigma, UK).

The ganglion cells were dissociated by passing the solution through a glass Pasteur pipette heat polished to an internal diameter of 1 mm (triturated). The triturated ganglion in SCG/DRG growth media was briefly centrifuged i.e. spun until the centrifuge reached a speed of 168 *g*. Due to this centrifugation the isolated cells are largely contained in the supernatant, the remaining aggregated cells in the pellet. The supernatant from the centrifugation was transferred to a fresh tube. The remaining pellet was triturated in 2 ml of fresh growth media and centrifuged at 168 *g*; this step was repeated 4 times or until no visible pellet remained after centrifugation. After each centrifugation the supernatant was pooled. The pooled supernatants were centrifuged for 5 minutes at 168 *g*. The pellet was re-suspended in 400 µl SCG/DRG growth media per SCG ganglion or per 8 DRG ganglia.

The isolated cells were plated onto either 35 mm diameter plastic petri dishes (Nunc, Denmark) or 12 mm (diameter) thickness 0 glass coverslips (Assistant, Germany). The glass coverslips were dipped in 70% ethanol and passed through a flame, then sterilised under UV light for 20 min. Prior to plating the petri dishes and/or coverslips were pre-coated with 10 µg/ml laminin, (from Engelbreth-Holm-Swarm murine sarcoma basement membrane, (Sigma, UK)) for a minimum of 2 hours at 37˚C in 5% CO_2. The laminin was removed and the dishes were washed with SCG/DRG growth media, this was removed and 100 µl of the cell suspension was plated onto each petri dish or coverslip.

The plated cells were allowed to adhere to the substrate for 6 hours before the SCG/DRG growth media was replaced, removing the dead or dying neurons. After adhesion the media surrounding the cells was replaced with fresh SCG/DRG growth media. Cells were maintained at 37°C with 5% CO_2 until required for experimentation. For all experiments cells were kept for a maximum of one week.

2.1.2 CULTURE OF RAT KERATINOCYTES

Rat keratinocytes were cultured through by a modification of methods previously described by (Dlugosz et al., 1995). Keratinocytes were cultured from 3 day old rats which had been killed by dislocation of the neck in accordance with Schedule 1 of the Animals (Scientific Procedures) Act 1986. The skin from the back and abdomen was excised in one piece. The excised skin was sequentially washed for 2 minutes in the following solutions: PBS with 1% antibiotic-antimycotic solution (0.01 M Phosphate Buffered Saline containing 1% Antibiotic-Antimycotic (100X) liquid (Invitrogen, UK)); 70% ethanol and finally PBS 1% with antibiotic-antimycotic solution.

Mammalian skin is comprised of two main layers the dermis and the epidermis, see figure 2.1. Keratinocytes are contained within the epidermis of the skin. In order to isolated these cells this layer needs to be isolated from the dermis. After the washes the skin was placed dermis side up into a 72 cm diameter plastic petri dish (Nunc, Denmark). The subcutaneous tissue (fat) was removed by gently scraping with constant pressure using a scalpel with a no.15 blade (VWR, UK). The dermis was dissociated from the epidermis by enzymatic digestion as follows. The skin was placed dermis side down, in a dish containing trypsin 0.25% (w/v)-EDTA solution (Invitrogen, UK). The skins were incubated with the enzyme solution at 4°C overnight, approximately 15 hours.

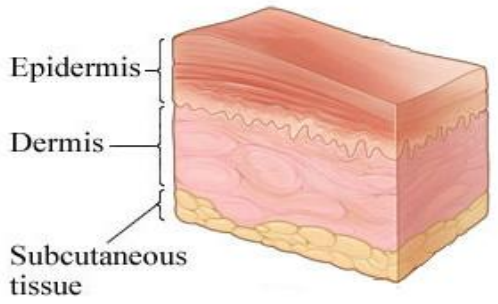

Figure 2.1 The basic structure of the skin (Blahd, 2011)

The skin was transferred then into a petri dish with the dermis facing up. Residual dermal tissue was removed by gently scraping with a scalpel with a no.15 blade.

The epidermis was sliced into approximately 1 cm wide sections and placed into a sterilised Erlenmeyer flask. Keratinocyte serum free media (Keratinocyte-SFM) (Invitrogen, UK) with 10% foetal bovine serum (FBS) (Invitrogen, UK) and 1% antibiotic-antimycotic (100X) liquid (Invitrogen, UK) was added to the flask and the tissue was stirred with a sterile magnetic flea on a magnetic stirrer for 30 minutes at room temperature.

To isolate the keratinocytes within the epidermis the suspension was passed through a nylon mesh cell strainer 70 μm (BD Falcon, USA) into a plastic centrifuge tube (VWR, UK). The cells were centrifuged for 5 minutes at 168 *g*. The resultant pellet of cells was then re-suspended in 15 ml of Keratinocyte growth-SFM, (Keratinocyte –SFM + 1% v/v Antibiotic-Antimycotic (100X) liquid) then 1 ml of the cell suspension was plated into 35 mm^2 plastic petri dishes or into each well of 12-well Multiwell plate (Nunc, Denmark). The keratinocytes were allowed to adhere without disruption overnight in a 5% CO_2 in an incubator at 37˚C.

After overnight incubation the unattached cells were removed by media replacement with fresh Keratinocyte growth-SFM. This procedure was repeated every 48 hours and the cells were maintained for up to 3 weeks or until they reached confluence.

2.2 IMMUNOFLUORESCENT STAINING

2.2.1 ISOLATED CELLS

In all experiments, 12 mm (diameter) thickness 0 glass coverslips (Assistant, Germany) were used. Cultured cells were washed (x2) at room temperature with PBS (0.01 M Phosphate Buffered Saline) followed by fixation with 4% paraformaldehyde (PFA), (EMS Diasum, USA) in PBS (PFA/PBS), for 15 minutes.

After fixation, the cells were washed (x3) for ten minutes with PBS. To reduce non-specific binding of the antibody the cells were incubated with a blocking solution; comprised of PBS with either 3% v/v of the serum of the host of the secondary antibody or 1% BSA w/v. To permeabilise the membrane of the cells 0.3% v/v Triton X-100™ or 0.3% TWEEN®20 was added to the blocking solution. The cells were incubated in blocking solution for a minimum of one hour at room temperature. The blocking solution was washed and primary antibodies were added at dilutions that are described in table 2.1. The final dilutions utilised were either the manufacturer's recommendation or as optimised in SCG cells which are known to contain the Kv7/M-channel.

Antibody/ Epitope and species	Source	Host	Final Concentration
Kv7.2 peptide / aa578-593 rat Kv7.2	Alomone, Israel	Rabbit	0.7 µg/ml.
Kv7.2/ aa850 to the C-terminus human Kv7.2	Abcam, UK	Rabbit	0.3 mg/ml
Kv7.2 (monoclonal) Neuromab clone N26A/23 fusion protein of aa1-50 human KCNQ2	Neuromabs, USA	mouse	1:100
TRPV1 (VR1 / aa4-21 rat VR1)	Abcam, UK	Rabbit	1:1000.
Anti-βIII Tubulin / C-terminus (EAQGPK) m βIII tubulin	Promega, USA	Mouse	0.5 µg/ml
Tyrosine Hydroxylase / Two different regions in gene shared between mouse and human	Abcam, UK	Chicken	1:1000
N52 /C-terminal segment of pig neurofilament 200	Sigma, UK	Mouse	1:1000
Peripherin/Recombinant full length rat peripherin	Abcam, UK	Rabbit	1:1000

Table 2.1: List of primary antibodies: *(aa: position in amino acid sequence of protein)*

The cells were incubated with the primary antibodies overnight at 4˚C.

Where available the primary antibody's epitope peptide was utilised to test for specificity of the binding of the primary antibody. The epitope peptide was incubated in 10 times molar excess of the working dilution of the primary antibody as described in table 2.1 above, at room temperature for at least an hour prior to addition of antibody to the cells. To test for specificity of the secondary antibody, in each experimental set, a control where the primary antibody was omitted was included.

After overnight incubation the primary antibody solution was removed and the cells were washed for 5 minutes in PBS (x3).

2.2.1.1 Conventional secondary antibody staining protocol: monoclonal Kv7.2 antibody or non-Kv7.2 primary antibodies

Conventional immunofluorescent secondary staining methods, see figure 2.2 (A), were used to stain the cells that had been incubated in primary antibodies that were either monoclonal Kv7.2 antibodies or non-Kv7.2 antibodies. Fluorphore conjugated secondary antibodies specific to the host of each primary antibody; as shown in table 2.2, were incubated with the cells for a minimum of one hour at room temperature in the dark.

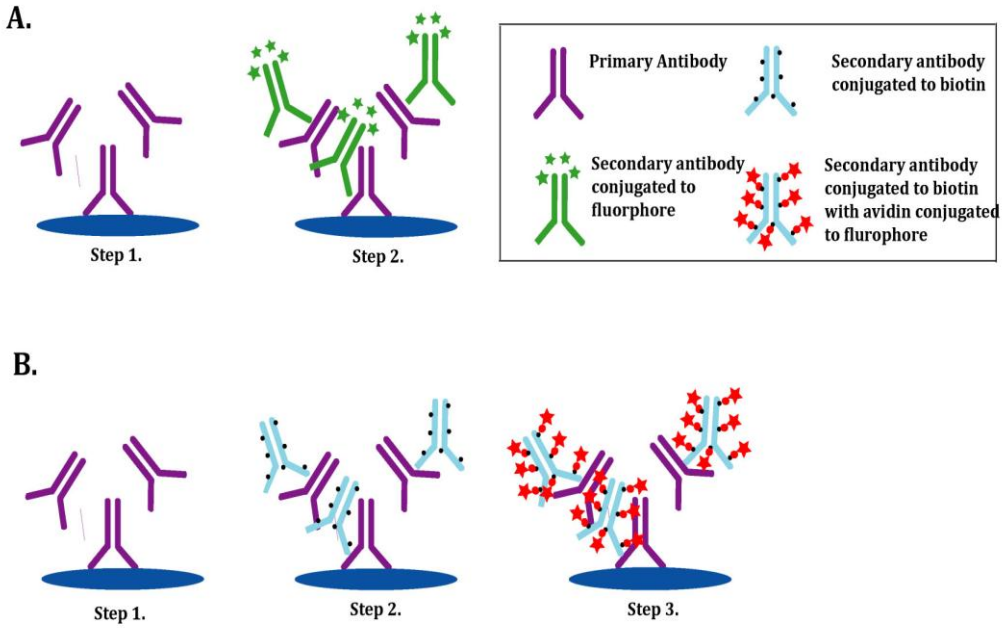

Figure 2.2: Summary of conventional and amplified immunofluorescent staining protocols. *(A) Conventional secondary antibody staining; Step 1. Primary antibody binds to substrate, Step 2. Secondary antibody with conjugated flurophore binds to primary antibody. (B) Amplification of secondary antibody staining; Step 1. Primary antibody binds to substrate, Step 2. Secondary antibody with multiple conjugated biotins binds to primary antibody, Step 3. Fluorphore conjugated to streptavidin binds to biotin.*

2.2.1.2 Amplification of secondary antibody staining protocol: polyclonal primary antibodies

A biotin/streptavidin amplification step was included in the staining with the polyclonal Kv7.2 primary antibodies. Biotin has a high affinity and multiple binding sites for streptavidin, consequently using a biotinylated secondary antibody and a streptavidin with multiple fluorphores facilitates the amplification of the fluorescent signal, see figure 2.2 (B). A biotinylated anti-rabbit secondary antibody diluted 1:333 in PBS was applied to the cells for a minimum of 1 hour. After incubation the antibody was removed and the cells were washed (x3) for 5 minutes in PBS. The cells were incubated with Cy3 conjugated to streptavidin diluted 1:100 in PBS for a minimum of one hour in the dark. Refer to table 2.2 for details of the biotinylated secondary antibody and Cy3 streptavidin.

Antibody/ Source	dilution	Absorption/ emission (nm)
Goat anti-mouse FITC/ Sigma, UK	1:63	492 / 518
Biotinylated Goat anti-rabbit/ Vector Laboratories, UK	1:333	Not applicable
Cy3 conjugated strepavidin	1:320	552 / 565
Rabbit anti-chicken FITC/ Sigma, UK	1:320	490/525
Goat anti-mouse Rhodamine/ Invitrogen, UK	1:100	570/590
Rhodamine Red™-X Goat Anti-Rabbit IgG/Invitrogen, UK	1:100	573/590

Table 2.2: List of secondary antibodies used for immunofluorescence experiments

Throughout the remainder of the protocol the exposure of the cells to light was kept to a minimum. Following the incubation with either Cy3 conjugated-streptavidin or the flurophore conjugated secondary antibody the cells were washed (x5) in PBS for 5 minutes then washed in dH_20. The cover slips were mounted on to SuperFrost® Plus glass slides (VWR International, UK) using Fluorescence Mounting Medium (Dako, UK) and placed in the dark overnight at room temperature to allow the mounting medium to set. The following day the coverslips were sealed around the edges using clear nail polish. Slides were stored at 4˚C.

2.2.2 ISOLATED TISSUES

2.2.2.1 Tissue perfusion and isolation

In accordance with schedule 1 of the Animals (Scientific Procedures) Act 1986 and under Home office personal licence certification (modules 1-4) a 150-200g Sprague Dawley rat was terminally anaesthetised via overdose of a species appropriate anaesthetic, intra-peritoneal injection of 1 mg/kg ketamine/xylamine (Wolfensohn and Lloyd, 2003). Terminal anaesthesia was defined as being established when leg withdrawal and corneal reflexes were abolished.

A midline incision was made through the abdomen exposing the diaphragm, sternum and internal organs. The sternum was cut and the rib cage was removed. A hypodermic needle (25G X 16 mm) (Tyco healthcare, UK) attached to a gravity-driven perfusion system was inserted into the left ventricle of the heart and the animals were perfused with 50 mls of ice cold heparinised saline (9% w/v NaCl (VWR, UK), 50000U/l Heparin). The aorta was severed to avoid recycling and to allow efflux of the perfusant. When the efflux of perfusant from the vena cava was clear and the liver was completely blanched, thus ensuring that all blood had been cleared from the circulatory system, the animals were then perfused with 50 – 100 ml of chilled 4% PFA/PBS.

The tissue was dissected and left in fixative (4% PFA / PBS) for at least 3 hours, post-fixation. After post fixation the tissue was rinsed with PBS, (x3) for 30 minutes and stored in a 30% Sucrose w/v / 0.01 % sodium azide / PBS solution for 3 – 5 days before sectioning.

2.2.2.2 Cryosectioning

The tissue was cyrosectioned using Leica Freezing Microtome SM 2000R (Leica Microsystems, Germany). A section of skin or ganglion, approximately 5 mm^3 was positioned on the stage and held briefly in place to allow adhesion via freezing. The base of the tissue was attached by applying 30% Sucrose / 0.01 % sodium azide / PBS solution using a small artists brush. The tissue was covered with powdered dry ice for 5 minutes to allow the tissue to freeze completely. When the tissue was frozen, the surrounding dry ice was carefully removed and 40 μm thick sections were sliced. Each section was transferred to a 12-well multiwell plate, (Nunc, USA) containing PBS using a small artists brush.

2.2.2.3 Staining of isolated tissue sections

Immunofluorescent staining of tissue sections was performed as described section 2.2.1 the exception being that the PBS washes and the incubations with secondary antibodies being at least twice as long. Throughout the staining protocol the tissue sections were placed on a rocking platform shaker (VWR, UK).

2.2.2.4 Mounting of tissue sections onto slides

Immunofluorescent stained tissue sections were mounted onto gelatinised slides using a small artist brush. Gelatinised slides were prepared as follows: super premium microscope slides (0.8-1.0 mm thick frost (VWR, UK)) were dipped for 30 seconds in a solution containing 3.75 % w/v gelatine and 0.25% w/v chromium (III) potassium sulphate dodecahydrate then air dried.

2.2.3 CONFOCAL IMAGE ACQUISITION AND ANALYSIS

Immunofluorescent staining was imaged via Leica DM RBE, fitted with a TCS SP2 confocal head (Lecia, Germany) using Leica Confocal software for SP2 (Lecia, Germany) and either 40x or 63x oil immersion objectives. During image acquisition the wavelength was optimised for the excitation and emission spectra for each flurophore to minimise photo bleaching. When comparing within the same experiment i.e. between the primary/secondary antibody test samples and secondary antibody only control samples the gain and exposure was maintained at the same level. The images obtained were further analysed using the following software: Openlab software (Improvision, UK), Corel Photo paint 10 (Corel Corporation, USA), Adobe Photoshop Pro (Adobe, USA) and Adobe Illustrator CS (Adobe, USA).

2.3 EXTRACELLULAR RECORDING FROM VAGUS NERVE

The protocol for the extracellular recording of the vagus nerve was based on the recording set up described by (Marsh et al., 1987).

2.3.1 DISSECTION OF THE VAGUS NERVE

The parameters of the recording chamber from which electrophysiology measurements were obtained required the dissection of the maximal possible length of vagus nerve, approximately 5 cm, therefore adult rats were used in this protocol. The rats were terminally anaesthetised as previously described in accordance with Schedule 1 of the Animals (Scientific Procedures) Act 1986 via asphyxiation by rising CO_2.

The rats were positioned ventral side up on a dissection stage. The skin surrounding the neck was excised and the muscles underneath were removed exposing the trachea and providing access to the vagus nerve, which runs parallel to the carotid artery. The carotid artery was separated from the vagus nerve by blunt dissection. HEPES buffered Krebs solution (142 mM NaCl, 2 mM KCl, 1.5 mM $MgCl_2$, 1.5 mM $CaCl_2$, 10 mM HEPES, 11 mM Glucose adjusted to pH 7.3) was frequently applied to the tissue throughout the protocol to prevent potential desiccation of the tissue. The vagus nerve was excised and carefully de-sheathed of the surrounding epineurium. A ligature was tied to each end of the desheathed nerve which was then placed into ice-cold HEPES buffered Krebs solution and stored at 4°C for 2 hours prior to experimentation. Care was taken throughout the dissection and during consequent handling of the nerve to minimise any damage to or stretching of the nerve.

2.3.2 RECORDING BATH SET UP

Extracellular recordings from the vagus nerve were completed in a plexiglass recording bath separated into three chambers separated by four adjustable upper and lower partitions as illustrated in figure 2.3 (A). Silver/silver chloride recording electrodes (World Precision Instruments, UK) were inserted into the base of chambers 1 and 2, (figure 2.3 (B)) to facilitate the recording of evoked electrical potentials. The partitions contain a small groove on one edge allowing the nerve to pass through the partitions without compression. The grooved edges of the lower partitions were coated with silicone grease and the partitions were positioned with the grooves facing up into the recording bath creating chamber 2. The bath was filled with Krebs solution to the top of the lower partitions. The edges of the upper partitions were coated with silicone grease along the non-grooved side. The nerve was placed in the bath in chamber 1. The ligature attached to the nerve was secured to the outside of the bath and the nerve was threaded over the grooves in the lower partitions. The greased upper partitions were promptly inserted and pressure was applied to seal the

compartments and seal around the nerve. The chambers were then completely filled with Krebs solution.

The nerve was manoeuvred in chamber 3 so that it was in contact with the central platinum stimulating electrodes. A continuous perfusion system was applied to chamber 2 to permit the addition and removal of drugs to that chamber alone. All recordings were performed at room temperature (~21- 25 °C) in order to minimise noise and improve stability.

Prior to experimentation 1 mM procaine (Sigma, UK) or 0.5µM tetrodotoxin (TTX; Tocris, UK) was added to chamber 1 so that monopolar action potentials were recorded.

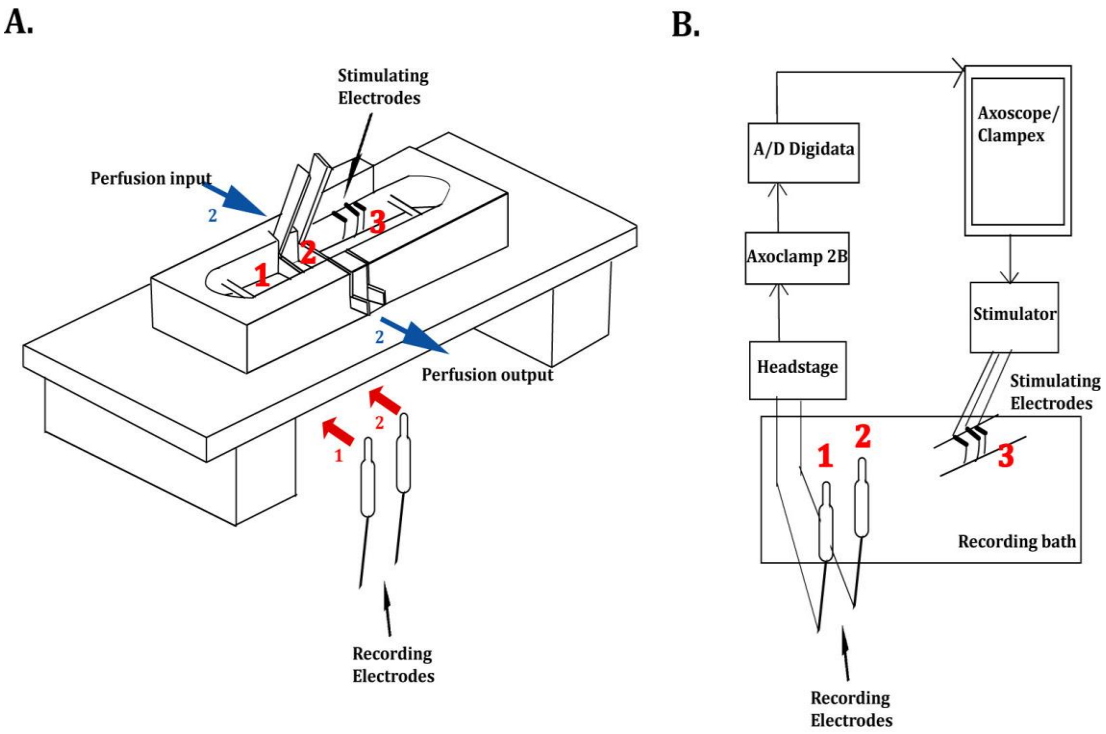

Figure 2.3: Schematic of set up for extracellular recording of vagus nerve.

(A) Extracellular recording bath. (B) Extracellular recording circuit. The numbers refer to the different chambers, 1, 2, and 3 within the bath; this is elaborated further in the text

2.3.3 EXTRACELLULAR RECORDING FROM THE VAGUS NERVE

The evoked compound action potentials (CAP) from within the rat vagus nerve were generated and visualised using the recording circuit as illustrated in figure 2.3 (B).

pCLAMP 10 software (Molecular Devices, USA) controlled both the stimulus via an isolated stimulator DS2 (Digimeter, UK) and the acquisition of the evoked potentials. The Ag/AgCl recording electrodes (World Precision Instruments, USA) were connected to the headstage HS-2A (0.1X LU) of an AxoClamp 2B amplifier (Molecular Devices, USA) in current-clamp mode using an output filter set at 10 kHz. Acquisitions were recorded to a computer via a Digidata 1200 A/D interface (Molecular Devices, USA) at a sampling rate of 20 kHz.

The change in axonal polarisation throughout the experiment was recorded in parallel at 1 kHz using a USB attached Mini Data analogue to digital converter and Axoscope 10.1 acquisition software (Molecular Devices, USA). Post-acquisition display and analysis was undertaken using Clampfit 10 (Molecular Devices, USA). The vagus nerve was stimulated at a rate of 0.3 Hz, with a stimulus width of 1 ms and stimulus voltage of 10-30 V, which had been optimised for the preferential recording of C-fibres. The stimulus amplitude was adjusted until it achieved a maximal peak C-fibre compound action potential and then the stimulus voltage was increased by a further 50% to ensure that supra-maximal stimulus was always being applied. The baseline drift of the electrode was 0.1 mV/hour.

2.4. INTRACELLULAR RECORDING FROM KERATINOCYTES

Intracellular recordings from keratinocytes were undertaken using conventional whole-cell recording techniques. Keratinocytes were cultured onto 35mm plastic culture dishes and mounted onto a Nikon Diphot 300 microscope utilising a Perspex perfusion chamber. Recordings were made using Clampex acquisition software controlling an Axopatch 200A integrated patch-clamp amplifier (Axon instruments, USA). The head stage (CV 201A; Axon instruments, USA) of which was mounted on a Narishige micromanipulator (MX-1; Narishige, Japan). All recordings were made at a sampling frequency of 5 kHz and filtered using a low pass Bessel filter at 2 kHz. The current and voltage outputs from the amplifier was digitised using a Digidata 1440A acquisition system (Molecular devices, USA) before being processed by Clampfit 10.2 (Molecular Devices), Excel 2003 (Microsoft, UK), and Microcal Origin 6.0 or 8.6. (OriginLab Corporation, USA) on a Dell PC.

Patch pipettes were fabricated from thin walled, filamented borosilicate capillary glass (GC150TF-10; Harvard Apparatus Ltd, UK) using a Narishige PC-10 vertical puller (Narishige, Japan). The tips of the pipette were 'fire-polished' using a glass polished platinum wire on a Narishige microforge (MF-830; Narishige, Japan). The pipette resistance when filled with the intracellular solution was ~5–10 MΩ.

A silver/silver chloride (Ag/AgCl) reference electrode, was electroplated at 9 V in a 0.9% (w/v) NaCl solution for approximately 5 minutes in order to coat the wire with AgCl.

For the recordings the cells were perfused with an external solution containing: NaCl (144 mM), KCl (2.5 mM), $MgCl_2$ (0.5 mM), $CaCl_2$ (2 mM), HEPES (5 mM), Glucose (10 mM), (pH adjusted to 7.4 with NaOH).

The internal solutions for recordings comprised: KCl (30 mM), CH_3C0_2K (80 mM), HEPES (40 mM), EGTA (3 mM) $MgCl_2$ (3 mM) and $CaCl_2$ (1 mM), (pH adjusted to 7.4 with NaOH).

Recordings were made in two configurations whole-Cell and perforated-patch. In whole-cell mode after gaining access to the intracellular compartment, cells were allowed to stabilise to allow full dialysis (5-10 mins). Keratinocytes were then subjected to a voltage ramp from -100 mV to +100 mV for 25 s to assess any voltage dependent conductances or changes in membrane current induced by drugs.

The perforated-patch method was utilised for the recording of the membrane potential of keratinocytes. The perforated-patch method uses a pore forming agent to allow access to the intracellular compartment without dialysing away components that may affect ion channel gating or regulation. In these experiments the pore forming agent was Amphotericin B. Amphotericin B was dissolved in DMSO (100 mg/ml), ultrasonicated to aid dissolution before being dissolved in intracellular solution to a final concentration of 0.2 mg/ml and filtered through a 0.45 μm filter. Electrodes were dipped in amphotericin–free intracellular solution before being backfilled with the amphotericin containing intracellular solution to aid attachment to the cell surface.

For all recordings the patch pipette was mounted within an electrode holder with a side attachment to which negative pressure could be applied following the lowering of the electrode onto the cell surface. Prior to contact with the cell the pipette current was 'zeroed' to remove any standing potential generated between the recording electrode and bath earth. A 'gigaseal' (> 1 GΩ was achieved by applying gentle suction via a tube attached to the side arm of the electrode holder. For the perforated patch recordings after a 'gigaseal' was attained the cell was left in cell attached mode until sufficient perforation had occurred. This often took up to 20 minutes and was accessed by monitoring the

capacity transient induced by a hyperpolarising (-10 mV) voltage step. The final series resistance was in the range 20-30 MΩ.

2.5 ASSAY OF ATP RELEASE FROM KERATINOCYTES

ATP release from the keratinocytes was measured via a modification methods described in (Koizumi et al., 2004) and the CellTiter-Glo®Luminescent Viabillity Assay (Promega, USA). This assay utilises the ability of luciferase to convert luciferin, oxygen and ATP into oxyluciferin with the emission of light via the reaction described in figure 2.4. The light released can then be measured with a luminometer (Model 20E, Promega, USA).

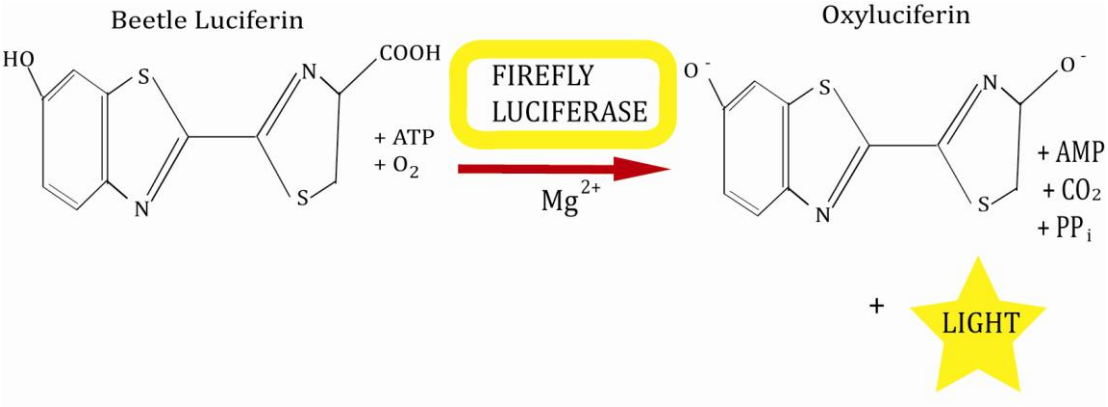

Figure 2.4: The Luciferase reaction. *Mono-oxygenation of luciferin is catalysed by luciferase in the presence of Mg2+, ATP and oxygen (Promega, USA)*

The luciferase assay has been used before in other studies to explore the release of ATP from keratinocytes (Mizumoto et al., 2003). To investigate a possible functional role of Kv7.2 channels in keratinocytes, ATP release was measured in cultured rat keratinocytes in response to Kv7 modulating drugs including XE991, linopirdine and retigabine. These drugs were applied alone or in combination with the TRPV3 agonist Carvacrol, since TRPV3 is known to be expressed in and linked to ATP release in keratinocytes (Mandadi et al., 2009).

The keratinocytes were cultured until they reached confluence, between 1-3 weeks. The keratinocyte growth-SFM was replaced with HEPES buffered Krebs solution (144 mM NaCl, 2.5 mM KCl, 0.5 mM $MgCl_2$, 2 mM $CaCl_2$, 5 mM HEPES, 10 mM glucose adjusted to pH 7.4) and incubated for an hour at room temperature (~21-25°C). This was important for two reasons. Firstly, keratinocyte growth-SFM is low in calcium in order to facilitate proliferation, (Hennings et al., 1980) and secondly any ATP released due mechanical disruption or temperature change would have been metabolised.

Drugs were applied for 10 minutes. In order to control for experimental errors due to mechanical disruption of the keratinocytes an equivalent volume of HEPES buffered Krebs as that of drug, was added to control set of dishes where possible.

A 50 µl sample of Krebs from the top surface of the dish was removed to which an equal volume of CellTiter-Glo® Reagent was added. This was vortexed and equilibrated for 10 minutes to allow the luminescent reagent to stabilise. The sample was transferred to a disposable cuvette (8 x50 mm) (Promega, USA) which was measured in a luminometer. The parameters of the luminometer and the assay were initially defined by measuring known concentrations ATP with this assay.

2.6 COMPOUNDS AND DRUGS

The Kv7/M-channel modulators XE991 and linopirdine were obtained from Tocris, (UK) and retigabine was obtained from Neurosearch, (Denmark). All other reagents that were used throughout this study, except where otherwise stated were obtained from Sigma, UK and VWR, UK. For the luminometer readings the Kv7 channel modulating drugs and/or carvacrol were made up as a stock in HEPES buffered Krebs solution.

2.7 ANALYSIS

All analysis, statistical or other wise and graphic display of data in this study was completed using either Microsoft Excel (Microsoft, USA) or OriginPro 8.6 (Origin lab, USA). Image design and analysis was completed using Openlab 3.1 (Improvision, UK) Corel Paintshop (Corel, USA), Adobe Photoshop Pro (Adobe, USA) and Adobe Illustrator CS (Adobe, USA). All statistical analysis of data obtained with the keratinocyte ATP release assay was completed using a Student's t-test.

2.8. RNA ISOLATION AND REVERSE TRANSCRIPTION PCR (RT-PCR) FROM KERATINOCYTES

2.8.1 RNA ISOLATION AND QUANTIFICATION

Keratinocytes were cultured as previously described (section 2.1.2) into one 72 cm diameter plastic petri dish (Nunc, USA). These were maintained in culture until the dish reached confluence, 1-2 weeks. Total RNA was isolated from the keratinocytes using the GenElute™ Mammalian Total RNA Miniprep Kit (Sigma, UK).

The concentration of total RNA in the sample was determined via the Beer-Lamberts law,

$$A = e\,C\,l$$

A is the measured absorption at 260 nm
e is the RNA extinction coefficient (25 µl/µg/cm)
C the RNA concentration
and l is the path length of the cuvette (1 cm)

The absorbance at 260 nm was measured by a SmartSpec™ Plus spectrophotometer, (Bio-Rad, UK) using a quartz cuvette. Prior to reading the

RNA sample the spectrophotometer was zeroed with an equivalent volume of the buffer that the RNA was dissolved in.

The purity of the RNA sample was measured by calculating the ratio of the absorbance at 260 and 280 nm, the 260/280 ratio. This ratio gives an indication of the level of protein contamination as the absorbance maximum of protein and nucleic acid is 280 nm and 260 nm, respectively. Pure RNA has a 280/280 ratio of 2 (Turner, 2005).

2.8.2 REVERSE TRANSCRIPTION-PCR REACTION

Reverse transcription was completed on the total RNA as follows: deoxyribonuclease (DNase I; Promega, USA) treated RNA (0.2µg) was denatured by heating to 65°C for 10min and then placed onto ice. The denatured RNA was reverse transcribed into cDNA using Moloney Murine Leukemia Virus M-MLV reverse transcriptase; the components of the reaction are as follows: M-MLV 5x reaction buffer, 0.5 mM deoxyadenosine triphosphate (dATP), 0.5 mM deoxycytidine triphosphate (dCTP), 0.5 mM deoxythymidine triphosphate (dTTP), 0.5 mM deoxyguanosine 5'-triphosphate (dGTP), oligodeoxynucleotide primers (Promega, USA), recombinant RNasin RNAase inhibitor 1 U/µl H_2O molecular biology grade. The reaction was incubated at 37°C for one hour followed by denaturation of the M-MLV reverse transcriptase at 80°C for ten minutes. The reverse transcribed cDNA sample either immediately underwent PCR or was stored at -20°C.

One tenth of the volume of the resulting reverse transcribed cDNA was subjected to PCR amplification. The PCR primers were intron spanning as described by (Shah et al., 2002) the details of which are below:

rKCNQ2 (2900s): AGTCGGATCAGAGTCTC

rKCNQ2 (3126a): GCTCTGATGCTGACTTTGAGGC

rKCNQ3 (746s): CAGCAAAGAACTCATCACCG

rKCNQ3 (906a) : ATGGTGGCCAGTGTGATCAG

rKCNQ4 (40s): CCCTCCAAGCAGCATCTG

rKCNQ4 (420a): TTGATTCGTCCCAGCATGTCCA

rKCNQ5 (995s): GGAACCCAGCTCCAACCTCAT

rKCNQ5 (1101s): CTTTCTTGGTAGGGTGCAG

The PCR was completed using the components and protocol as optimised for the Vent$_R$® DNA Polymerase (NEB, USA) and was completed under the following PCR cycle conditions:

For KCNQ2 and KCNQ4

- 94° for 5 min
- 30 cycles
    - 94 °C for 30 sec
    - 55°C for 30
    - 72°c for 1 min
- 72°C for 10 min
- 4°C forever

For KCNQ3 and KCNQ5

- 94° for 5 min
- 30 cycles
    - 94 °C for 30 sec
    - 60°C for 30
    - 72°c for 1 min
- 72°C for 10 min
- 4°C forever
-

The amplified products were analysed by electrophoresis through a 1% agarose gel containing ethidium bromide then visualised under UV light.

2.9 MEASUREMENT OF CHANGES IN INTRACELLULAR CALCIUM IN KERATINOCYTES

Intracellular calcium was monitored using the cell permeable acetoxymethyl (AM) ester of Fura-2, Fura-2 AM (Invitrogen, UK). Fura-2 is a dual excitation flurophore which facilitates the ratiometric measurement of intracellular Ca^{2+} (Grynkiewicz et al., 1985). The binding of Ca^{2+} shifts the peak of the excitation spectrum from 380 nm to 340 nm while the emission wavelength remains unchanged at 510 nm. Unfortunately, due to wavelength specific attenuation by the fibre-optic cable connection from the polychrome unit to the microscope, 340nm could not be used; thus, 350nm was utilised instead

Fura-2 AM was dissolved in DMSO with 10 % pluronic acid (Invitrogen, UK). The keratinocytes were incubated for one hour at room temperature (22-25 ° C) with Fura-2 AM (final concentration 5 μM). The cells were perfused with HEPES buffered Krebs containing: NaCl (144 mM), KCl (2.5 mM), $MgCl_2$ (0.5 mM), $CaCl_2$ (2 mM), HEPES (5 mM), Glucose (10 mM), 0.1% w/v sulfinpyrazone (Sigma, UK), (pH adjusted to 7.4 with NaOH) for 20 minutes prior to recording to facilitate cleavage of the ester groups by endogenous esterase's.

The imaging and measurement of changes in intracellular calcium in keratinocytes was completed using the apparatus set up as shown in figure 2.5.

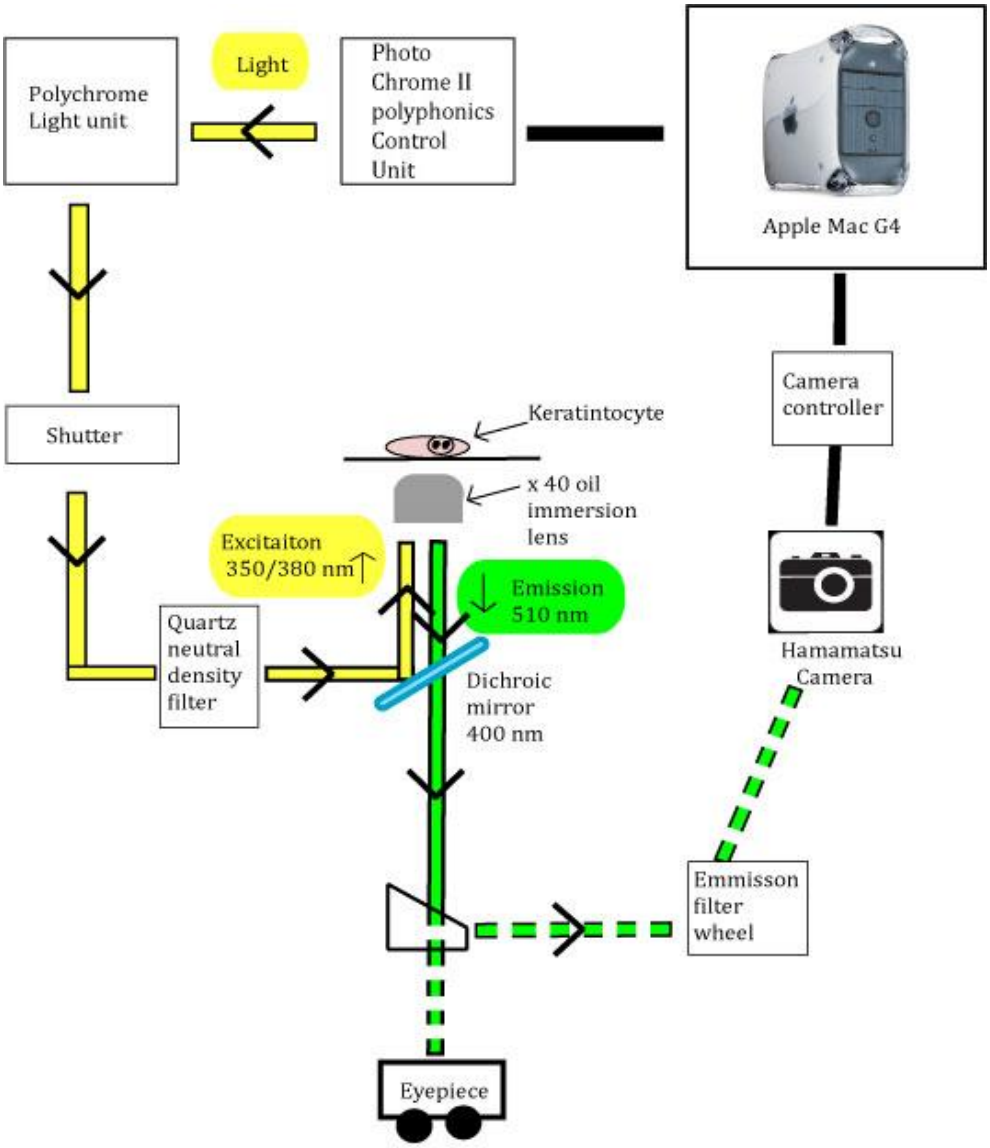

Figure 2.5: Set up of apparatus used for measuring changes in intracellular calcium. *A xenon short arc lamp within a monochromator (polychrome light unit, Till Photonics, Germany) provided the excitation light under the control of Openlab acquisition software via an Apple Mac. The incident excitatory light was controlled by the computer via a shutter and intensity was controlled by quartz density filters .The excitation/emission wavelengths were 'split' using a 400 nm dichroic mirror and a 510 nm emission filter. Images were monitored using a Hamamatsu CCD camera (Hamamatsu, Japan).*

Cells were visualised on a Nikon diaphot 300 inverted phase contrast microscope (Nikon instruments, USA) using an oil immersion x40 fluorescent objective (Nikon, USA). The excitation light was supplied by a xenon short arc

lamp (XBO; Osram, UK) within a Polychrome II monochromator (TILL Photonics, Germany) which was controlled by Openlab 3.1 Image acquisition software (Improvision, UK) on an Apple Mac G4 computer. Excitation light intensity was regulated using quartz neutral density filters to reduce photo-bleaching of the fluorescent probe.

Emitted light was passed via a dichroic mirror (400 nm) through a bandpass filter (520 ± 20 nm) before being redirected to a 12 bit greyscale Hamamatsu C4880-80 camera, (Hamamatsu, Japan). A Hamamastu CCD camera controller enabled the control of exposure times and facilitated image capture. Suitable pseudo-colour palettes were overlaid onto the images to enhance visualisation. To minimise photo bleaching experiments were performed in a dark room and exposure times were kept to a minimum.

The images acquired at 350 and 380nm excitations were subjected to a ratio-metric algorithm undertaken following background light subtraction undertaken at each of the wavelengths. For each cell an area of cytoplasm was selected from which the changes in mean 350:380 ratio with time were plotted as a two dimensional graph.

RESULTS

CHAPTER 3.

SELECTION AND OPTIMISATION OF Kv7/M- CHANNEL PRIMARY ANTIBODIES

The primary objective of this study was to investigate whether Kv7/M-channels are expressed in nociceptive neurons and fibres within the peripheral nociceptive pathway, which in this study is comprised of peripheral neurons the cell bodies of which lie within the dorsal root ganglion and whose processes terminate within the skin. The dorsal root ganglion contains various neurons which can be broadly defined by their conduction velocity, from fastest to slowest Aβ, Aδ and C-fibres. It is the slower Aδ and C-fibres that are believed to be responsible for nociception.

In order to investigate the expression of Kv7/M-channels in nociceptive neurons immunofluorescent staining was used. This chapter details the optimisation of the immunofluorescent protocol, which was achieved by optimising the antibodies in neurons that express Kv7/M-channels.

3.1 Kv7.2 IS THE Kv7-CHANNEL IN THE PERIPHERAL NERVOUS SYSTEM

The Kv7/M-channel family is comprised of 5 different subunits Kv7.1-5 encoded by *KCNQ* genes *KCNQ* 1-5. The Kv7 subunits can be combined as homomers or heteromers to form a tetrameric channel. The Kv7 subunits are differentially expressed throughout the body and it is the Kv7.2- 5 subunits that are expressed neuronally (Jentsch, 2000). The endogenous M-channel is comprised of a Kv7.2/Kv7.3 heteromer which has an almost identical electrophysiological profile to native M-channels when the channel subunits were expressed in *Xenopus* oocytes (Wang et al., 1998) or Chinese hamster ovaries cells (CHO's) (Hadley et al., 2003). It appears that the expression pattern in peripheral neurons comprises either a Kv7.2/3 heteromer or a Kv7.2 homomer (Devaux et al., 2004;Schwarz et al., 2006). Therefore Kv7.2 provides the best target for immunofluorescent staining in elucidating whether Kv7/M-channels are present in nociceptive somatosensory neurons.

3.2 Kv7.2 ANTIBODY SELECTION

The structure of the Kv7/M-channel limits the availability of epitopes from which antibodies can be produced. Kv7.2 is a trans-membrane protein in which a considerable amount of the protein is contained within the plasma membrane restricting the sequence available for selection of an epitope (see figure 3.1). Also the c-terminal tail of Kv7.2 has binding sites for regulatory proteins including A-kinase anchoring protein (AKAP), phosphatidylinositol-4,5-bisphosphate (PIP2) and protein kinase C (PKC), (Delmas and Brown, 2005). Consequently the availability of epitopes on the c-terminal tail will depend on the state that the channel was in when the tissue or cell was fixed. The comparatively long length (relative to other voltage gated potassium channels) of the c-terminal tail, may lead to local protein folding which may mask possible antibody epitopes. Although all these factors are taken into account when antibodies are designed this design is based on the current structural knowledge of M-channels, which in turn is largely based on the structure of models of similar channels therefore these limitations cannot be completely negated. Thus to enhance the probability of localisation of the channel preliminary studies were conducted with more than one Kv7.2. antibody directed at different parts of the amino and carboxy tails of the Kv7.2 protein.

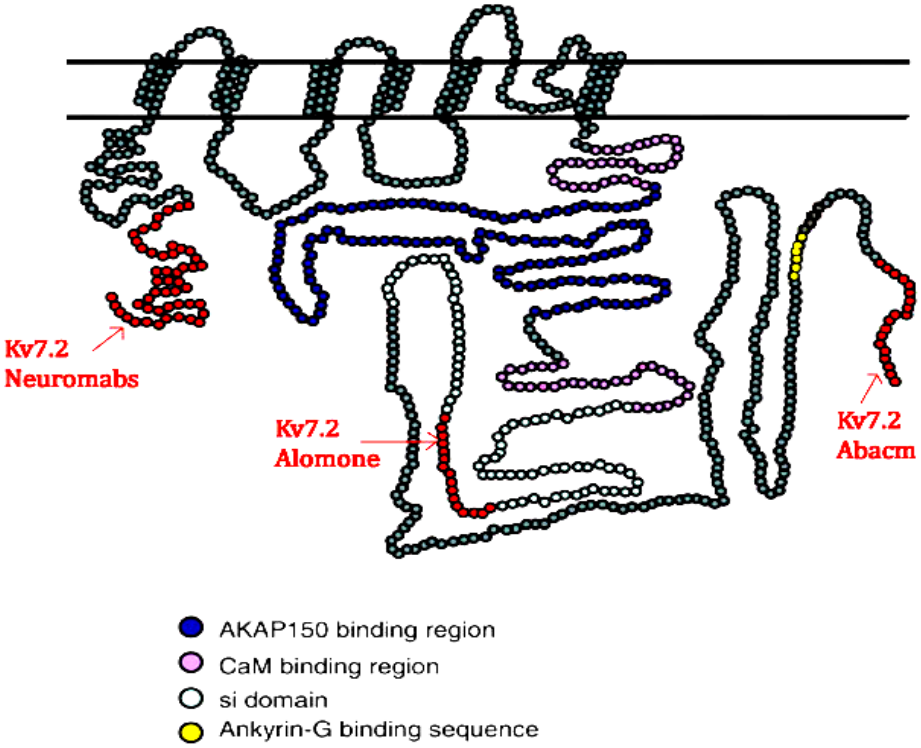

Figure 3.1: Location of Kv7.2 antibodies epitopes within the Kv7.2 protein.
The position of the epitope for each antibody within the amino acid sequence is highlighted in red (adapted from Rasmussen et al., (2007)).

The Kv7.2 antibodies utilised are detailed in table 2.1 in the methods section. Throughout the remainder of this study the antibodies are referred to as Kv7.2 followed by the company from which they were sourced i.e. Kv7.2 Alomone, Kv7.2 Abcam and Kv7.2 Neuromab. A schematic of the amino acid sequence location within the Kv7.2 structure from which antibodies are derived is given in figure 3.1. The antibodies were not all available at the initiation of this study and were integrated in the following order, Kv7.2 Alomone, Kv7.2 Abcam and Kv7.2 Neuromab.

The Kv7.2 antibodies were initially tested in cultured SCG neurons as these cells have been widely studied and are known to express functional Kv7/M-channels (Wang et al., 1998;Hadley et al., 2003).

3.3 Kv7.2 ANTIBODY OPTIMISATION

3.3.1 CONVENTIONAL IMMUNOFLUORESCENCE STAINING WITH Kv7.2 ANTIBODIES

Conventional immunofluorescence staining was initially attempted with the Kv7.2 antibodies. Conventional immunofluorescent staining involves the incubation of the tissue or cells with primary antibody followed by incubation with a secondary antibody which is conjugated to flurophore. A typical result achieved using this staining technique is shown in figure 3.2

.

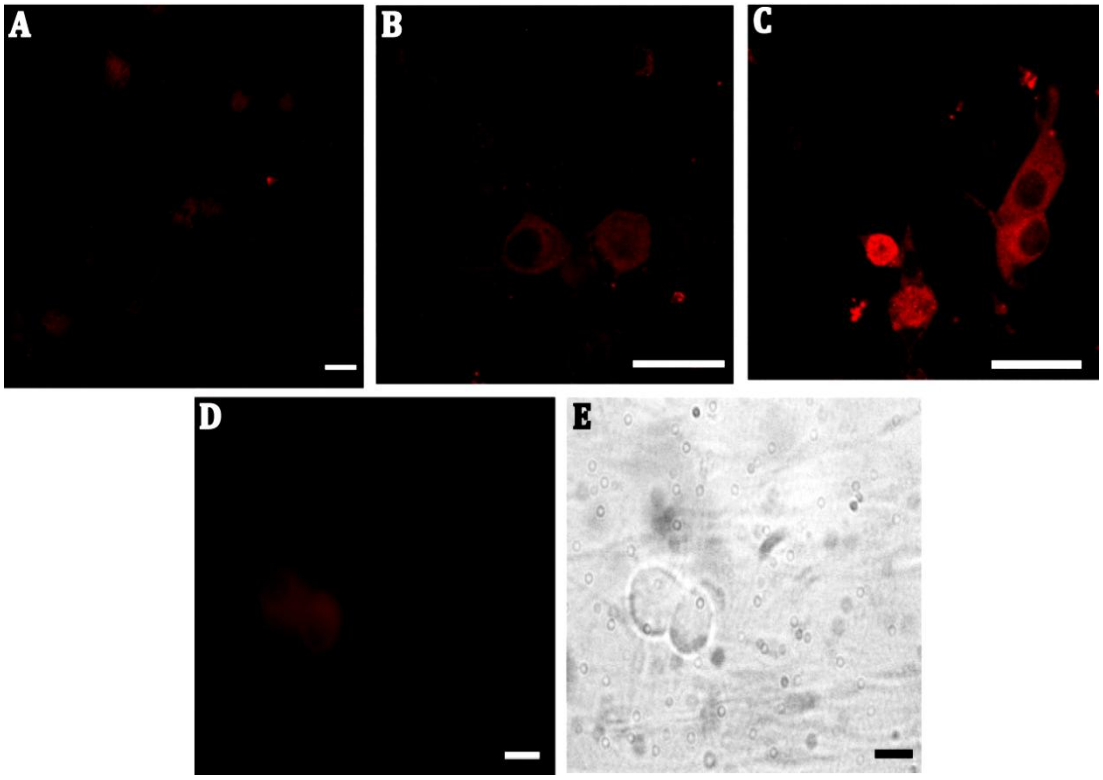

Figure 3.2: Conventional immunofluorescence staining of cultured SCG neurons with Kv7.2 antibodies and secondary antibodies*. (A) Kv7.2 Abcam with rhodamine anti-rabbit. (B) Kv7.2 Alomone with rhodamine anti-rabbit. (C) Kv7.2 Neuromabs antibody with rhodamine anti-mouse. (D) Representative secondary only immunofluorescence at maximal exposure, rhodamine anti-mouse (similar results were achieved with rhodamine anti-rabbit only). (E) Transmitted image of D. Scale bar = 20 µm*

The amount of immunoreactivity achieved with the different Kv7.2 antibodies, reflected by the brightness of the stained cells, was extremely variable; very little immunoreactivity could be detected with the polyclonal antibodies, Kv7.2 Alomone and Kv7.2 Abcam, figure 3.2 (A) and (B). This was indistinguishable from the levels achieved with the secondary antibody only staining, figure 3.2 (D). A higher level of immunoreactivity was detected with the monoclonal Kv7.2 Neuromab antibody.

To surmount the low level of immunoreactivity for Kv7.2 obtained with conventional immunofluorescent staining, particularly with the polyclonal antibodies for Kv7.2 from Alomone and Abcam, an additional amplification step was included in the protocol as described below.

3.3.2 AMPLIFICATION OF IMMUNOFLUORESCENT SIGNAL OF THE Kv7.2 ANTIBODY STAINING

Amplification of the fluorescent signal was achieved through the use of secondary antibodies to which multiple conjugated biotins are attached. Avidin, with multiple conjugated fluorphores, is then applied after the biotinylated antibody. This facilitates specific amplification of the immunofluorescent signal because biotin has a high affinity for avidin. The affinity constant of streptavidin for biotin is 10-14 M^{-1} (Green, 1990) which is indicative of a very strong bond; picomolar affinity constants are unusual for non-covalent bonds.

The immunofluorescent signal was improved by this amplification technique (see figure 3.3). Particular improvement of the signal occurred with the polyclonal Kv7. 2 antibodies, figure 3.3 (A) and (B). The staining achieved with all (primary) antibodies was clearly distinguishable from the staining with secondary antibodies alone; this suggested that the staining was due to primary antibody binding rather than non-specific binding of the secondary antibody

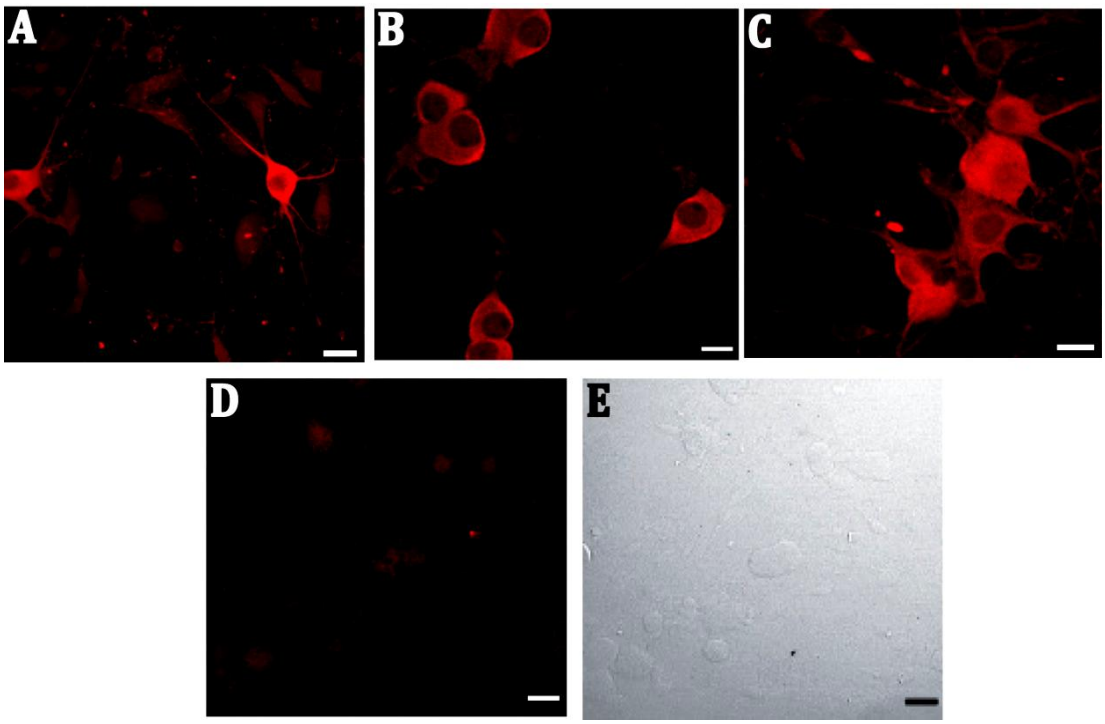

Figure 3.3 Amplification of immunofluorescent signal of Kv7.2 antibodies in cultured SCG neurons. *(A) Kv7.2 Alomone antibody with biotinylated anti-rabbit / Cy3-strepavidin. (B) Kv7.2 Abcam antibody with biotinylated anti-rabbit / Cy3-strepavidin. (C) Kv7.2 Neuromab antibody with biotinylated anti-mouse/ Cy3-strepavidin. (D) Representative secondary only immunofluorescence at maximal exposure, biotinylated anti-rabbit / Cy3-strepavidin. (similar results were achieved with biotinylated anti-mouse / Cy3-strepavidin only (E) Transmitted image of D. Scale bar = 20 µm*

3.4 CONFIRMATION OF SPECIFICITY OF THE PRIMARY ANTIBODY

The specificity of the secondary antibody was tested by the inclusion of a secondary only control in each experimental run; this consistently revealed little if any staining when imaged at the maximum exposures utilised for the corresponding primary antibody containing samples

The specificity of the primary antibody can be tested by pre-incubating the primary antibody with the epitope peptide from which the antibody was produced prior to application to the cells. Unfortunately, the only epitope peptide available was for the Kv7.2 Alomone polyclonal antibody. The epitope peptide was incubated at 10x molar excess, for 1 hour at room temperature, with the primary antibody then applied to the cells. The remainder of the protocol was carried out as previously described (see section 3.3.2).

Pre-incubation of the Kv7.2 Alomone antibody with the epitope peptide reduced the immunofluorescent signal achieved to a level no greater than that yielded by the secondary antibody alone (see figure 3.4).

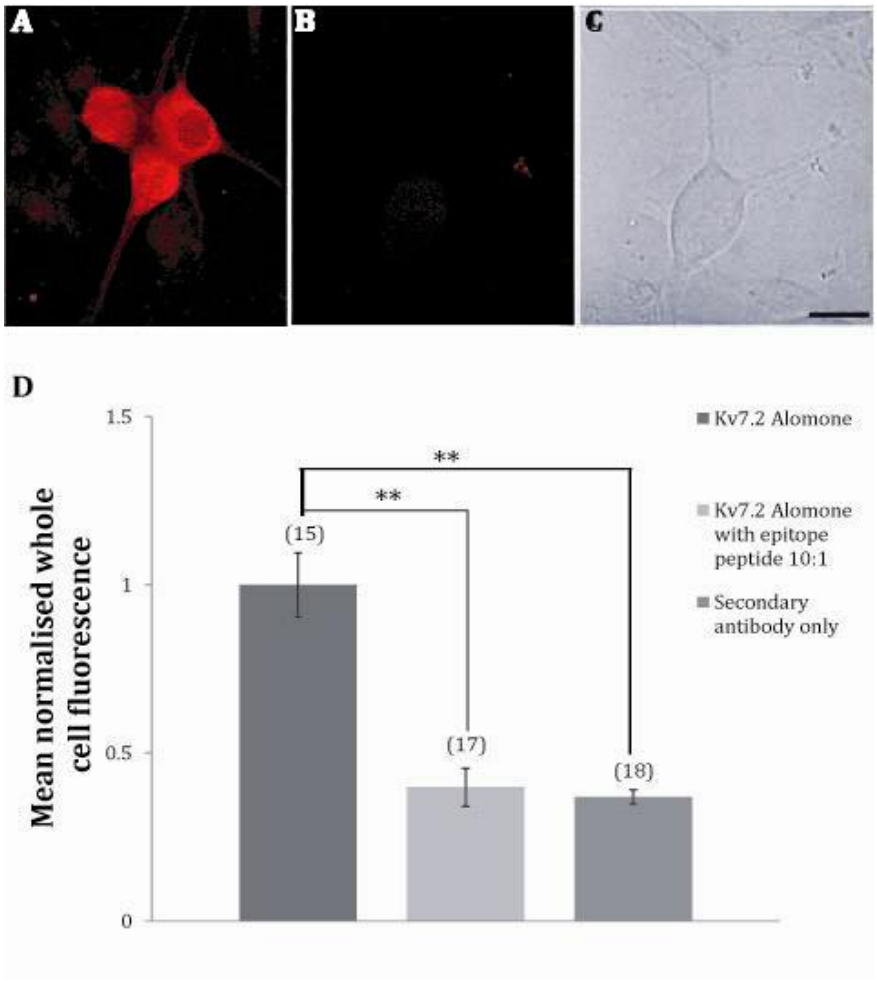

Figure 3.4: Reduction of the immunofluorescent signal following pre-incubation with the epitope peptide of the Kv7.2 Alomone antibody. *(A) Kv7.2 Alomone with biotinylated anti-rabbit / Cy3-strepavidin. (B) Epitope peptide pre incubation of Kv7.2 Alomone with biotinylated anti-rabbit / Cy3-strepavidin. (C) Transmitted light image of B. (D) Specificity test of Kv7.2 Alomone antibody. ** p <0.01 compared to immunoreactivity of Kv7.2 Alomone. Scale bar = 20 µm*

Pre-incubation of the Kv7.2 primary antibody from Alomone with its epitope led to a significant ($p<0.01$) reduction in the immunofluorescent signal. There was no significant difference in immunofluorescent signal from the cells pre-incubated with the epitope peptide and that from that of the secondary antibody only containing cells, indicating that this antibody is highly specific for the Kv7.2 protein.

3.5 CONCLUSIONS

Using the biotin/streptavidin immunofluorescent signal amplification protocol Kv7.2 protein could be detected in cultured SCG neurons using antibodies to the N-terminus (Kv7.2 Neuromab), C-terminus (Kv7.2 Abcam and Kv7.2 Alomone). The immunofluorescent signals detected with all 3 antibodies following amplification were clearly distinguishable from that detected from use of the secondary antibodies alone. Thus, all 3 antibodies were deemed suitable for use in the investigation of the expression pattern of Kv7/M-channels in peripheral nociceptive neurons.

The main determinant of which antibodies were selected for each staining run was the availability of the antibody. Ideally all three antibodies were used in a staining run and the best staining achieved (defined as the highest level of immunoreactivity with little immunoreactivity in the corresponding secondary antibody only containing control) were selected for analysis or publication in this thesis.

CHAPTER 4.

Kv7/M-CHANNEL CO-LOCALISATION WITH DRG NEURONAL-TYPE MARKERS

Several studies have shown that intaplantar injection of Kv7/M-channel modulators can alter responses to locally applied thermal or mechanical stimuli (Linley et al., 2008;Brown and Passmore, 2009;Passmore et al., 2012). The localisation of this effect suggests that functional Kv7/M-channels are located at or close to the peripheral nerve terminals where they play an important role in controlling excitability. The somatosensory sensory pathway is comprised of neurons whose cell bodies lie within the dorsal root ganglion (DRG) (for the hind paw this is specifically DRGs from spinal vertebrae L4 and L5) and whose processes terminate within the dermis and epidermis of the skin.

Previous studies have identified functional M-channels, the mRNA signal and immunoreactivity for Kv7.2, Kv7.3 and Kv7.5 in cultured DRGs (Passmore et al., 2003). However, culturing may alter protein expression from the endogenous in vivo state. Indeed the M-current increases with time in cultured SCGs from days 1-3 (Winks, 2004) and in cultured DRGs (personal communication, Dr G.M. Passmore). This implies that culturing neurons may alter Kv7 channel expression or function.

Thus, the co-localisation of the Kv7/M-channel was investigated in sliced frozen sections of rat DRGs from spinal vertebrae L4 and L5 (the spinal levels corresponding to the area of the hind paw form which recordings in Passmore et al., (2012) were fixed by perfusion and acutely isolated, using the antibodies optimised for staining for Kv7.2 as previously described in chapter 3.

4.1 Kv7.2 CO-LOCALISATION IN TRPV1-STAINING NOCICEPTIVE NEURONS

TRPV1 is a member of the transient receptor potential vanilloid family (TRPV) first cloned in 1997 and identified by its activation by capsaicin (Caterina et al., 1997). Further studies revealed that the TRPV1 channel can also be activated by noxious heat ≥42°C, acidic pH and other substances including lipoxygenase and ethanol and is primarily expressed within peripheral nociceptive neurons (Patapoutian et al., 2003). Functional Kv7/M-channels channels have been identified in capsaicin-responsive cultured DRG neurons (Passmore et al., 2003). My aim was to find out if Kv7.2 protein co-localised with TRPV1 in sliced DRGs.

Immunoreactivity for the Kv7.2 antibody co-localised with that of TRPV1 nociceptive neurons in some small/medium sized DRG neurons (see figure 4.1 and 4.2). The Kv7.2 Abcam and TRPV1 antibody also independently stained many neurons. Thus some neurons that stained for TRPV1 did not stain for Kv7.2, and conversely (see figure 4.2). Therefore, Kv7.2 maybe more ubiquitous in its expression than TRPV1 nociceptive neurons.

A histogram based on the estimate of the sizes of the visible neurons (figure 4.2 (A) was composed, the size of the neuron is considered to be an estimate as the apparent size will depend on the position of the cell within the slice. Interestingly the majority of larger and presumably myelinated neurons (<30 μm) appear to be Kv7.2 negative. Due to the thickness of the slices (40 μm) it was difficult to obtain clear transmitted images, i.e., ones from which the morphology could be differentiated. Hence, corresponding transmitted light images could not be included with every fluorescent image for the images within this staining set and others described in this chapter.

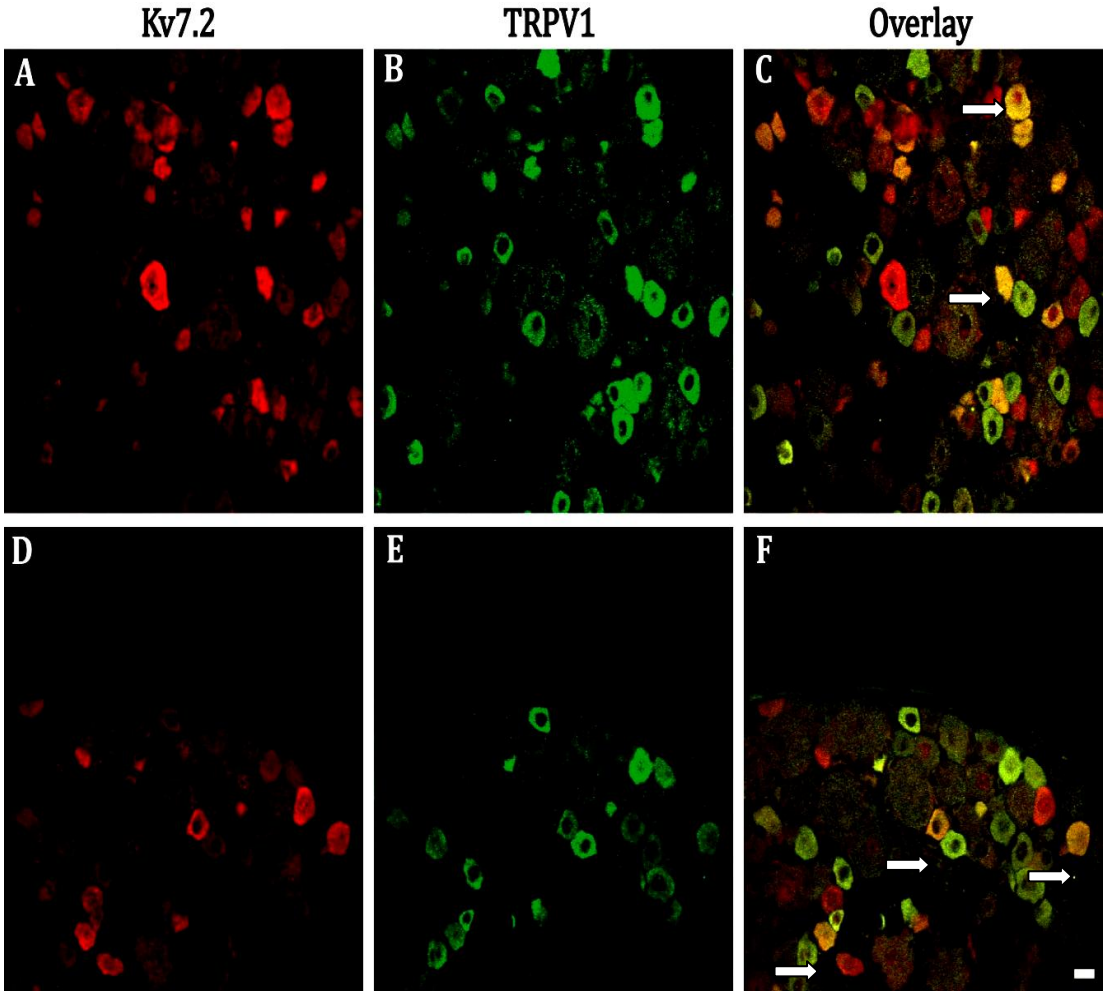

Figure 4.1: TRPV1 co-localises with Kv7.2 Abcam in a subset of neurons in the sliced DRG preparation. *(A) and (D) Kv7.2 Abcam, (B) and (E) TRPV1 (C) and (F) overlay. Arrows illustrate examples of co-localisation. Scale bar=20 µm.*

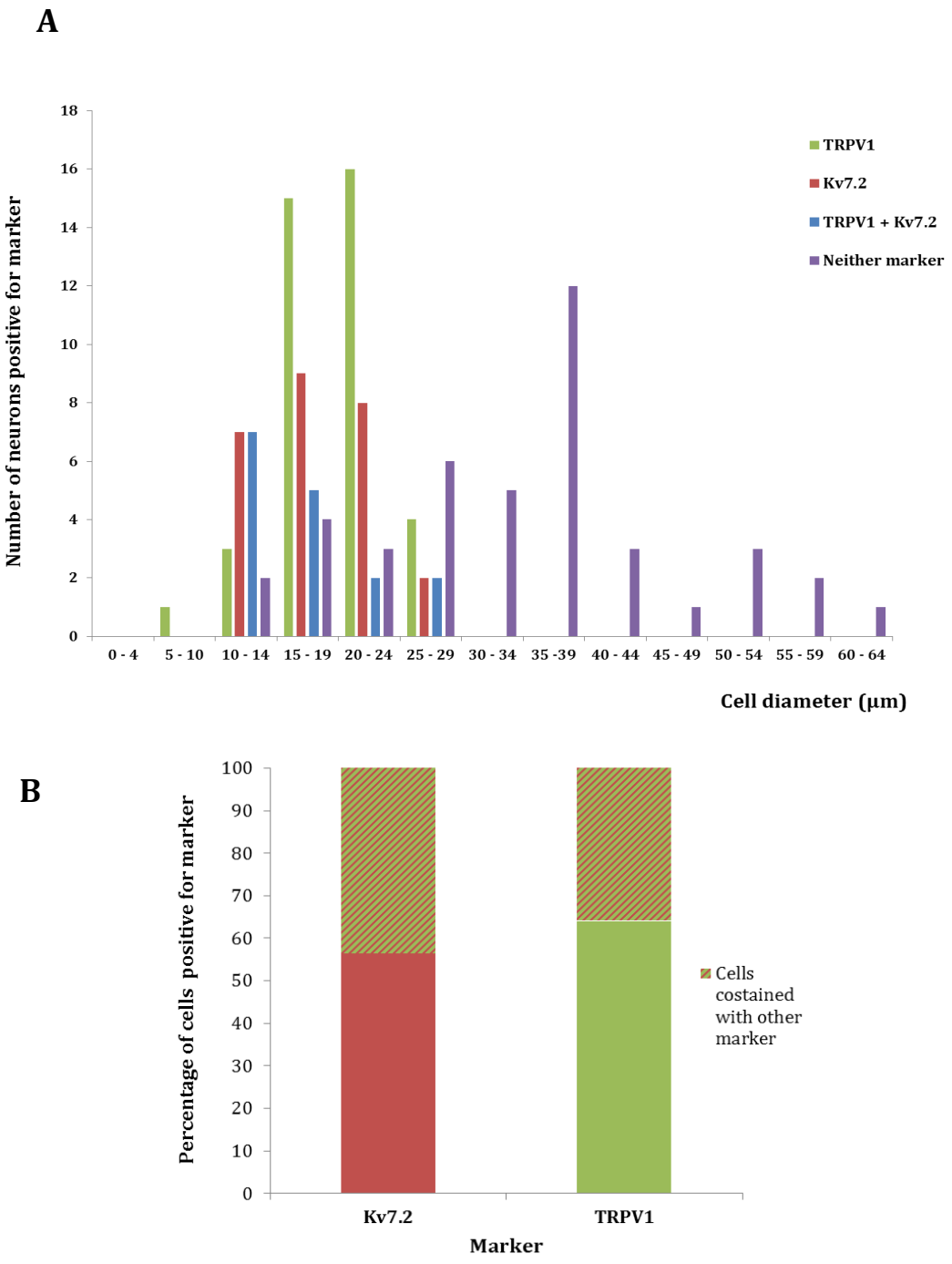

Figure 4.2: Semi- quantitation of the co-localisation of immunoreactivity of Kv7.2 with TRPV1. *(A) Histogram of the estimated size distribution of cells within sections of sliced DRG (B) Percentage of Kv7.2 or TRPV1 cells immunoreactive for the other marker, TRPV1 or Kv7.2.*

4.2 Kv7.2 CO-LOCALISATION IN IB4 POSITIVE DRG NEURONS

Small unmyelinated DRG neurons can also be defined by their differential expression of peptides (Jankowski MP, 2010). These can be broadly be defined as either non-peptide expressing isolectin B4 (IB4)-binding neurons or peptide expressing CGRP (calcitonin gene-related peptide) (Brumovsky et al., 2007).

IB4 binds to α-D-galactose carbohydrate on the cell surface and the intensity of IB4 staining is strongly associated with C-type (unmyelinated) nociceptive DRG neurons (Fang et al., 2006). My aim was to determine if Kv7.2 immunoreactivity localised in C-type nociceptive neurons of the non-peptidergic IB4 positive type.

Some of the DRGs that stained positive for IB4 also exhibited immunoreactivity for the Kv7.2 antibodies (see figure 4.3 and 4.4). Interestingly, some of the IB4-*negative* cells were also immunoreactive for Kv7.2 indicating that Kv7.2 may be present in peptidergic expressing neurons of another small DRG neuronal type. The Kv7.2 positive, IB4-*negative* cells could also be larger myelinated DRG neurons as the from the histogram of estimated size of neurons within the DRG slice (figure 4.4 (A)) there appears to be a small population of larger DRG which appear to be in the size range of Aδ neurons.

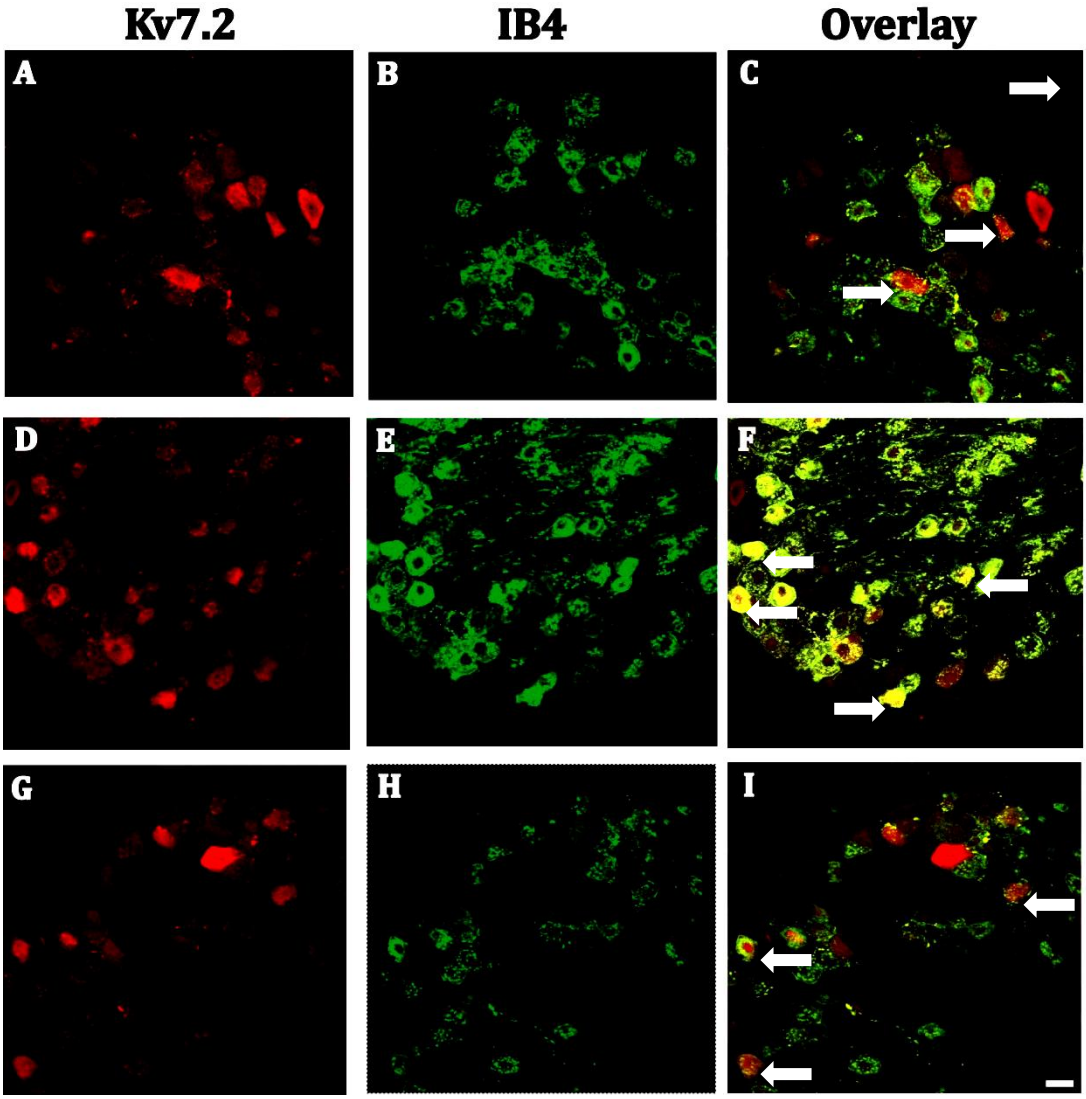

Figure 4.3: Kv7.2 Abcam co-localises with IB4 in a subset of small DRG neurons. *(A), (D) and (G) Kv7.2 Abcam, (B), (E) and (H) IB4, (C), (F) and (I) overlay. Arrows illustrate examples of co-localisation. Scale bar=20 μm*

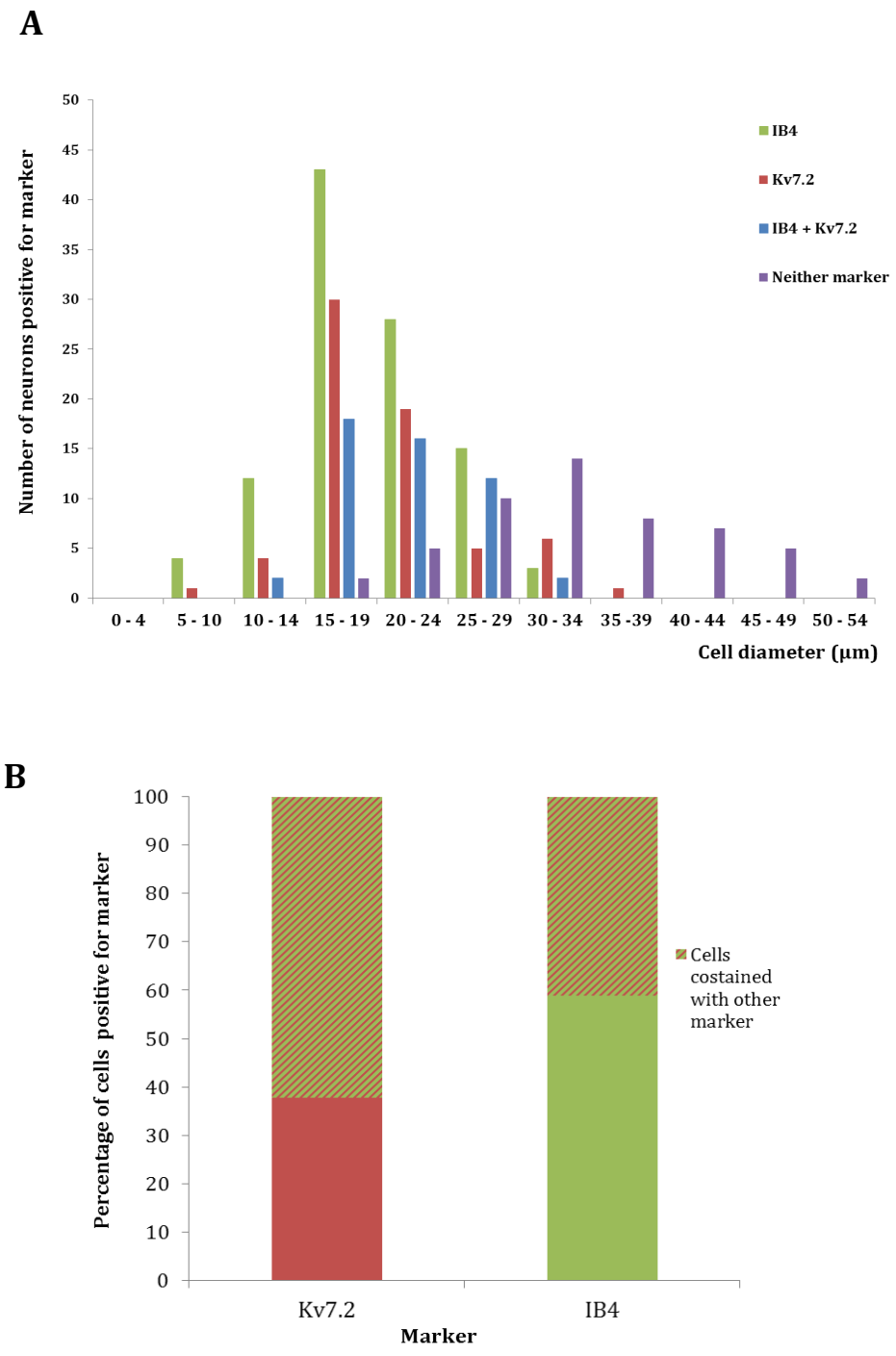

Figure 4.4: Semi- quantitation of the co-localisation of immunoreactivity of Kv7.2 with IB4. *(A) Histogram of the estimated size distribution of cells within sections of sliced DRG (B) Percentage of Kv7.2 or IB4 cells immunoreactive for the other marker, IB4 or Kv7.2.*

4.3 Kv7.2 CO-LOCALISATION IN 'MYELINATED' DRG NEURONS

DRG also contains neurons with myelinated axons: large diameter, heavily myelinated Aβ- and medium diameter, lightly myelinated Aδ- fibres. These large diameter neurons can be identified by their immunoreactivity to neurofilaments, including neurofilament NF200 (Ruscheweyh et al., 2007).

Previous results in this chapter (figure 4.4 (A)) indicate that there is a population of Kv7.2 positive neurons comparable to sizes of myelinated DRG neurons (table 1.1). It is important to further investigate this as Aδ fibres are also involved in nociceptive transmission (Woolf and Ma, 2007) and recordings from Aδ afferents in the skin nerve preparation revealed a sensitisation to noxious heat following Kv7 channel block (Passmore et al., 2012), experiments were carried out to determine if Kv7/M-channels are expressed in the corresponding DRG neurons.

There are various antibodies available to NF200 (also called neurofilament H); in this study, the monoclonal NF200 antibody clone N52 was used for immunofluorescent staining in sliced DRGs.

Co-staining Kv7.2 with NF200 revealed that some myelinated neurons contain the Kv7/M-channel protein but the majority of Kv7.2 positive neurons fall within the smaller unmyelinated neuron category (figure 4.5 and 4.6). Due to issues with resolution of the images it was difficult to obtain size estimates of neurons that were not positive for either marker. However, from the histogram of estimated neuronal size of there appears to be few if any Kv7.2 positive neurons of the larger somata Aβ neuronal type. This may explain why the majority of NF200 immunoreactive cells were not co-immunoreactive for Kv7.2 see figure 4.6 (B).

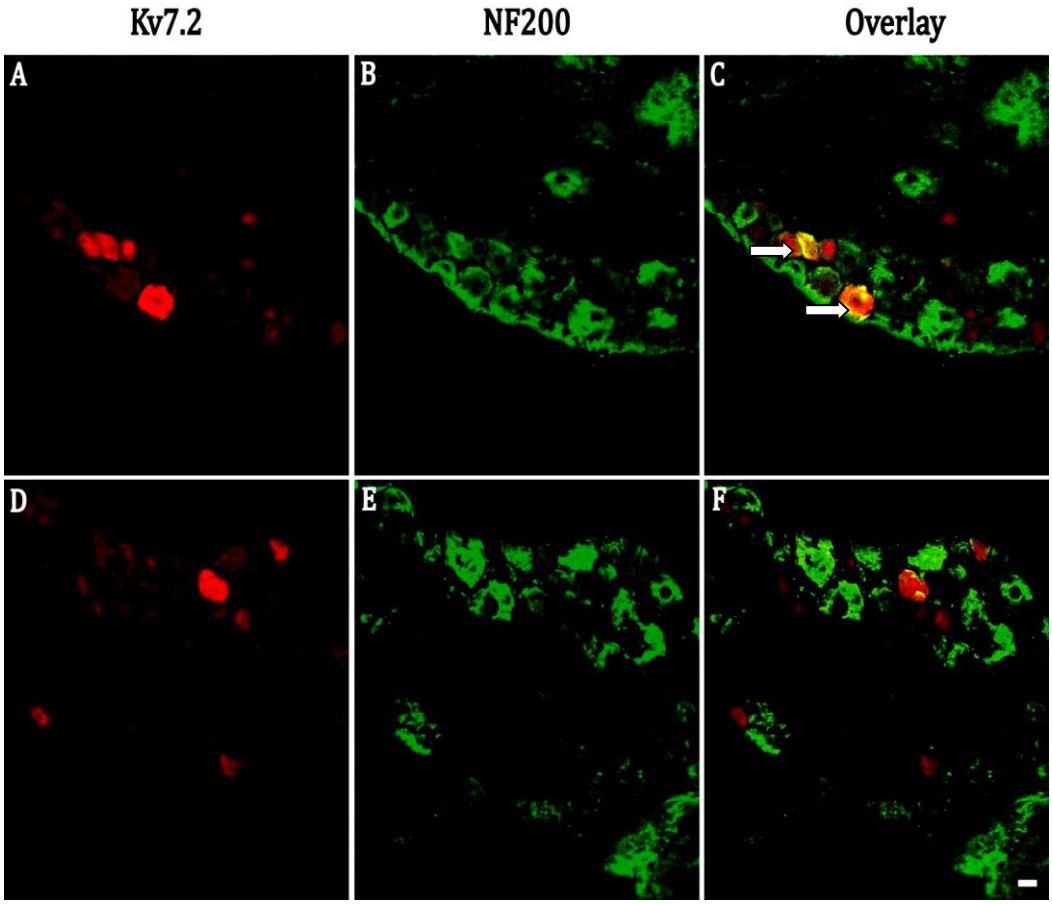

Figure 4.5: Immunoreactivity to NF 200 co-localises with Kv7.2 Abcam in a subset of large DRG neurons*. (A) and (D) Kv7.2 Abcam (B) and (E) NF 200, (C) and (F) overlay. Arrows illustrate examples of co-localisation. Scale bar=20 µm*

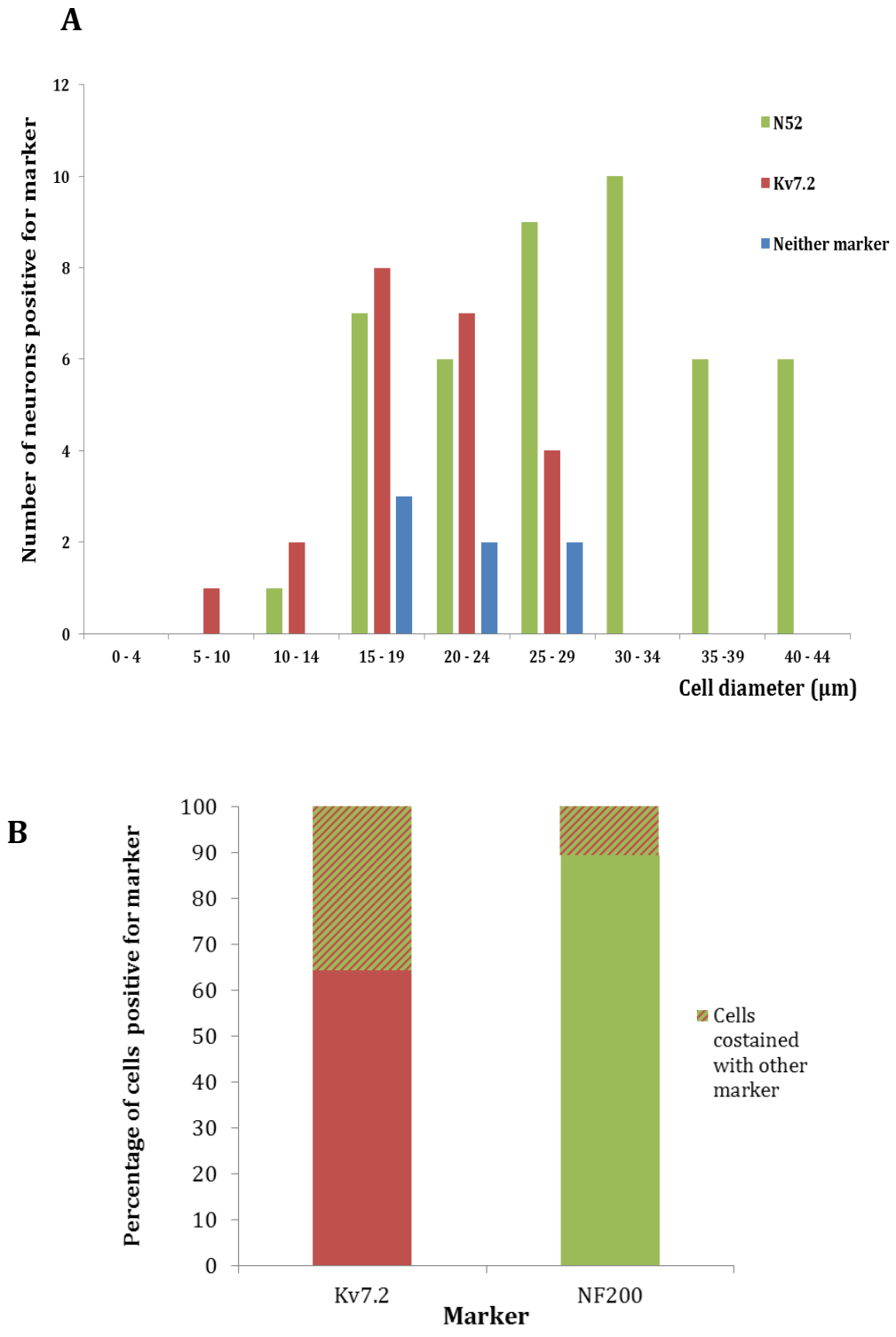

Figure 4.6: Semi- quantitation of the co-localisation of immunoreactivity of Kv7.2 with NF200. *(A) Histogram of the estimated size distribution of cells within sections of sliced DRG (B) Percentage of Kv7.2 or NF200 cells that we also immunoreactive for other marker.*

4.4 CONCLUSIONS

Kv7/M-channels have previously been described in cultured DRGs in different DRG neuron types, including TRPV1-positive (capsaicin sensitive) nociceptive neurons (Passmore et al., 2003;Linley et al., 2008). Culturing DRG may alter ion channel expression; examining expression in acutely isolated DRG slices may provide a more accurate reflection of localisation.

The results in this chapter reveal that Kv7.2 is mainly expressed in small unmyelinated C-type nociceptive DRG neurons, as defined by somatic immunoreactivity to IB4 and TRPV1. The Kv7.2 antibody also stained other DRG neuron types including the somata of NF200 positive myelinated fibre neurons, some of which maybe nociceptive Aδ DRG neurons. After the conclusion of these experiments a similar size distribution of Kv7.2 positive neurons and similar expression patterns of Kv7.2 coimmunolocalisation with the neuronal markers was demonstrated in a paper published by Rose et al., (2011).

Immunoreactivity to Kv7.2 occurred in about half of the population of the small neuronal markers, TRPV1 and IB4, but was not exclusive to either maker. The NF200 antibody co-localised less frequently with Kv7.2 antibody compared to the small nociceptive markers. This observation is likely to be due to preferential expression of Kv7.2 within the Aδ-type DRGs as the size of these neurons correlates with the estimated size of the larger Kv7 positive neurons., this could not be categorically confirmed as the diameters of neurons measured in this study are only estimates as the apparent size the neuron depends on the position within the slice when the DRG slice was taken. The expression of the Kv7/M-channel in Aδ provides further support for a role of these channels in this nerve fibre types previously demonstrated through *in vivo* studies where Aδ fibres have been demonstrated to respond to Kv7/M-channel modulators in response to noxious heat (Passmore et al., 2012).

The results obtained in this study differ from the staining and electrophysiological evidence obtained from cultured DRG neurons (Passmore et al., 2003) where the Kv7/M-channel is present in all DRG neuron types. This difference may be due to an artefact of culturing or due to the presence of other Kv7/M-channel subunits e.g. Kv7.3 and Kv7.5 expressed in the DRG, which was not investigated in this study.

The Kv7/channel is associated with the control of neuronal excitability. In general under normal conditions repetitive discharges from DRGs do not occur, but can occur after an insult. For example, nerve ligation can lead to ectopic firing of neurons in the DRG (Liu et al., 2000); this might be a consequence of Kv7/M-channel reduction since peripheral nerve injury also reduces Kv7.2 mRNA levels in ipsilateral DRGs (Rose et al., 2011) and transcriptional repression of Kv7.2 expression increase DRG neuron excitability (Mucha et al., 2010). Further, the ability of DRG neurons to generate repetitive discharges is enhanced by the acute inhibition of M-current by M-channel blockers (Passmore et al., 2003;(Mucha et al., 2010)) or by inflammatory mediators ((Crozier et al., 2007); Liu et al., 2010;(Linley et al., 2012)). Thus, Kv7/M-channels appear normally to play a prominent role in dampening the excitability of nociceptive DRG neurons, and their decreased expression linked to pain and pain pathology. Further, the broad distribution of Kv7.2 immunoreactivity in DRG neurons also suggests that they may play a part in regulating other forms of somatosensory transmission such as tactile mechanotransmission (Heidenreich et al., 2011).

CHAPTER 5.

Kv7.2 IMMUNOREACTIVITY IN PERIPHERAL TERMINALS WITHIN THE SKIN

The results from the previous chapter indicate that the Kv7/M-channel subunit Kv7.2 is present in the cell bodies of DRG corresponding to the peripheral nerve fibres that terminate in the skin, specifically the hind paw. Sensory nerve recordings from the terminal endings of these fibres using the isolated rat skin-nerve preparation (Passmore et al., 2012) have shown that local application of the Kv7/M-channel enhancer retigabine and the blocker XE991 to the skin of the rat's paw respectively reduced and enhanced afferent nerve firing induced by local application of noxious heat. This suggests that Kv7/M-channels might be present within the nerve terminal endings that lie within the skin, or possibly in other tissues contributing to the overall sensory nerve response to heat. To assess this, immunohistochemical analysis of skin slices was performed using hairy skin as employed for the electrophysiological recordings.

5.1 STRUCTURE OF MAMMALIAN HAIRY SKIN

Mammalian skin can be separated into two main types: hairy and plantar. As the names suggest, these are differentiated primarily by the presence of hair follicles. The skin can then be further differentiated into two structural layers, the dermis and epidermis (see figure 5.1). The images obtained within this chapter were taken in close proximity to the epidermal border with the dermis, or near to the epidermal layer surrounding the hair follicle within the dermis.

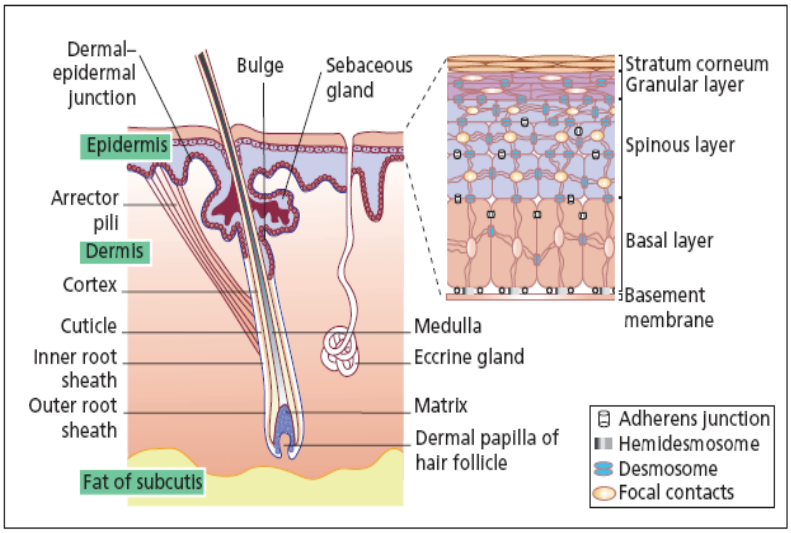

Figure 5.1: The structure of hairy skin *(McGarth et al., 2012).*

5.2 Kv7.2 IMMUNOREACTIVITY WITHIN THE EPIDERMIS

Initial staining of sliced hairy skin revealed immunoreactivity to Kv7.2 Alomone which appears confined to a region corresponding to the epidermis (figure. 5.2). This cellular epidermal staining is investigated further in chapter 6. Obvious staining of nerve fibres could not be discerned. This is probably due to the small size of the free nerve endings (≥0.2 µm diameter (Schalow, 2005)), coupled with the thickness of the slice (40 µm), which made it difficult to discriminate actual staining from the background. Also the staining of these nerve endings might be punctate rather than diffusely spread along the axon. Hence, the skin was co-stained with the markers previously used with the DRG slices and with other markers of peripheral neurons and their axons.

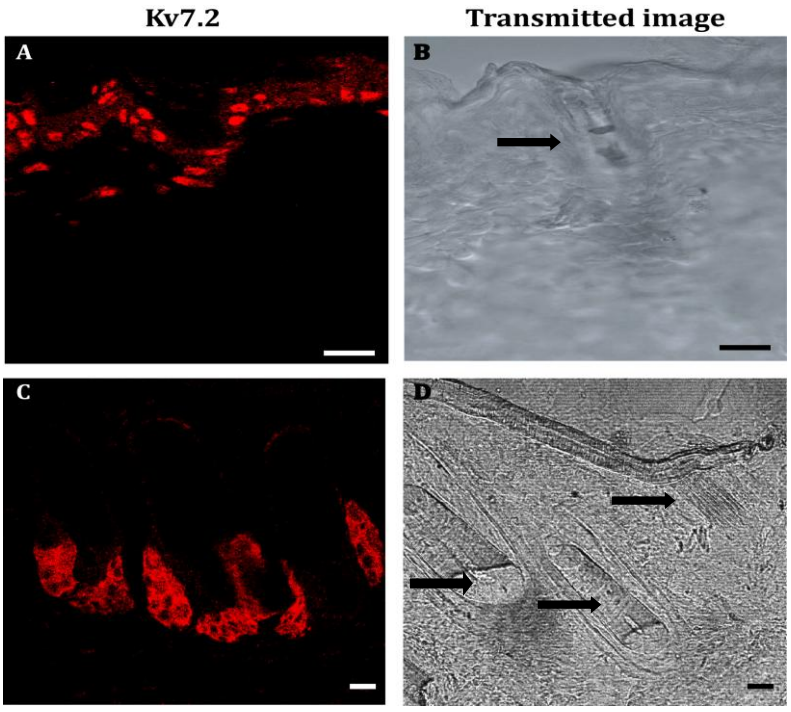

Figure 5.2: Staining within keratinocytes with the Kv7.2 antibodies. *(A): Keratinocytes immunoreactive to Kv7.2 Alomone within the outer epidermal layer. (B): transmitted light image of (A). (C): Keratinocytes immunoreactive to Kv7.2 Abcam within the epidermal layer surrounding the hair follicle. (D): transmitted light image of (C). The arrows in (B) and (D) point to hair follicles. Scale bar 40µm*

5.3 Kv7.2 IMMUNOREACTIVITY IN HAIRY SKIN WITH A NEURONAL MARKER (NON-SPECIFIC)

Neuron specific beta III tubulin (an isoform of tubulin that is only expressed in neuronal tissue) is a broad spectrum neuronal marker (Alexander et al., 1991). Co-staining with antibodies to tubulin beta III and to the Kv7.2 channel demonstrated a degree of co-localisation, implying that Kv7.2 is present within nerve endings in the skin. This co-localisation was predominantly found in the nerves that are in close proximity to the hair follicle and in the epidermal tissue that surrounds the hair follicle, as illustrated in figure 5.3. Beta III tubulin immunoreactive fibres are seen to co-localise with Kv7.2 Abcam immunoreactivity near to where a section of the epidermis envelops the hair follicle, as denoted by the arrow head.

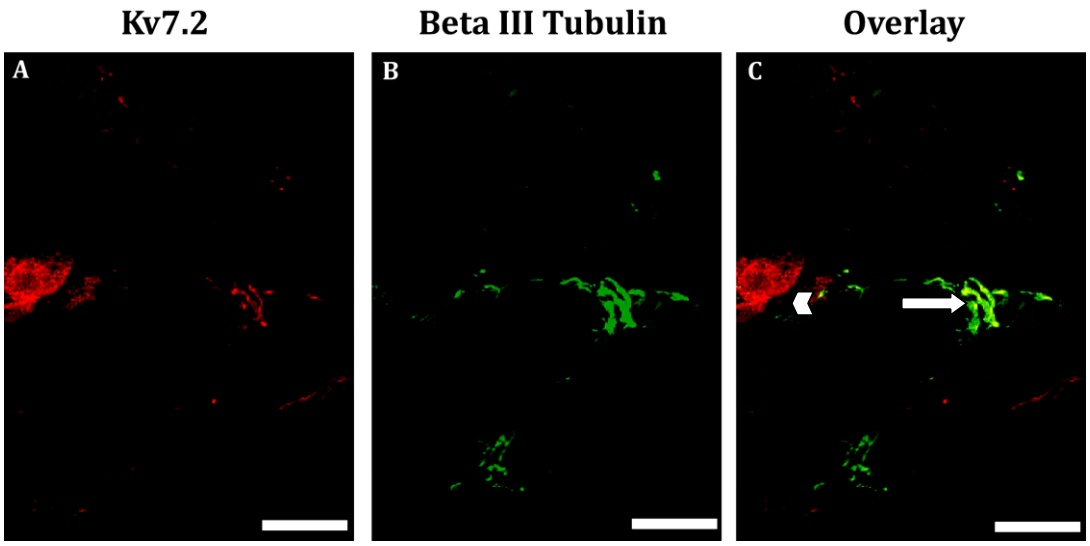

Figure 5.3: Kv7.2 immunoreactivity is present in neurons within hairy skin as denoted by Beta III immunoreactivity. *(A) Kv7.2 Abcam (B): Beta III tubulin (C) Overlay of (A) and (B). The arrow points areas of co-localisation and the chevron to possible epidermal tissue surrounding a hair follicle. Scale bar 40μm*

5.4 Kv7.2 IMMUNOREACTIVITY IN HAIRY SKIN WITH TRPV1

The co-localisation of Kv7.2 with beta III tubulin, as shown in figure 5.3, suggests that Kv7.2 channels are expressed in the peripheral neurons that innervate the skin. As shown previously (section 4.1) TRPV1, a marker of nociceptive neurons, co-localised with Kv7.2 in some neurones in sliced DRG. The question is whether this co-localisation of expression is confined to the soma of DRG neurons or whether Kv7.2 and TRPV1 also co-localise at the peripheral terminals.

The staining of TRPV1 nociceptive fibres revealed co-localisation with the Kv7.2 Neuromab antibody, indicating that this M-channel subunit is not only present in nociceptive neuron somata but also in the peripheral terminals (figure 5.4). Given the diameter of the fibres in figure 5.4 they could conceivably be single fibres from C-type nociceptors but more likely they are comprised of bundles of the smallest fibres.

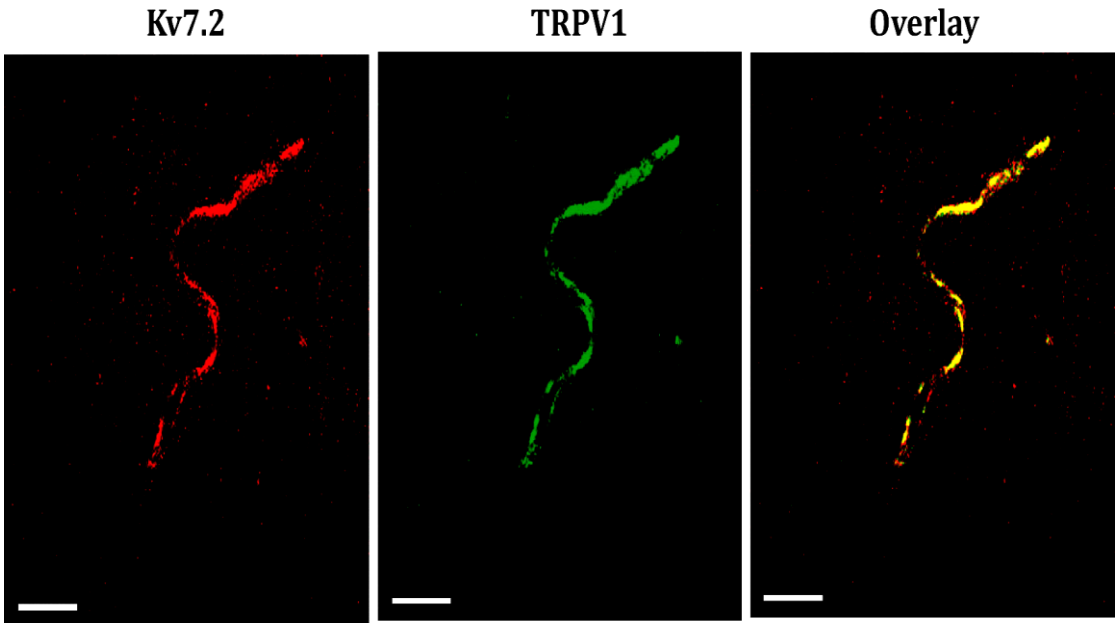

Figure 5.4: Kv7.2 immunoreactivity is present in TRPV1 expressing nociceptive neurons within hairy skin *(A): Kv7.2 Neuromab, (B): TRPV1, (C): Overlay of (A) and (B). These images were obtained near the dermal-epidermal border. Scale: 20μm*

5.5 Kv7.2 IMMUNOREACTIVITY IN UNMYELINATED PERIPHERAL FIBRES IN HAIRY SKIN

TRPV1 is present in some but not all unmyelinated fibres. To identify the presence of K_V7/M-channels in other unmyelinated populations' peripheral neuronal fibres were co-stained with an antibody to peripherin. Peripherin is a marker of intermediate neuronal filaments that is specifically expressed in unmyelinated fibres (Fornaro et al., 2008). The results from co-staining skin slices with peripherin and Kv7.2 Neuromab (figure 5.5) revealed co-localisation of immunoreactivity in some but not all unmyelinated fibres. This concurs with the somatic unmyelinated DRG neuron maker IB4 staining observed in the sliced DRGs in the previous chapter (figure 4.3), where some, but not all, IB4 positive unmyelinated neurons co-stained with Kv7.2. Therefore Kv7.2 appears to be expressed in only some peripheral unmyelinated fibres.

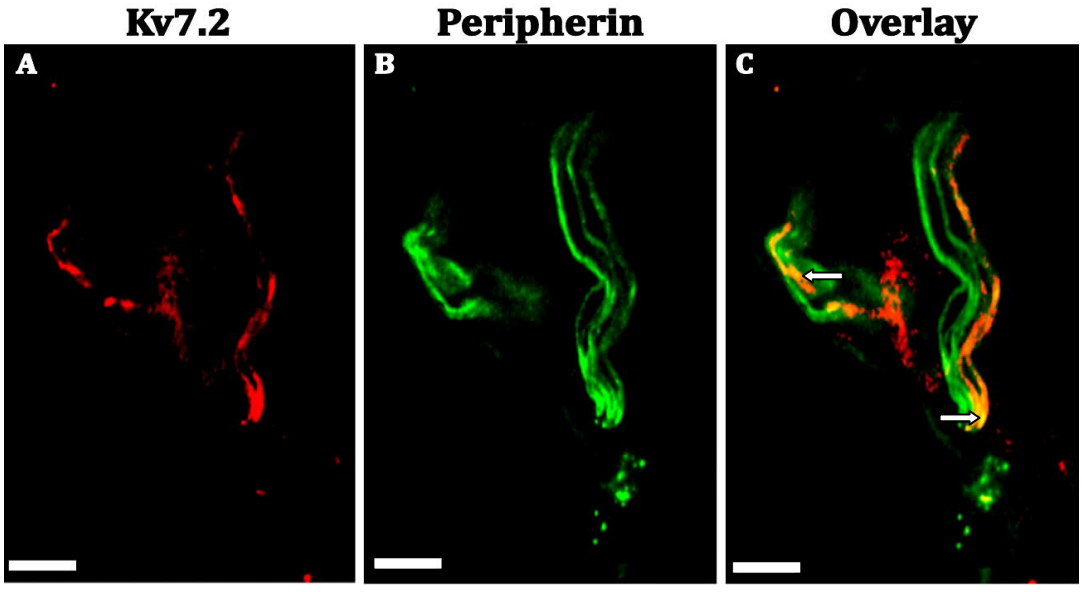

Figure 5.5: Kv7.2 immunoreactivity is present in peripherin-expressing unmyelinated neurons within hairy skin *(A): Kv7.2 Neuromab, (B): peripherin, (C): Overlay of (A) and (B). The arrow points to co-localisation. Scale: 10μm*

5.6 Kv7.2 IMMUNOREACTIVITY IN MYELINATED PERIPHERAL FIBRES IN HAIRY SKIN

Kv7.2 immunoreactivity in sliced DRG also co-localised with a marker of myelinated neurons, NF200. Since some of these fibres are likley to be of the Aδ type which are nociceptive and furthermore as Aδ fibre responses to noxious heat are facilitated by the M-channel modulator XE991 (Passmore et al., 2012) it was of interest to investigate whether terminals of these myelinated fibres also express Kv7.2. For this I again used NF200 as the A-fibre marker (De Schepper et al., 2008). As was observed in DRG slices (figure. 4.5), Kv7.2 staining was observed in some, but not all, NF200-staining fibres (figure 5.6). Whether this indicates localisation in Aδ fibres and not in other myelinated fibres cannot be determined.

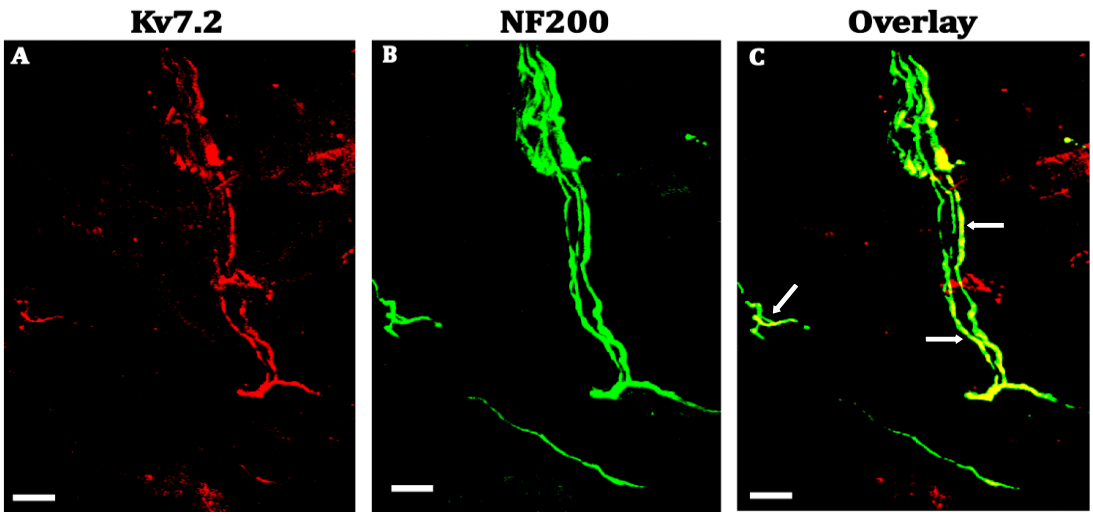

Figure 5.6: Kv7.2 immunoreactivity is present in neurofilament H (NF200) expressing myelinated fibres within hairy skin *(A): Kv7.2 Neuromab, (B): Neurofilament H (NF200), (C): Overlay of (A) and (B). These images were obtained near the dermal-epidermal border. The arrows points to co-localisation. Scale: 20µm*

5.7 Kv7.2 IMMUNOREACTIVITY IN SYMPATHETIC PERIPHERAL FIBRES IN HAIRY SKIN

Sympathetic fibres also innervate the skin, where they are important in vasomotor control. Rat sympathetic neurons possess large M-currents, and the M-channel subunits Kv7.2, 7.3 and 7.5 are expressed in sympathetic neuron somata (Hadley et al., 2003).

To investigate whether the Kv7/M-channel is also present at these terminals within the skin sliced cryosections of hairy skin were co-stained for immunoreactivity for Kv7.2 and tyrosine hydroxylase, a marker for sympathetic neurons, was observed in some nerve bundles. Kv7.2 protein was found in some but not all sympathetic fibres (see figure 5.7) suggesting that Kv7/M-channels are not only present in the somata of sympathetic neurons but also at their peripheral terminals.

Previous studies have also shown that functional Kv7/M-channels are present at sympathetic nerve endings. Retigabine, the M-channel enhancer, has been shown to block nicotinic stimulation of muscle cells in co-culture with sympathetic neurons (Zaika et al., 2011b). Further evidence come from the ability of the Kv7/M-channel to modulate neurotransmitter release from processes of isolated cultured sympathetic neurons (Lechner et al., 2003;Hernandez et al., 2008).

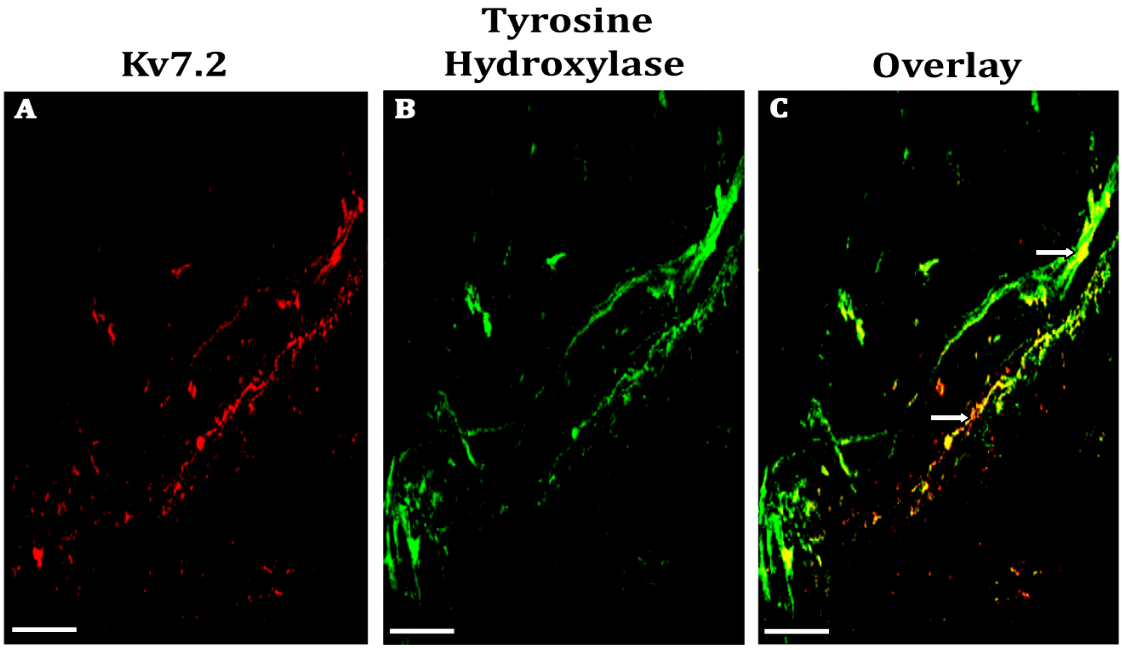

Figure 5.7: Kv7.2 immunoreactivity is present in tyrosine hydroxylase expressing neurons within hairy skin *(A): Kv7.2 Neuromab, (B): tyrosine hydroxylase, (C): Overlay of (A) and (B). These images were obtained near the dermal- epidermal border. Scale: 40µm*

5.8 CONCLUSIONS

In summary the results from this chapter indicate that Kv7/M-channels have broad expression in many cutaneous neuronal fibres including TRPV1-positive, myelinated and unmyelinated neurons, and that this expression is not confined to the soma of the neuron but is also present within the cutaneous peripheral terminals and in sympathetic nerve endings.

The presence of Kv7/M-channels within the peripheral terminals including fibres which are of nociceptive origin suggests that these channels may have an important role in this regulating the initial stages of nociceptive transduction and action potential initiation. Indeed, results from previous studies suggest effects of M-channel modulators on the afferent discharges from Aδ fibres peripheral nerve terminals in response to noxious heat in the isolated rat skin-nerve preparation(Passmore et al., 2012) , and also intra-plantar injections of

XE991 altered both WDR cell responses (particularly Aδ fibres response) to noxious heat (Passmore et al., 2012) and induced nocifensive behaviour (increased latency of hind paw withdrawal) to thermal stimuli in the rat paw (Linley et al., 2008).

These results do not address the possibility of other Kv7 subunits being present at the peripheral terminals. Thus, recent immunohistological evidence has indicated that Kv7.5 is the principal subunit of the Kv7/M-channel in sciatic C-fibres (King and Scherer, 2012), while Kv7.4 is the main functional subunit in dermal mechanoreceptors (Heidenreich et al., 2012). Nevertheless, Kv7.2 is the dominant subunit of the Kv7/M-channel in nodes of Ranvier in the sciatic nerve (Schwarz et al., 2006), and in baroceptors (Wladyka et al., 2008). Further, the reduced expression of Kv7.2, after partial sciatic nerve ligation, accompanied by an enhanced sensitivity to thermal hyperalgesia, coupled with the frequently-reported analgesic effect of M-channel enhancers in animals and man (Wickenden and McNaughton-Smith, 2009) provides further evidence for an important role of M-channels in controlling pain.

The epidermal staining does raise the question whether Kv7 modulators work solely by interacting with Kv7/M-channels in the peripheral nerve terminals themselves, or also by acting on the Kv7/M-channel within non-neural elements within the skin to modify the intradermal release of nociceptive mediators this would require the Kv7/ M-channels localised within the non-neural epidermal cells to be functionally involved in regulating activity. This is addressed in the final results chapter of this thesis.

CHAPTER 6.

LOCALISATION AND FUNCTION OF Kv7.2/M- CHANNELS IN UNMYELINATED FIBRES OF THE VAGUS NERVE

The previous chapter provides evidence for the expression of Kv7/M-channel in the cell bodies and peripheral terminals of nociceptive neurones. The question remains: are these channels present at these locations alone or are Kv7/M-channels present along the unmyelinated axons, where channels may have function in the transmission nociceptive signals. Prior to the initiation of this study Kv7.2 had been co-localised at axon initial segment and the nodes of Ranvier along myelinated peripheral axons (Devaux et al., 2004;Schwarz et al., 2006) but their presence along nociceptor axons that are unmyelinated (or only lightly myelinated) had yet to be elucidated. To investigate these immunofluorescent and electrophysiological techniques were utilised to study unmyelinated fibres in the vagus nerve.

6.1 THE VAGUS NERVE A MODEL FOR STUDYING UNMYELINATED NERVES

The vagus nerve is the tenth, often referred to as cranial nerve X, and longest cranial nerve. Originating in the medulla, the vagus nerve branches to innervate the heart and other internal organs (see figure 6.1).

The vagus nerve is made up of sensory and motor fibres that serve several important roles: the parasympathetic control of visceral organs and the relay of sensory information from these organs to the brain. Approximately 80-90% of the nerve fibres in the vagus nerve are sensory nerves. The majority (~80%) of vagal fibres in the rat are unmyelinated C-fibres (Soltanpour and Santer, 1996); an electron micrograph illustrating this is shown in figure 6.1(B). Thus, the vagus is convenient for studying Kv7 channel localisation and function in mammalian unmyelinated fibres.

A

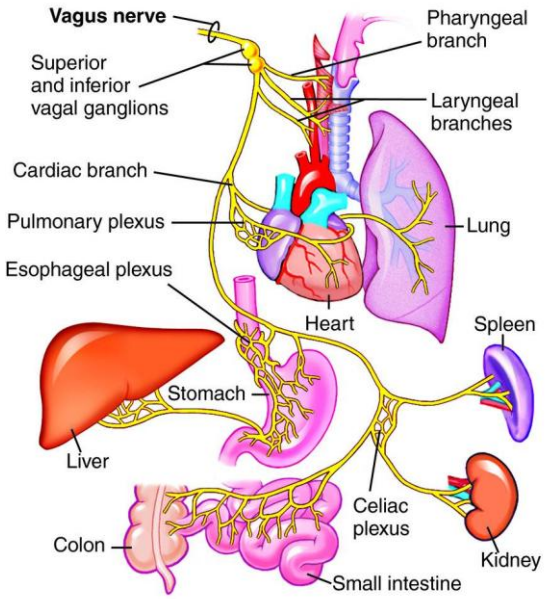

B

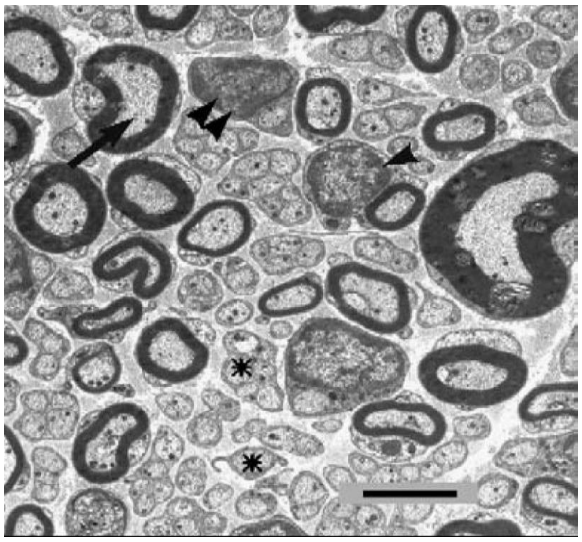

Figure 6.1: The vagus nerve *(A) The pathway of the vagus nerve (Anderson et al., 1998). (B) Electron micrograph of a cross section of the rat vagus nerve; large myelinated axons (arrow), small unmyelinated axons (asterisks), myelinating (single arrowheads) and non-myelinating (double arrowheads) Schwann cells . Scale 5µm.(Pfeiffer-Guglielmi et al., 2006)*

6.2 Kv7.2 IMMUNOREACTIVITY ALONG UNMYELINATED VAGAL FIBRES

The acutely isolated and fixed vagus nerve was teased and co-stained with antibodies for Kv7.2 Abcam and peripherin, a marker for unmyelinated neurons. Substantial co-localisation of Kv7.2 with peripherin was observed (figure 6.2), indicating the abundant presence of the Kv7.2 M-channel subunit along the length of vagal unmyelinated fibres.

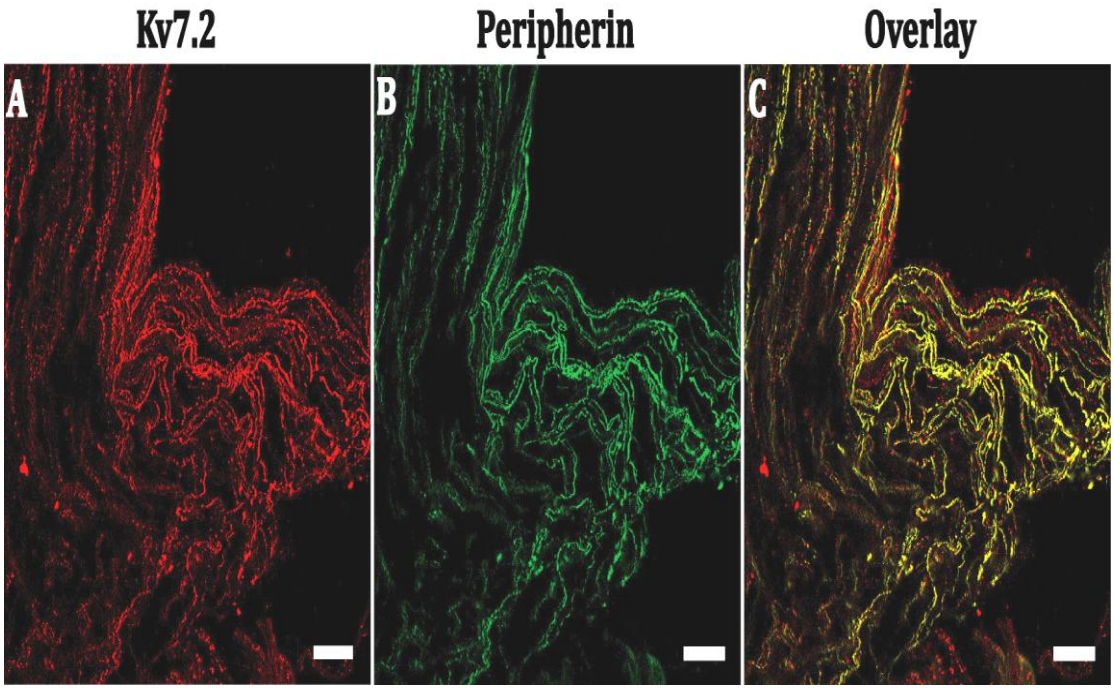

Figure 6.2: The Kv7.2 subunit is present in unmyelinated fibres of the vagus nerve. *Confocal image of immunofluorescent staining reveals co-localisation of Kv7.2 with peripherin in a teased vagus nerve (A.) Kv7.2 Abcam antibody. (B.) Peripherin antibody. (C.) Overlay of A and B. Scale = 10 µm*

6.3 C-FIBRE/UNMYELINATED NERVE COMPOUND ACTION POTENTIALS (CAPS) IN THE VAGUS NERVE.

The role of M-currents in C-fibres was inferred from the action of M-channel blockers and enhancers on compound C-fibres action potentials and surface demarcation potentials, using extracellular recording from the isolated vagus trunk as described by (Marsh et al., 1987) (see Methods). Some of the results described in this section were obtained in collaboration with Vanessa Keasbury. Her contribution is indicated with an asterisk (*) at the appropriate points below.

Compound action potentials were recorded using stimuli of 1ms duration; voltage was optimised for C-fibre recording. The C-fibre CAP could be distinguished from the A-fibre response by (a) its longer latency (reflecting slower conduction from the point of stimulation to the point of recording, figure 6.3A; see Methods, figure 2.4(A)), and (B) its lower excitability as indicated by the strength-duration curve in figure 6.3 (B).

In this study, the conduction velocity of rat vagal C-fibres was estimated as 0.6 ms-1; this is within the range ($\leq$2 ms^{-1}) used to classify C-fibres (Harper and Lawson, 1985) and is similar to the conduction velocity of 0.9ms^{-1} previously obtained using this experimental arrangement (Marsh et al., 1987). For further experimentation, the stimulus was optimised for C-fibre responses by increasing the stimulus strength until the C-fibre CAP reached its maximum, then using a constant stimulus of 1.5 times this value.

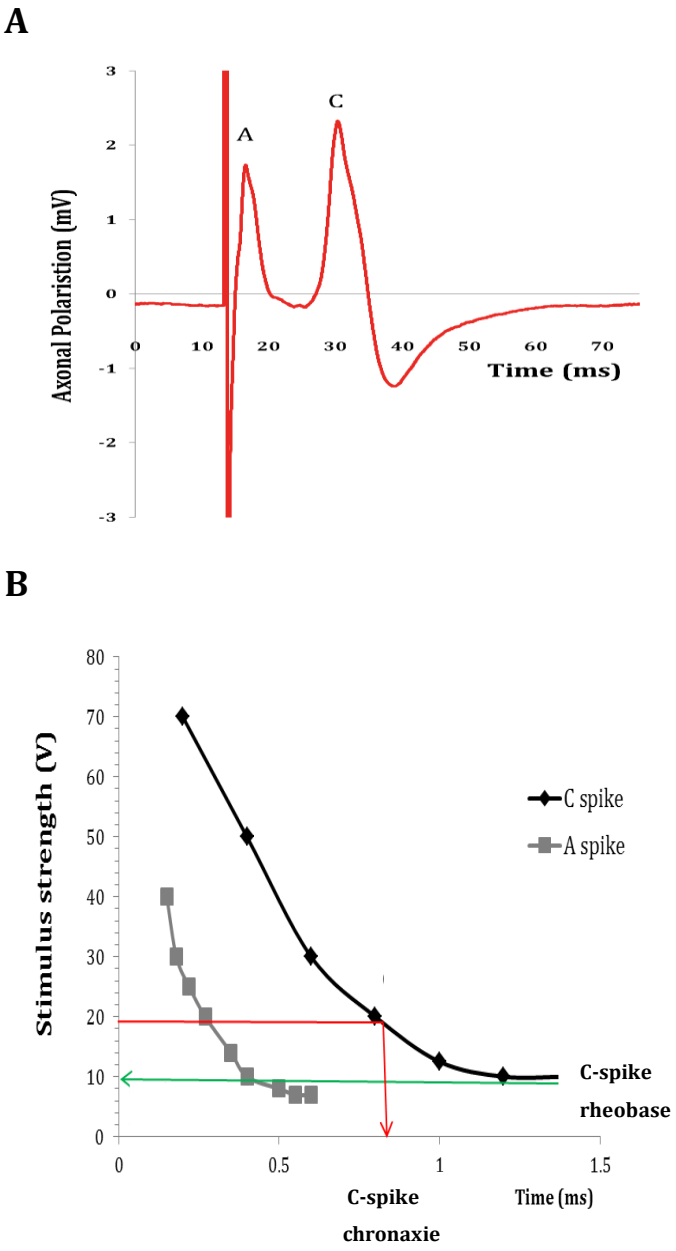

Figure 6.3: Differentiation of C-fibre (unmyelinated) CAP. *(A) A-fibre and C-fibre CAPs generated by a 1 ms, 10-30 V stimulus. (B) plot of stimulus strength against stimulus duration. Rheobase – minimum strength required to evoke a response; chronaxie =minimum duration required for the C-spike the rheobase is 9 V and the chronaxie is 0.75 ms*

6.4 EFFECTS OF Kv7/M-CHANNEL MODULATORS ON UNMYELINATED FIBRES

To test for the presence of functional M-channels in the unmyelinated fibres of the vagus nerve the effects of the M-channel 'enhancer' retigabine and of two M-channel blockers XE991 and linopirdine (see Introduction), on C-fibre spikes and vagus nerve surface demarcation potentials were determined.

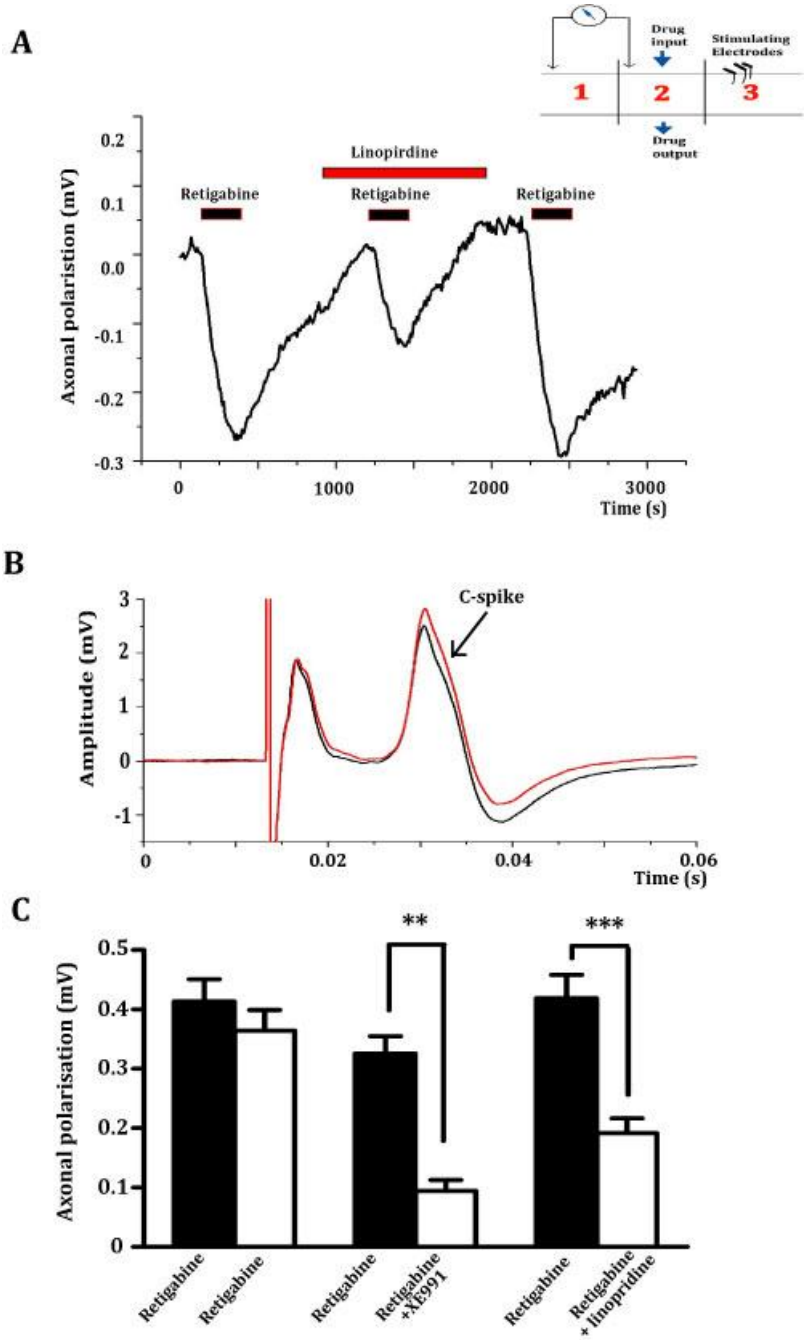

Figure 6.4: Retigabine induced a linopirdine–sensitive hyperpolarisation of the rat vagus nerve with concomitant changes in the compound action potential generated by the unmyelinated axons (C-spike). *(**A**). 10 μM retigabine applied for 3 min induced a prolonged hyperpolarisation of the vagus nerve that was reversibly inhibited by 30 μM linopirdine. Hyperpolarisation was recorded as the change in surface demarcation potential between the central drug-perfused chamber (2) and the distal chamber containing the cut nerve ending (1) (summary of Methods, figure 2.4 in top right corner). (**B**). The C-fibre compound action potential amplitude (arrowed) was increased and the spike after-hyperpolarisation was decreased by retigabine (red trace). Data has been baseline subtracted for ease of comparison. (**C**). Mean (± SEM) demarcation potential changes produced by retigabine. The retigabine-induced hyperpolarisation (black columns) was reproducible when reapplied after 1 hour (first pair, open column; n= 8) and significantly inhibited when the second application was preceded by 10 μM XE991 (second pair, n = 7; **P< 0.01) or 30 μM linopirdine (third pair, n = 11 ***P<0.005). [Illustrated recordings by JMR. J. Keasberry contributed additional data included in that summarised in (C)]*

6.4.1 EFFECT OF Kv7/M-CHANNEL MODULATORS ON SURFACE DEMARCATION POTENTIALS

Retigabine (10 μM) produced a consistent, reversible and reproducible increase in the steady surface demarcation potential/axonal polarisation between the segment of the nerve exposed to the drug in the central chamber (2) and the drug-free segment in the distal chamber (1) (see Methods, figure 2.4). The average change in axonal polarisation produced by retigabine was *0.38 ± 0.022 mV (n = 33). Control applications of the retigabine solvent DMSO (1:1000 v/v) had no effect on axonal polarisation.

This indicates that retigabine hyperpolarised the vagus nerve. This is likely to be due to an effect on the C-fibres since these fibres make up a vast majority of the fibres in vagus nerve and therefore will contribute the largest component to the axonal polarisation and also the surface potential change was accompanied by a change in C-fibre, but not A-fibre, CAP amplitude (see 6.4.2). Similar effects on axonal polarisation by other drugs acting selectively on C-fibres have been

observed using this preparation (GABA, carbachol:(Brown and Marsh, 1978); capsaicin: (Marsh et al., 1987))

The effect of retigabine on the surface demarcation potential was substantially reduced by co-application of 10 μM XE991 or 30 μM linopirdine (figure 6.4 (A), (C). *Linopirdine reduced the retigabine-induced potential change from 0.42 ± 0.04 to -0.19 ± 0.02 (n = 10; P<0.005). XE991 reduced the potential change from 0.33 ± 0.03 to 0.09 ± 0.02 mV (n=7; P<0.01). This indicates that the effects of retigabine could be attributed to an action on the M-current.
[*Includes data obtained by V.Keasberry]

In contrast, linopirdine and XE991 applied in the absence of retigabine did not produce a significant change in demarcation potential (the mean increases with 10-30 μM linopirdine 0.071 ± 0.015 mV (n = 10) and with 10 μM XE991 0.048 ± 0.016 mV (n = 6) respectively. Since all of these preparations had previously been exposed to retigabine, it is likely that this small response was due to block of residual retigabine-enhanced M-currents, not endogenous (unenhanced) currents.

6.4.2. EFFECT OF Kv7/M-CHANNEL MODULATORS ON COMPOUND ACTION POTENTIALS

Retigabine increased the amplitude of the C-fibre CAP and reduced the post-spike hyperpolarisation (figure 6.4 (B)), without changing spike width. In contrast, no clear effect on the A-fibre CAP* could be discerned. These effects would be expected to follow a selective hyperpolarisation of C-fibres. This would increase CAP height by reducing sodium channel inactivation, but reduce the after-hyperpolarisation by reducing the driving force for the potassium current.
[*Includes data obtained by J.Keasberry.]

6.5. CONCLUSIONS

The immunohistochemical analysis revealed the presence of at least one subunit of the M-channel (Kv7.2) in the unmyelinated fibres of the vagus nerve, and the electrophysiological tests confirm that they form functional M-channels, or part thereof.

It is possible that M-channels in these fibres are Kv7.2 homomers, rather than the more usual Kv7.2/7.3 heteromers, as may be the case in some peripheral myelinated axons (Schwarz et al., 2006). This could be tested from their differential sensitivity to tetraethylammonium (Hadley et al., 2000) but this would require direct measurement of the M-current when activated by depolarisation. This cannot be done on single unmyelinated fibres but might be possible using sucrose-gap recording (Marsh, 1982). I also cannot exclude the presence of other subunits, such as Kv7.5 (King and Scherer, 2012) but their functional contribution is likely to be small since the effects of retigabine (see below) were sensitive to reasonably low concentrations of XE991, which would not be expected were the responsive channels composed of Kv7.5 subunits (XE991 IC50 against Kv7.5 = 65μM; Kv7.2/Kv7.3 heteromers = 0.6 μM (Schroeder et al., 2000)).

Evidence that the Kv7/M-channel protein is functional stems from the hyperpolarising effect of retigabine. This was due to an action on M-channels since the hyperpolarisation was reduced by the M-channel blockers linopirdine and XE991.

Retigabine produces a hyperpolarising shift in the M-current voltage activation curve (Tatulian et al., 2001). Hence, even very few channels are open at the normal resting potential (see below), their open probability will be greatly increased by retigabine, producing a large outward current and inducing a membrane hyperpolarisation. Further evidence for the presence of M-channels in peripheral unmyelinated fibres is provided by the experiments of (Lang et al., 2008), who showed that retigabine reduced the excitability of C-fibres in human

sural nerves which could be blocked by XE991 but like the results obtained in this study the observed no effect with XE991 application alone.

In contrast, vagal fibres were not clearly depolarized by XE991 or linopirdine in the absence of retigabine. This suggests that either very few Kv7/M-channels were open at rest potential, or if there are channels open, the effects on the resting membrane potential of blocking the channel were countered by the influence of other resting membrane currents, such as twin-pore (K2P) potassium currents (Kang and Kim, 2006;Dobler et al., 2007;Plant, 2012;Marsh et al., 2012;Cadaveira-Mosquera et al., 2012) , Na-activated potassium channels (Alloui et al., 2006;Tamsett et al., 2009;Nuwer et al., 2010), plus currents generated by the electrogenic sodium pump (Rang and Ritchie, 1968).

Notwithstanding a variety of other currents, the interpretation that few channels are open at normal resting potential might be favoured by the observation of Lang et al (2008) that XE991 alone did not reduce the excitable threshold of sural nerve C-fibres. This observation is different to that which would be expected if the Kv7/M-channel conductance contributed a substantial fraction of resting membrane conductance.

CHAPTER 7.

Kv7/M-CHANNELS IN KERATINOCYTES

The epidermal Kv7.2 immunoreactivity described in chapter 5 raises the question what cells are being recognised by the antibody and what possible role could the Kv7/M-channel have in these cells?

7.1 Kv7.2 IMMUNOREACTITVITY IN THE EPIDERMIS

The Kv7.2 antibody revealed immunoreactivity within the epidermis at the surface of the skin and also in the epidermis surrounding the hair bulb (figure 7.1 (A)). The majority of the cells within the epidermis, approximately 90%, are keratinocytes (Brouard et al., 1999;McGarth et al., 2012). Epidermal keratinocytes differentiate with age and progress through the epidermis from the epidermal layer that is adjacent to the dermis to the outer epidermis. This leads to distinct stratified layers within the epidermis.

The Kv7.2 immunoreactivity within the sliced hairy skin appeared to be broadly spread throughout the epidermis. The epidermis of hairy skin is relatively thin compared to that of plantar skin. To get an idea of whether the Kv7.2 immunoreactivity is confined to a particular layer within the epidermis plantar skin was stained with the Kv7.2 antibodies, (figure 7.1 (B)-(D)).The staining observed with the Kv7.2 antibody was particularly intense in the layers adjacent to the dermal-epidermal border, in the stratum germinativum and stratum spinosum. These two basal layers of cells are comprised of the only keratinocytes capable of undergoing mitosis, enabling a culture of these cells to be produced. Cultured keratinocytes allow for direct testing for immunoreactivity to Kv7.2, and also allows the testing of possible roles for the Kv7/M-channels within these cells.

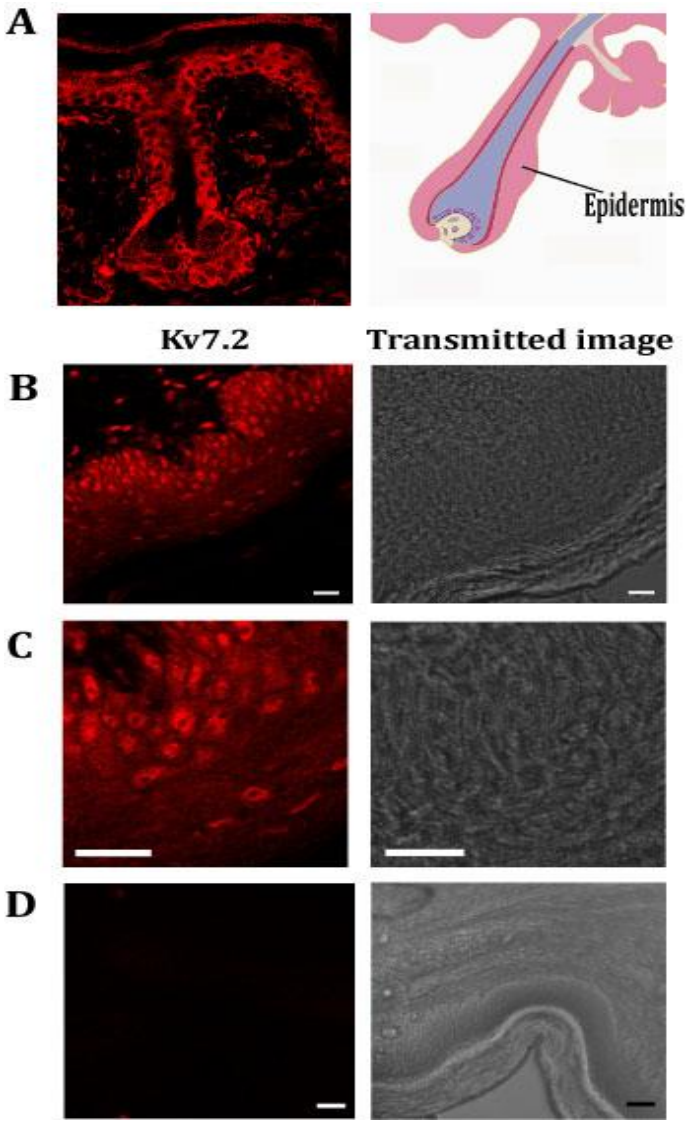

Figure 7.1: Immunoreactivity for Kv7.2 within the epidermis of hairy and plantar skin. *(A) Immunoreactivity for Kv7.2 Abcam within the epidermal tissue surrounding the hair follicle with a cartoon of the hair follicle structure where the epidermis is denoted by the area shaded in pink. (B) and (C) Kv7.2 Alomone immunoreactivity within rat plantar skin with corresponding transmitted images on the right (D) Secondary only antibody, plantar skin, with corresponding transmitted images on the right. Scale= 40 µm*

7.2 CULTURE OF RAT KERATINOCYTES

A protocol for obtaining viable and reproducible cultures of rat keratinocytes was developed from a protocol previously described for the isolation of keratinocytes from mouse ((Dlugosz et al., 1995).

Ideally, for continuity, keratinocytes would be cultured from the same skin location (hind paw) and same size animal (150 g) that was immunoreactive to Kv7.2 in the sliced skin, and which had also been used in the skin nerve experiments where Kv7/M-channel presence was detected in cutaneous nociceptive fibres (Passmore et al., 2012). Unfortunately, a viable culture of keratinocytes could not be obtained from animals of the equivalent age or size, but only from rats aged 1 day.

The keratinocyte culture needed to be maintained at sub-confluence as confluence induces differentiation, upward migration and apoptosis, as would normally occur *in vivo* (Lippens et al., 2005). Defined keratinocyte–serum free media (keratinocyte-SFM) from Invitrogen (see methods 2.1.2) was used for the culture of keratinocytes and was stated by the manufacturer to be selective for keratinocytes over other possible contaminant cells such as fibroblasts. Keratinocyte–SFM medium is also low in Ca^{2+} (<0.1 mM): this is important in maintaining the cells in the growth phase as an increase in intracellular Ca^{2+} induces keratinocyte differentiation (Hennings et al., 1980;Watt, 1989;Denda et al., 2001).

7.3 Kv7.2 IMMUNOREACTIVITY IN CULTURED RAT KERATINOCYTES

The cultured keratinocytes were tested for immunoreactivity to Kv7.2 with two of the Kv7.2 antibodies that had tested positive in epidermal cells in the sliced skin experiments, Kv7.2 Abcam and Kv7.2 Neuromab. The results are illustrated in figure 7.2 below.

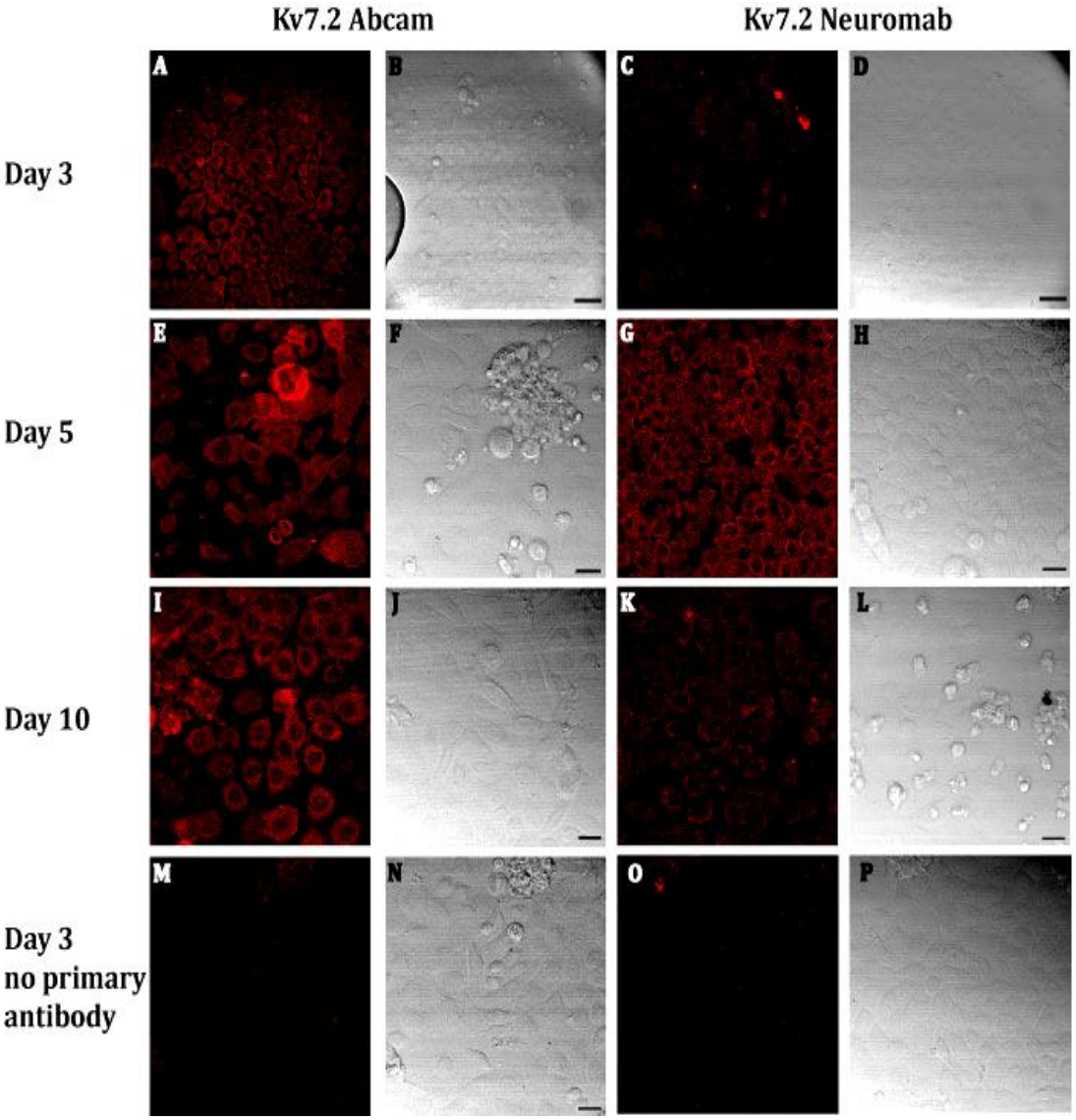

Figure 7.2: Immunoreactivity to Kv7.2 channel in cultured rat keratinocytes.
(A) Day 3 in culture Kv.7.2 Abcam. (B) Transmitted image of A. (C) Day 3 in culture Kv.7.2 Neuromab. (D) Transmitted image of C. (E) Day 5 in culture Kv.7.2 Abcam. (F) Transmitted image of E. (G) Day 5 in culture Kv.7.2 Neuromab. (H) Transmitted image of G. (I) Day 10 in culture Kv.7.2 Abcam. (J) Transmitted image of I. (K) Day 10 in culture Kv.7.2 Neuromab. (L) Transmitted image of K. (M) Day 3 in culture secondary only (Kv7.2 Abcam). (N) Transmitted image of M. (M) Day 3 in culture secondary only (Kv7.2 Neuromab). (N) Transmitted image of M. Scale bar =20 μM.

The transmitted light images of the keratinocytes in figure 7.2 show similar morphology to those cultured to similar densities in other studies (Kolly et al., 2005). When confluence was reached the keratinocytes grew on top of each other and took on a rounded appearance, see figure 7.2 (E) and (L).

Immunoreactivity for both of the Kv7.2 antibodies was detected in the cultured keratinocytes. The immunoreactivity to the Kv7.2 Abcam antibody is present at all degrees of confluence: see figure 7.2 (A), (E) and (I). The immunoreactivity with the Kv7.2 Neuromab antibody appears to be more intense when the keratinocytes are near confluence: figure 7.2 (C), (G), and (K). The staining could not be quantified due to the large variability in size and shape of keratinocytes. There was little immunoreactivity in the secondary antibody-only control e.g., figure 7.2 (M) and (N). The secondary antibody-only control images were taken at the highest gain that had been used when imaging the Kv7.2 antibody-containing group indicating little, if any non-specific binding of the secondary antibody.

7.4 Kv7.2 IMMUNOREACTIVITY IN SLICED P1 RAT SKIN

Keratinocytes cultures were only successfully obtained from the epidermis of one day old (P1) rats. To determine if sliced skin from P1 rats exhibited similar Kv7.2 expression to that from adult rats, frozen sections of acutely fixed P1 rat skin were tested for immunoreactivity with the Kv7.2 Abcam antibody, which gave good immunoreactivity in cultured keratinocytes (figure 7.2) and previously in sliced skin (figure 7.1).

The immunoreactivity to the Kv7.2 Abcam antibody in sliced P1 rat skin was weak compared to that observed in adult skin and little if any morphology could be differentiated (figure 7.3). This may be due to the young age of the animal in which the tissue is more delicate and less differentiated, leading to difficulties in tissue preparation (e.g. fixation times and/or the slicing of the tissue).

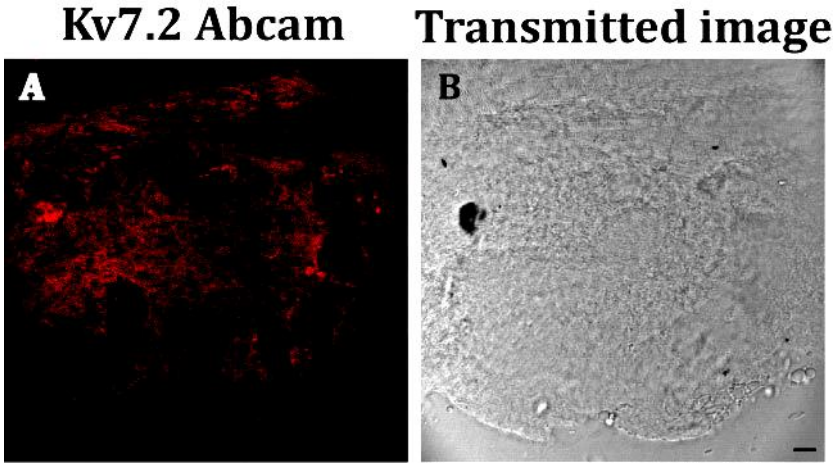

Figure 7.3: Weak immunoreactivity in P1 rat skin for the Kv7.2 Abcam antibody. *Scale bar = 20 µM*

7.5 Kv7 CHANNEL mRNA IN CULTURED KERATINOCYTES

Since Kv7.2 immunoreactivity in sliced P1 skin was weak, in order to corroborate the Kv7.2 immunoreactivity in the cultured keratinocytes, reverse transcriptase polymerase chain reaction (RT-PCR) was performed on the total RNA isolated from cultured keratinocytes (see Methods). RT-PCR also allows the RNA isolated from keratinocytes to be tested for other neuronal *KCNQ* mRNA.

The keratinocytes were cultured to near confluence (3-10 days), since the Kv7.2 staining appeared to be the most intense at this stage (see figure 7.2). The total RNA isolated from the cultured keratinocytes was quantified by spectrophotometry. The yield of RNA was 47 ng/µl and the absorbance coefficient (a measure of RNA purity) gave a 260/280 nm ratio of 1.8. This indicates that the sample was largely purified RNA, with some contamination by genomic DNA, protein, phenol or other contaminants, as a pure RNA sample should have a ratio of >2, (Lehninger, 1975).

The integrity of the isolated total RNA was confirmed on a 1% (w/v) agarose gel containing ethidium bromide and visualised under UV light, see figure 7.4. The gel revealed a single band of between 1500 and 2000 base pairs (bp). As this gel was non-denaturing, the RNA ran as a single, albeit wide, band rather than double bands (18S and 28S) that would result from a denaturing gel. The width of the band infers that there possibly is a degree of overloading of sample into the gel or some degradation of the RNA maybe present. No large molecular weight bands were observed, as would have been present had genomic DNA been a significant contaminant.

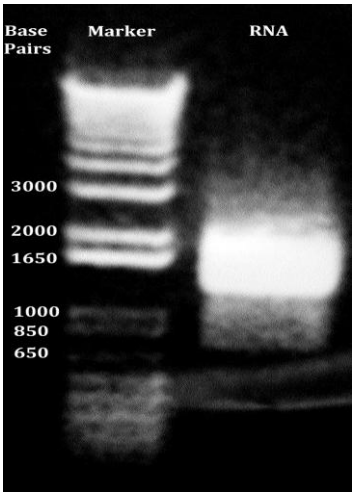

Figure 7.4: Total RNA isolated from cultured rat keratinocytes on a 1% (w/v) agarose gel. *Marker lane is TrackIt™ 1 Kb DNA Ladder*

The total RNA from the cultured keratinocytes was DNAase treated to remove any contaminant DNA, and then reverse transcribed using two different reverse transcriptases, Superscript™ or Moloney Murine Leukemia Virus (M-MLV). These were used in combination with either Oligo dT or random hexamer primers. After completion of reverse transcription the resulting cDNA was subjected to PCR using the intron-spanning primers for the Kv7 channel family members Kv7.2-5 previously described (Shah et al., 2002;Hadley et al., 2003).

The predicted size of the RT-PCR products using these primers are as follows

Kv7.2 = 226 bp

Kv7.3 = 160bp

Kv7.4 = 380 bp

Kv7.5 = 106bp

The PCR products were then run on a 1% (w/v) agarose gel containing ethidium bromide and visualised under UV light to determine if bands of predicted size; have been produced (see figure 7.5).

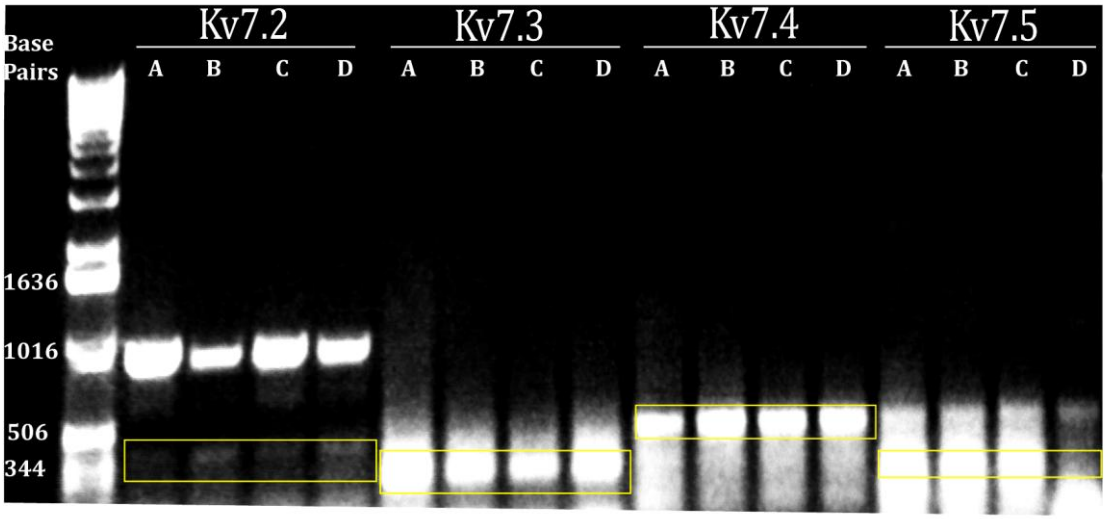

Figure 7.5: RT-PCR of Kv7/M-channel subunits Kv7.2, Kv7.3, Kv7.4 and Kv7.5 on mRNA purified from cultured rat keratinocytes. *RT-PCR products approximately the predicted size are highlighted in yellow. A-D refers to the reverse transcriptase and primer selection used for the reverse transcription reaction of the RT-PCR. (A) Superscript™/ Oligo dT (B) Superscript™/ random hexamer (C) Moloney Murine Leukemia Virus (M-MLV)/ Oligo dT (D) Moloney Murine Leukemia Virus (M-MLV)/ random hexamer.*

The RT-PCR products yielded bands of varying intensity near the predicted sizes expected for Kv7.2-5 (see figure 7.5). There was a lot of primer dimer on the gel (not shown) and the Kv7.2 produced an intense upper band of which could be due to PCR product dimer or amplification of a pseudogene (Williams et al., 2008). This indicates that this experiment ideally requires further optimisation as the unexpected band could possibly be due to template DNA contamination, although this would have been mitigated with the DNase treatment. Alternatively the PCR primers may need to be redesigned to ensure that all known isoforms of each Kv7 subunit are accounted for. However, the presence of bands of appropriate size for each of the primers provides some corroboration of the Kv7.2 immunoreactivity observed in keratinocytes and also infers that the other Kv7/M-channels subunits are expressed in cultured keratinocytes.

7.6 ELECTROPHYSIOLOGICAL RECORDING OF Kv7/M-CHANNELS IN CULTURED KERATINOCYTES

The Kv7/M-channel regulates excitability in neurons by maintaining the membrane potential of the cell at sub threshold levels. Keratinocytes are non-excitable cells therefore excitability could not be measured. Instead attempts were made to measure the change in membrane current and membrane potential produced by modulators of Kv7/M-channels.

Membrane current was measured in collaboration with Dr. V. Telezhkin. Keratinocytes contain desmosomes (plus other junctions) which, if left intact, would lead to a dissipation of the current, making voltage clamp extremely difficult. Hence, the keratinocytes were first trypsinised, washed with media, and re-plated as isolated cells.

After patching an isolated keratinocyte, a 25 s voltage ramp from -100 -+40 mV was applied to the patch-pipette and the current produced was recorded as shown in figure 7.6.

A.

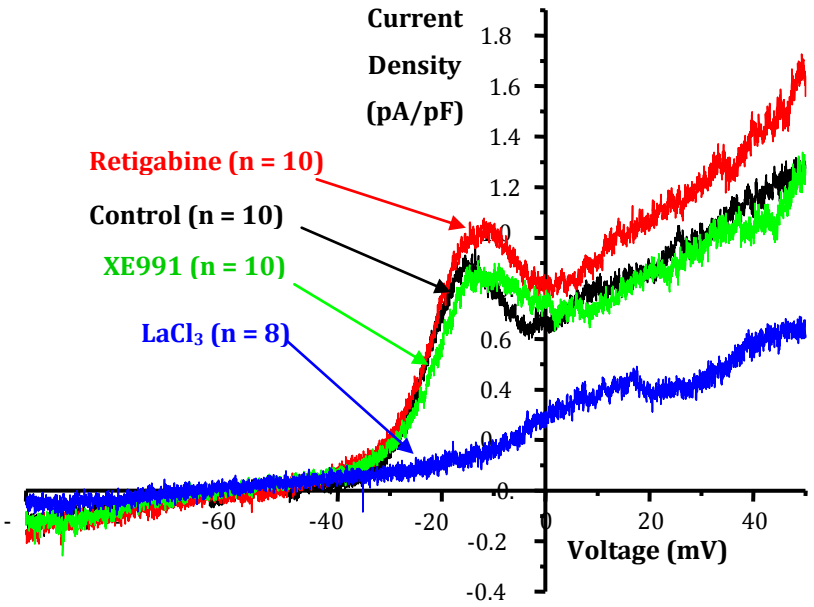

B.

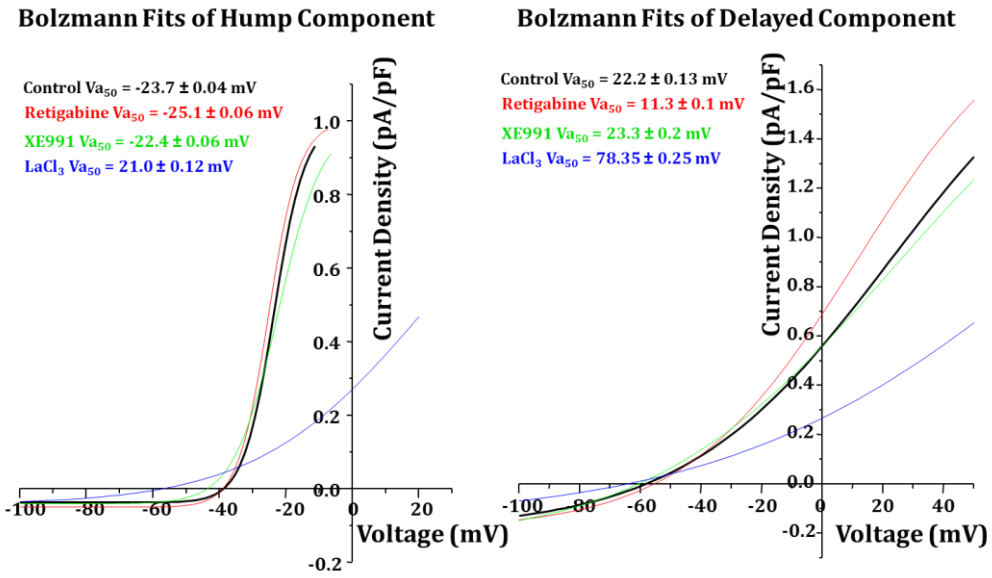

Figure 7.6: Kv7/M-channel modulators alter a component of the integral transmembrane current in a rat keratinocytes. *(A) Average effects of retigabine (10 μ; n=10), XE991 (10 μM; n=10) and $LaCl_3$ (1 mM; n =8) on integral transmembrane current in a rat keratinocyte generated by a voltage-ramp from -100 to +40 mV. (B) Boltzmann curve fits of the Hump-like and the Delayed components of the integral transmembrane current in rat keratinocytes in control and in presence of retigabine, XE991, and $LaCl_3$. [Experiment in collaboration with Dr. V. Telezhkin.] The curve illustrates the average responses of 10 cells (8 in the case of $LaCl_3$). For further details of recording conditions, refer to the methods section 2.4.*

The results from the voltage ramps indicate there are two components of the outward currents, figure 7.6 (A). One component maximises between -20 and -10 mV; this which I refer to as the "hump" component. The other component is the "delayed" component that appears from 0mV onwards. The majority of traces produced a "hump" current. The "hump" component currents were separated from the "delayed" component currents then fitted to the Boltzmann equation figure 7.6 (B).

The application of retigabine lead to an enhancement of the "delayed" component; a plot of the average results obtained is displayed in figure 7.6 (B). Retigabine also shifted the curve of the delayed component about 10 mV in the hyperpolarising direction. Although less than that observed in rat sympathetic neurons (~-20 mV shift) by Tatulian et al., (2001), this result suggests that the shift might be at least partly due to current passing through Kv7/M-channels. The effect of the M-channel blocker XE991 (10 μM) was small producing only a slight reduction in the outward current. The "hump" component was mostly eliminated by the application of La^{3+} which suggests that this component may be due to a Ca^{2+} activated K^{+} current activated by Ca^{2+} entry through TRP channels.

The effect of Kv7/M-channel modulators on the membrane potential of isolated keratinocytes was studied under current-clamp, in collaboration with Dr. G. Passmore. In these experiments, the keratinocytes proved extremely difficult to patch. A stable resting potential obtained in one cell which was retained for long enough to test retigabine. In this cell (resting potential -75 mV) retigabine (10 μM) produced a clear hyperpolarisation of 3 mV, as shown in figure 7.7. The membrane potential was restored after subsequent additional application of 3 μM XE991, suggesting that the effect of retigabine was due to activation of endogenous M-channels. All other cells had very depolarised resting potentials (between -25 and -10 mV) and therefore were not used.

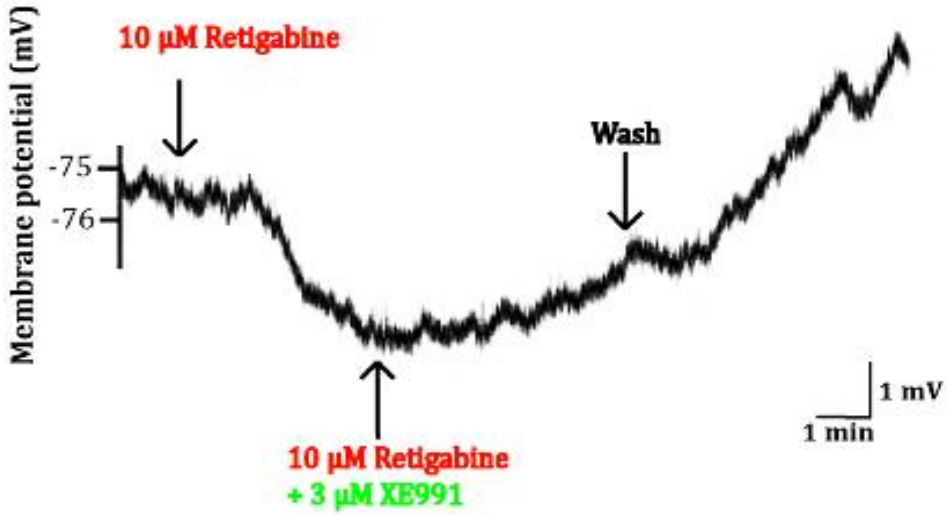

Figure 7.7: Retigabine hyperpolarises the membrane of Keratinocytes. *[Experiment in collaboration with G. Passmore] For further details of recording condition please refer to the methods section 2.4.*

These two electrophysiological studies, although limited due to the difficulties in obtaining recordings provide some preliminary evidence to suggest that functional M-channels are indeed present in keratinocytes.

7.7 THE EFFECT OF Kv7 MODULATORS ON TRPV3-INDUCED ATP RELEASE FROM KERATINOCYTES

The previous results provide evidence for the expression of M-channel subunits and some evidence for functional M-channels in keratinocytes. The next step was to investigate a possible physiological role for these channels such as moderating the stimulated release of ATP.

7.7.1 TRPV3 AND KERATINOCYTES

Ion channels of the TRP (Transient Receptor Potential) family are are associated with thermal and nociceptive sensation. TRPV1, 3 and 4 have been found on keratinocytes (Peier et al., 2002;Inoue et al., 2002;Chung et al., 2004b). Particularly strong expression was observed with the TRPV3 channel in keratinocytes where both the TRPV3 protein and mRNA signal has been detected (Peier et al., 2002;Chung et al., 2004b).

TRPV3 is a Ca^{2+} permeable cation channel activated at normally non-noxious 'warm' temperatures (≥ 32°C). Various compounds can activate or potentiate the activation of TRPV3 including 2-Aminoethoxydiphenyl borate (2-APB) (Chung et al., 2004a) and structurally related plant-derived compounds such as camphor, carvacol and thymol (Nilius, 2007).

Thermal activation of cultured keratinocytes can induce the release of ATP from keratinocytes, which in turn can lead to calcium rises in adjacent sensory neurons, implying a possible role for the keratinocytes in conveying sensory information (Mandadi et al., 2009) TRPV3 activation also leads to a membrane depolarisation, so voltage-gated M-channels might regulate the extent of this depolarisation and indirectly the amount of ATP released.

ATP release in cultured keratinocytes can be measured via the luciferase assay and a luminometer (see Methods). In the following experiments, the amount of

ATP released in response to TRPV3 activation and the effect of Kv7/ M-channel modulators on this release was measured.

7.7.2 DESIGN OF AN ATP RELEASE ASSAY FROM KERATINOCYTES

The luciferase assay uses luciferase's to convert luciferin and ATP in the presence of oxygen, into a photon of light. The amount of light released can then be measured with a luminometer.

The range over which the luminometer could measure ATP was established. This was completed by measuring on a luminometer with solutions of known concentrations of ATP via the luciferase reaction (see section 2.5). The resulting standard curve of ATP concentration and luminometer reading is illustrated in figure 7.8.

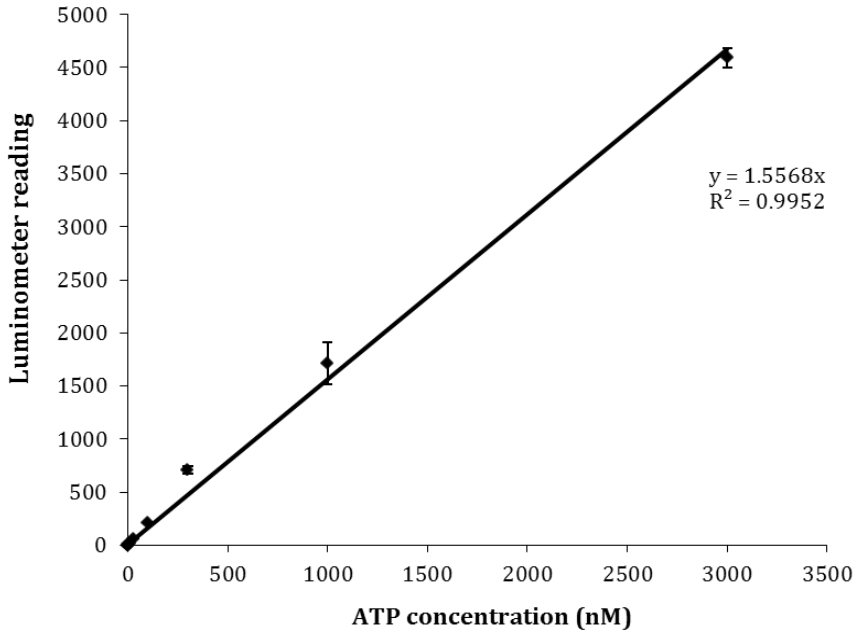

Figure 7.8: Semi-quantitative dynamic range for ATP with the luciferase assay measured using a luminometer. *The equation of the line of best fit is shown on the chart as is the correlation coefficient. (n=3)*

This graph provides a guide to the dynamic range over which the concentration of ATP could be measured, up to 3 μM ATP. The correlation coefficient of the line of best fit of this linear regression is 0.9952. Therefore the ATP concentration is proportional to the luminometer reading which allows the equation of the line of best fit to be utilised to the calculate an estimate of amount of ATP released from the cells.

The estimated amount of ATP from each assay is given as:

$$\frac{\textbf{Luminometer reading (y)}}{\textbf{1.56}} = \textbf{Concentration of ATP (nM)}$$

The amount of ATP that is released is dependent on the number of cells present in each sample, therefore to make comparisons between treatment groups an equal number of cells needed to be contained within each sample within an experiment. To achieve an equal distribution of the cells in each sample the suspension of keratinocytes obtained at the final stage of culture was plated in equal volumes into equally-sized dishes (1.9 cm^2), each dish being a separate sample which would be compiled into treatment groups later. Due to discrepancies between the yields from separate cultures, comparisons between the amounts of ATP released with different treatments could only be made within cultures, not across cultures. In all ATP release experiments an internal control for any mechanical disruption of the keratinocytes was included this involved the addition of an equivalent volume of HEPES buffered Krebs (50 μl) to the cells as that of the treatment solution, HEPES buffered Krebs with drug (50 μl) and is termed 'control' in all experiments. After 10 minutes a 50 μl sample was removed from the extracellular fluid for ATP measurements.

Prior to experimentation the cells were cultured until near confluence as it was at this stage that the cells appeared to have the strongest immunoreactivity for Kv7.2 antibodies and where KCNQ2 mRNA was detected (see figure 7.2 and figure 7.5). Keratinocyte growth media contains very little calcium (<0.1mM),

since low calcium is required for cells to remain mitotic (Xu et al., 2006). As the TRPV3 channel requires calcium, the entire volume (500 µl) of keratinocyte growth-SFM was replaced with an equivalent volume of HEPES-buffered Krebs solution containing 1.5mM $CaCl_2$. This was completed an hour before addition of any drugs as mechanical disruption of keratinocytes by replacing the media is known to induce ATP release (Burrell et al., 2005). After the replacement of the growth media with the HEPES buffered Krebs the remainder of the experiment was conducted at room temperature (22-25 °C) in order to limit any effect temperature change may have on the results.

To ensure that the ATP released from the cultured keratinocytes could be measured by this assay, an experiment estimating maximum stimulated release of ATP from the confluent cells was conducted. This was completed by the application of a strong irritant. Previous studies have shown that keratinocytes release ATP in response to strong irritants such as 4% sodium hydroxide (Dixon et al., 1999;Mizumoto et al., 2003). The design of this and subsequent experiments was as follows. Each sample contained 500 µl of HEPES buffered Krebs, to which a 50 µl of X10 drug that had been dissolved in HEPES buffered Krebs was added.

When 4% NaOH was applied to the confluent cultured keratinocytes an average of 420 pmol of ATP was released (total ATP minus the ATP release due to mechanical disruption calculated from the control), which was significantly larger than that released by application of the control Krebs solution (figure 7.10) .

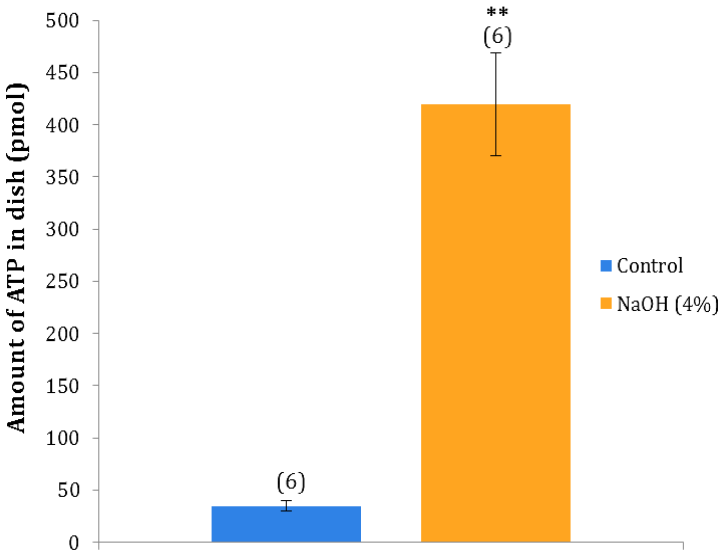

Figure 7.9: The mean amount of ATP released from cultured keratinocytes by application of 4% NaOH. *All recordings were made from a 50 µL sample of the supernatant following 10 minutes exposure to the drug or the HEPES buffered Krebs only control. The number of samples in each treatment group is defined in brackets above the bars. Error bars are S.E.M ** p<0.01. See appendix 1 for raw data.*

7.7.3 TRPV3 INDUCED ATP RELEASE FROM KERATINOCYTES

Previous reports have indicated that TRPV3 channels can be activated by camphor (5-10mM) (Chung et al., 2004b;Moqrich et al., 2005) carvacrol (500 µM) (Xu et al., 2006;Doerner et al., 2011) and 2-Aminoethoxydiphenyl borate (2-APB; 100 µM) (Chung et al., 2004a) a non-selective TRP agonist (Colton and Zhu, 2007). Camphor has also been reported to release ATP from cultured mouse keratinocytes (Mandadi et al., 2009). The effects of these compounds on the release of ATP from cultured rat keratinocytes was tested. Camphor (3 and 10 mM) proved ineffective, the amount of ATP released being no greater than that of the control (figure 7.10) this may be due to issues with solubisation. 2-APB (100 µM) with this assay also produced an insignificant release of ATP (figure 7.11). Treatment of the keratinocytes with carvacrol (1 mM) evoked a substantial release and which was significantly greater than that of the control (figure 7.11). Therefore carvarol was selected as the agonist for inducing ATP

release from keratinocytes in this study as this reponse was repeatable in across different cultures.

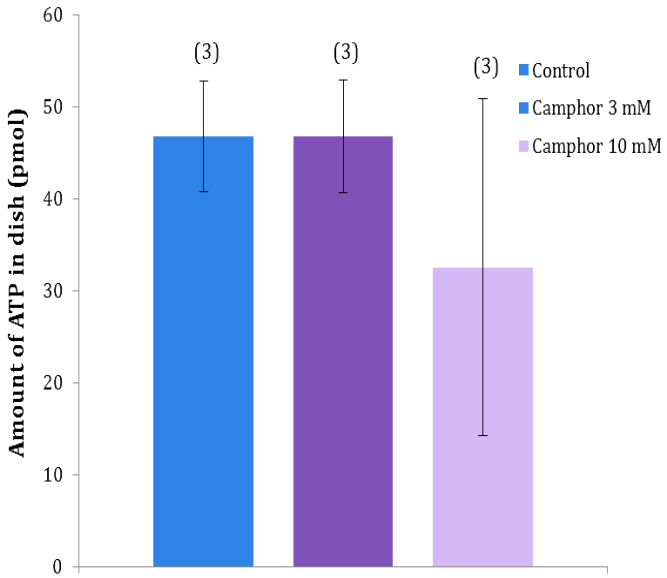

Figure 7.10: The TRPV3 agonist camphor (3, 10 mM) does not significantly increase ATP released from cultured rat keratinocytes. *All recordings were made from a 50 µL sample of the supernatant following 10 minutes exposure to the drug or the HEPES buffered Krebs only control. The number of samples in each treatment group is defined in brackets above the bars. Error bars are S.E.M ** p<0.01. See appendix 1 for raw data.*

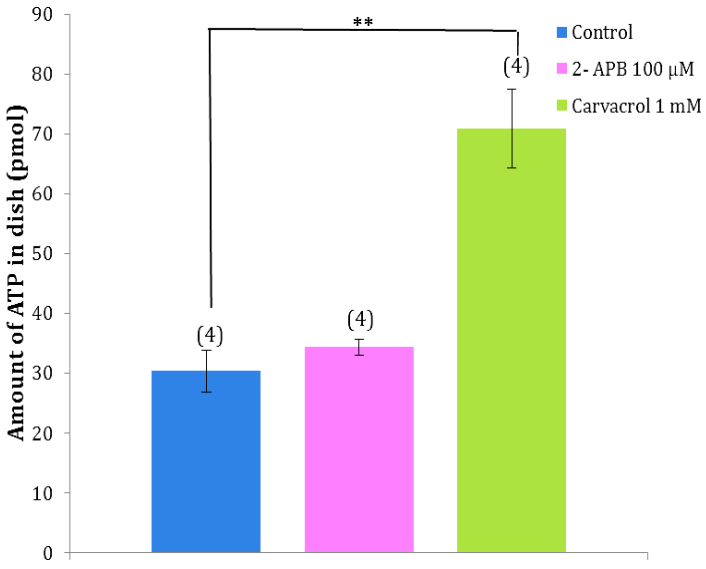

Figure 7.11: The TRPV3 agonist Carvacrol significantly increased ATP released from cultured keratinocytes. *There was no significant effect of 2-APB, a synthetic shared activator of TRPV1, TRPV2 and TRPV3 (Hu et al., 2004). All recordings were made*

*from a 50 µL sample of the supernatant following 10 minutes exposure to the drug or the HEPES buffered Krebs only control. The number of samples in each treatment group is defined in brackets above the bars. Error bars are S.E.M ** p<0.01. See appendix 1 for raw data.*

7.7.4 EFFECT OF Kv7/M-CHANNEL MODULATORS ON TRPV3-INDUCED ATP RELEASE.

To assess what effect M-channels in keratinocytes might have on TRPV3-evoked ATP release I first tested the effect of the M-channel enhancer retigabine. For this I used carvacrol to induce a TRPV3-dependent release of ATP, since this gave a consistent but submaximal release of ATP (see figure 7.12).

As shown in figure 7.12, 10 µM retigabine produced a substantial and consistent increase in carvacrol-induced ATP release, by an average of 340 % (pooled data from two cultures with 6 samples). Since retigabine was dissolved in 5% DMSO, I also checked whether DMSO had any effect. No significant effect on control ATP release was detected (5% DMSO) ([ATP]: controls 15.1± 8.6 nM, n=4; DMSO 12.0 ± 3.8 nM, n=4). No effect on the release of ATP due to carvacrol (plus XE991) was observed as although the release was significantly greater when compared with control but it was not significantly different from carvacrol application alone (figure 7.12(B)). Also, in separate experiments, was found to have no enhancing effect on the resting release of ATP in the absence of carvacrol ([ATP]: controls 15.2 ± 5.9 nM, n=4); retigabine 14.3 ± 7.8 nM, n=3)). This shows that the effect of retigabine shown in figure 7.13 was restricted to the TRPV3-activated release. XE991 (10 µM) in the absence of retigabine had no significant effect on either the spontaneous release ([ATP]: controls 73.3 ± 43.7 nM, n=4); XE991 98.4 ± 19 nM, n=3)) or the enhanced release produced by carvacrol ([ATP]: carvacrol 203.3 ± 32.9 nM, n=4; carvacrol + XE991 359.8 ± 84.5 nM, n=4).

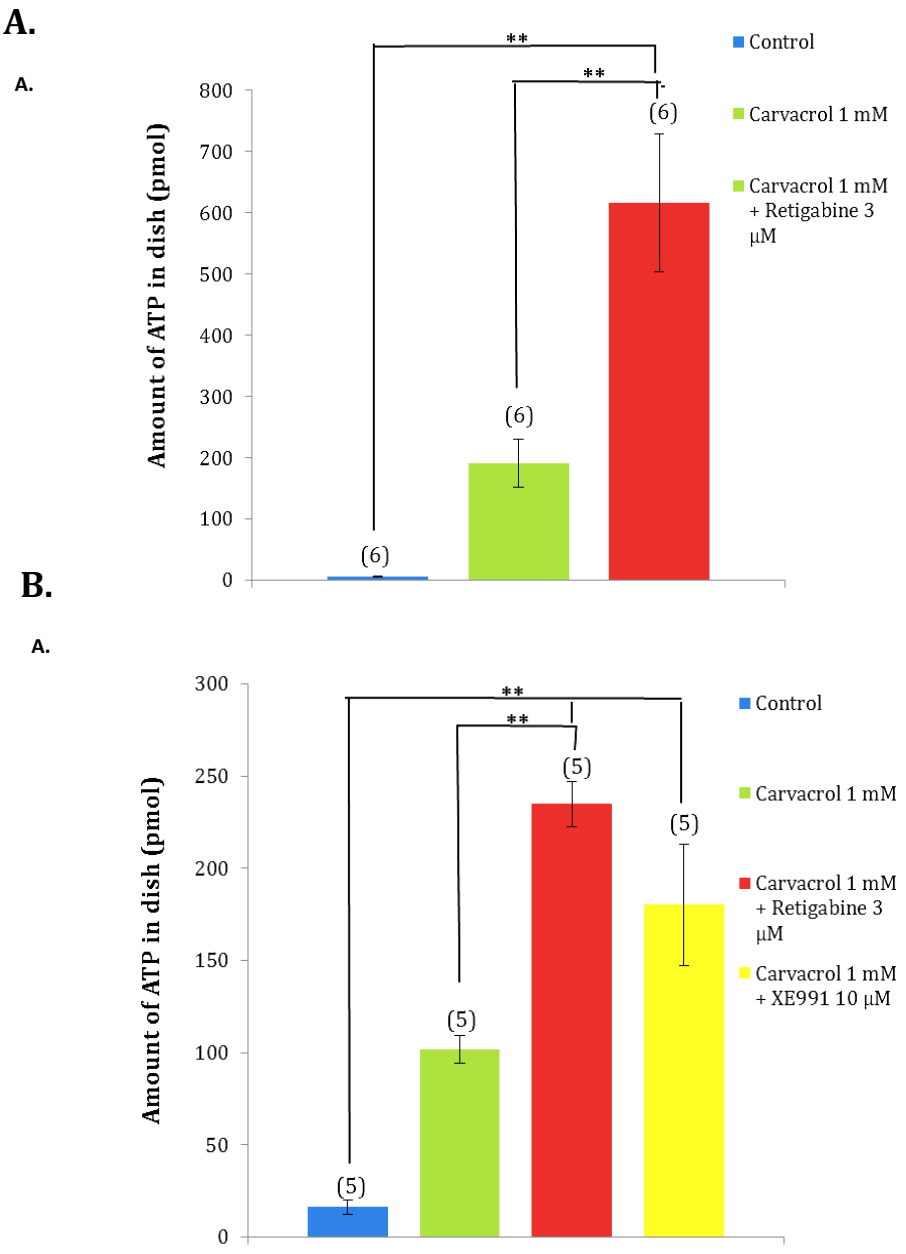

Figure 7.12: The Kv7/M-channel modulator retigabine significantly, potentiates the TRPV3 agonist carvacrol induced release increase from cultured keratinocytes. *(A) Significant potentiation of carvacrol induced ATP release by retigabine (B) Separate experiment showing significant potentiation of carvacrol induced ATP release by retigabine but no significant increase in ATP release with carvacrol due to 10 µM XE991. All recordings were made from a 50 µl sample of the supernatant following 10 minutes exposure to the drug or the HEPES buffered Krebs only control except in (B) where XE991 was added 2 minutes before initiation of experiment to ensure block of the channel. The release due to cavacrol (plus XE991) is significant compared with control but does not differ from cavacrol alone. The number of samples in each treatment group is defined in brackets above the bars. Error bars are S.E.M ** p<0.01. See appendix 1 for raw data.*

The M-channel blocker XE991 was also tested for any effects carvacrol-induced ATP release. Pre-incubation with 10 µM XE991 did not significantly affect the response to carvacrol (data not shown) but it did suppress the enhancement of carvacrol-induced release by retigabine (figure. 7.13). Thus, the enhanced response to carvacrol produced by retigabine may be attributed to activation of M-channels, though block of M-channels alone did not reduce cavacrol-induced ATP release.

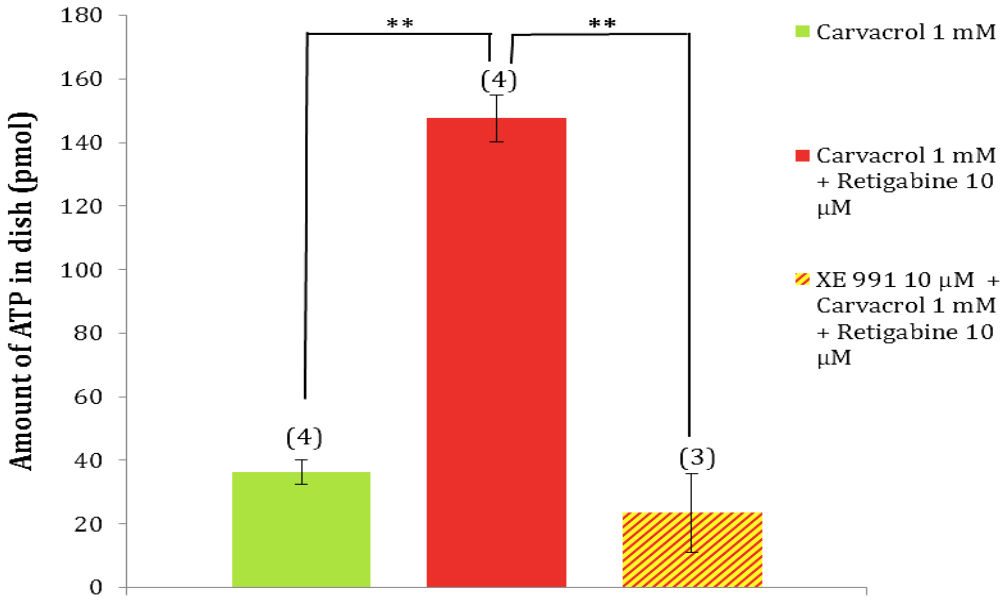

Figure 7.13: Enhancement of carvacrol-induced ATP release by retigabine (10 µM) was inhibited by co-application of 10 µM XE991*. All recordings were made from a 50 µL sample of the supernatant following 10 minutes exposure to the drug or the HEPES buffered Krebs only control. Number of samples in each treatment group is defined in bracket above the bars. Error bars are S.E.M ** p<0.01*

7. 8 THE EFFECT OF Kv7/M-CHANNEL MODULATORS ON TRPV3 INDUCED CALCIUM TRANSIENTS IN CULTURED KERATINOCYTES

The next question was how could retigabine be potentiating the stimulated release of ATP from the cultured keratinocytes?

It has been suggested that the release of ATP from keratinocytes by TRPV3 activation could be due to Ca^{2+} entry (Koizumi *et al.*, 2004), although there are other mechanisms in which ATP can be released from cells (Sabirov, 2005). One possibility is that retigabine increased the Ca^{2+} entry in the keratinocytes produced by carvacrol. To test this, changes in intracellular calcium were measured via fluorescence imaging using the Ca^{2+}-binding probe Fura-2 AM, (described in Methods, section 2.9). Fura-2 AM is a dual emission probe in which the binding of Ca^{2+} shifts the emission spectra from 380 nm to 350 nm. By measuring the fluorescence at both wavelengths and then calculating the 350:380 nm ratio, changes in intracellular calcium can be measured.

The 350:380 nm ratios of the keratinocytes containing Fura-2 AM were continuously recorded throughout the experiment. Carvacrol (1 mM) increased intracellular [Ca^{2+}] in cultured keratinocytes, a (figure 7.14 (A)). Fura-2 signals across different keratinocytes were highly variable but signals with repeated carvacrol applications to the same keratinocyte were reasonably consistent, though some desensitization occurred as previously reported in similar studies (Xu et al., 2006). Therefore in order to test whether retigabine affected the Ca^{2+} signal, carvacrol was applied twice to the same cell then 350:380 nm and the ratio of the second to first responses (R2/R1) on addition of either Krebs' solution or 10 μM retigabine 5 min before the second response can calculated (figure 7.14). As shown in figure 7.14 (B), the second response was smaller on average on adding Krebs solution (R2/R1 = 0.73 ± 0.10, n = 33) but was consistently increased after adding 10 μM retigabine (R2/R1 = 1.18 ± 0.04, n =24); the difference between the response to retigabine was significantly

different to that of Krebs' solution (P<0.01). Retigabine application on its own did not produce any consistent change in resting [Ca^{2+}]. The drugs were each applied for 3 min in the following order: carvacrol 1 mM, carvacrol 1 mM + retigabine 3 μM. Retigabine was applied 5 min before carvacrol. Cells were washed between each application there was no observed change in the 350:380 nm ratios when retigabine was applied alone. The size (peak ratio minus baseline ratio) of the responses to each treatment was measured (see figure 7.14).

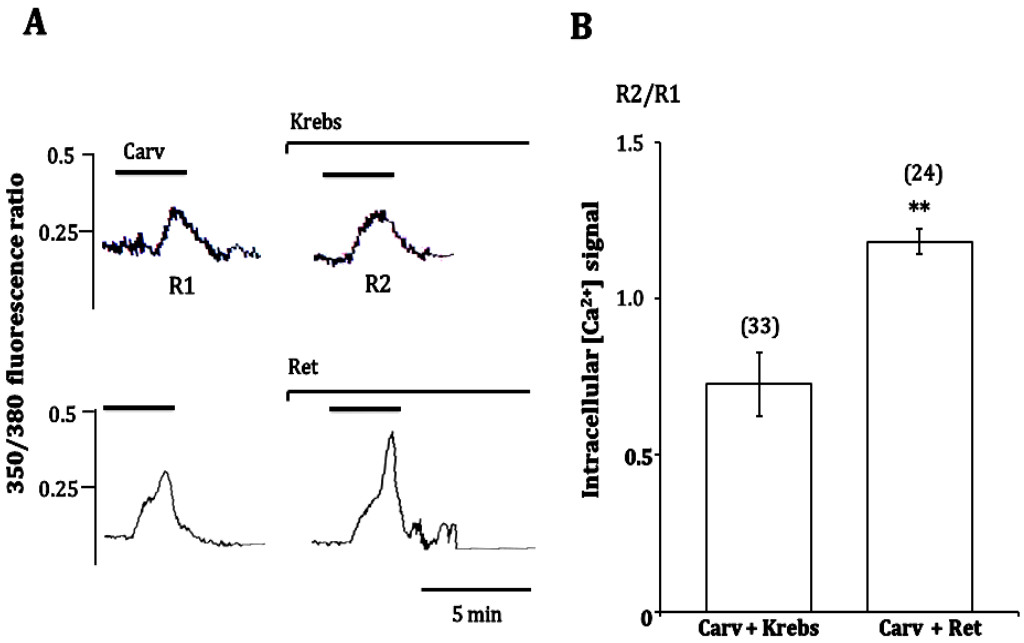

Figure 7.14: Retigabine enhances the increase in intracellular [Ca^{2+}] in cultured keratinocytes produced by carvacrol. *Retigabine enhances the increase in intracellular [Ca^{2+}] in cultured keratinocytes produced by carvacrol. (A) Representative Ca^{2+} signals, measured as increases in the 350:380 nm fluorescence signal in Fura-2 preloaded cells, and recorded from two keratinocytes following two applications to each of 1 mM carvacrol (carv) for 3 min. The top trace shows representative responses to two successive applications of carvacrol. In the lower trace the second carvacrol application was preceded by addition of retigabine (Ret: bath concentration 10 μM). (B) shows the mean ratio of the second-to-first responses (R2/R1) following addition of Krebs' solution (Carv + Krebs) or retigabine (Carv + Ret) before the second response. Bars are SEM, number of cells in brackets. The asterisk (**) indicated that the R2/R1 ratio is significantly greater when R2 was preceded by retigabine than when it was not (P<0.01).*

7.9 CONCLUSIONS

In this chapter cultured rat skin keratinocytes were utilised to confirm that the epidermal immunoreactivity for the Kv7.2 M-channel subunit observed in Chapter 5 was due to the expression in keratinocytes of this protein since Kv7.2 immunoreactivity could be shown in the cultured keratinocytes and the mRNA transcripts for four Kv7 subunits, Kv7.2, 7.3, 7.4 and 7.5, were detected by RT-PCR. These cultures were prepared (out of necessity) from 1 day-old rats. Rat skin at that age showed less *in situ* Kv7.2 immunoreactivity than that of older rats examined previously and less distinctive keratinocyte localisation than that seen in the cultured keratinocytes. The latter might reflect increased expression of the protein with time in culture.

There immunoreactivity to Kv7.2 also appears to correspond with potentially-functional Kv7/M-channels in the cultured keratinocytes. The M-channel enhancer retigabine produced a small but consistent enhancement of outward membrane current in a sample of cultured keratinocytes, accompanied by an 11 mV hyperpolarising shift in the voltage activation curve, as would be expected from previous observations with this compound (Tatulian *et al.*, 2001). In support of this observation, in one test retigabine produced a clear (3 mV) hyperpolarisation of the resting potential. Conversely, the blocking agent XE991 produced a very small reduction in outward current. These results suggest that the M-current appears to make a contribution, though minor to the keratinocyte membrane current and potential. The membrane currents in these cells have not previously been investigated and the nature of other outward currents was not examined in detail in the present experiments. However, they are likely to include a component of Ca-activated K^+ current, possibly carried through TRP channels since the currents were strongly reduced by La^{3+} (Ramsey *et al.*, 2006).

Further evidence for M-channel functionality in cultured rat keratinocytes emerged from measurements of ATP release following stimulation of TRPV3 channels with carvacrol. In these experiments, stimulated release of ATP was strongly amplified by the M-channel “enhancer” retigabine. This was clearly due

to an effect on the Kv7/M-channels as the amplification was entirely prevented by the co-application of the Kv7/M-channel blocker XE991. The M-channel blocker alone did not induce significant change in the carvacrol-induced ATP release from keratinocyte, although results were variable and warrant further investigation.

The release of ATP by TRPV3 could be due to the entry of Ca^{2+} through the TRPV3 cation channels (Koizumi *et al.*, 2004). This may provide one possible explanation for the enhanced release of ATP by retigabine and also why no change in release of ATP was observed with XE991 i.e. the Kv7/M–channel enhancement produces a voltage-dependent outward hyperpolarising current that opposes the depolarisation produced by activating TRPV3 channels and hence reduces Ca^{2+} entry. This response might be intensified if like TRPV1 channels (Zhang *et al.*, 2011) TRPV3 is closely associated with M-channels and induces a Ca^{2+}-dependent inhibition of the latter when activated: retigabine might then be able to counteract this inhibition (Zhang *et al.*, 2011). Direct measurements of carvacrol-induced Ca^{2+} increases in individual cultured keratinocytes gave rather varied results but retigabine appeared to produce a small enhancement in the carvacrol induced rise in intracellular calcium which suggests that the above hypothesis might not be implausible but further experiments are required to confirm this.

Notes on technical limitations: In seeking information regarding the functionality of the Kv7 channels in keratinocytes a number of technical problems were encountered: variations in the viability of the cultures; ability of the membrane patching and low amplitudes of membrane currents; variability of the amounts of ATP released from different cultures and susceptibility of release to large fluctuations following cell damage; and the large cell-to-cell variations in measurements of intracellular Ca^{2+}. These limited the scope of my present experiments but most should be rectifiable in future experiments.

CHAPTER 8.

GENERAL DISCUSSION

AND

CONCLUSIONS

The aims of this study were to determine the expression of the Kv7/M-channel within the peripheral nociceptive sensory pathway (here defined as the DRG neurons and their associated fibres terminating in the skin), and to evaluate aspects of their functional significance within this pathway. This study was initiated to accompany the functional studies of Kv7/M-channels in peripheral nerve terminals of the isolated rat skin saphenous nerve experiments completed by Dr G. M. Passmore (Passmore et al, 2012).

The principal findings of this study are as follows. The expression of the Kv7/M-channel was investigated through the use immunohistochemical techniques using antibodies to the Kv7.2 subunit of the channel, which is believed to be the most abundant subunit of the functional channel in the periphery (Devaux et al., 2004;Schwarz et al., 2006). Immunoreactivity to Kv7.2 was detected in a substantial proportion of DRG sensory neurons, including some (but not all) neurons that are presumed to be small nociceptive DRG neurons due to their immunoreactivity to TRPV1 or IB4. Although estimated measurements of size distribution of Kv7.2 staining indicates that the channel is predominantly expressed in small neurons of the C-type DRG neuron and in some larger, presumably Aδ-type DRG neurons this could not be conclusively determined as the apparent size of DRG neuron will depend on its position within the slice. Kv7.2 immunoreactivity was also present in some of the peripheral sensory nerve endings within the skin but did not appear to co-stain exclusively with a particular peripheral neuronal fibre type. Staining was observed in both myelinated and unmyelinated peripheral fibres including some fibres that showed co-immunoreactivity for the nociceptive marker, TRPV1 and the unmyelinated C-type neuronal fibre marker, peripherin. Immunoreactivity to Kv7.2 was also found to be diffusely spread along unmyelinated sensory C-fibres within the vagus nerve, defined by peripherin co-immunoreactivity. Electrophysiological measurement found that these fibres were hyperpolarised by the Kv7/M-channel 'enhancer' retigabine, this hyperpolarisation was sensitive to the channel blocker XE991, suggesting that there are functional Kv7/M-channels along these fibres. A novel location for the Kv7/M-channel

was also identified by immunoreactivity for Kv7.2 in keratinocytes, the predominant cell type of the epidermis. Results were obtained which imply that functional Kv7/M-channels are present in keratinocytes. Electrophysiological recordings revealed that retigabine and XE991 could modulate the current produced by a voltage ramp and also the membrane potential of keratinocytes. Retigabine also potentiated the induced release of ATP by carvacrol a TRPV3 agonist, this effect was blocked by XE991, suggesting a possible physiological role that the channels may have in keratinocytes.

Possible implications of these findings are as follows. The immunoreactivity to the Kv7.2 subunit identified in this study in both nociceptive (TRPV1/IB4 positive) and non-nociceptive (TRPV1/IB4 negative) small DRG neurons concurs with immunoreactivity observed in sliced DRGs by Rose et al., (2011) and also with M-current recordings obtained from both capsaicin sensitive and insensitive small DRG neurons previously by Passmore et al., (2003) and Linley et al., (2008) but contrasts the results observed in cultured DRG neurons where Kv7/M-channel subunits and an M-current were found in all DRG neuronal types (Passmore et al., 2003). This difference could be due to culturing imparting an affect channel expression or other Kv7/M-channel subunits which may contribute to the current observed in cultured DRGs. The somatic localisation and the apparent lack of immunoreactivity of the Kv7.2 antibody in many of the TRPV1/IB4 positive cells may be due a couple of factors. The first factor could relate to the sensitivity of the antibody. The staining obtained with the antibodies was in the soma of the neuron rather than in the membrane where the channel would be expected to be located. This could be due to an increased density of the channel this location compared to the membrane and the antibody may not be sensitive enough pick up these differences or alternatively the epitope for the antibody may be masked when the channel protein is inserted into the membrane. It is also possible that the lack of immunoreactivity could be due to the contribution of the other Kv7/M-channel subunits to the current. This idea is supported by an immunofluorescent results obtained from other studies. (Passmore et al., 2003;King and Scherer, 2012)

observed Kv7.3 expression was in small DRG neurons in the absence of Kv7.2 staining and a recent study by King and Scherer, (2012) reported that Kv7.5 was the dominate subunit within peripheral small neurons and fibres, although this was not confirmed with functional studies.

This results in this thesis also revealed immunoreactivity in possible *non-nociceptive* small neurons and larger myelinated (NF200 positive) DRG neurons which leads to the question as the whether Kv7/M-channels are involved in different modalities of sensory stimulation. M-currents have been recorded from larger myelinated DRG neurons (Passmore et al., 2003) and some of the large DRGs stained with Kv7.2 here could be of the Aδ nociceptive type whose nociceptive thermal responses were modified by retigabine and XE991 (Passmore et al., 2012). Kv7/M-channels may play a role in pressure sensation. Heidenreich et al., (2012) immunolocalised Kv7.4 in peripheral fibres in Meissner corpuscles mechanoreceptors and also found that the Kv7/M-channel blocker linopirdine and loss of function mutations in the Kv7.4 gene increased the excitability of rapidly adapting mechanoreceptors. These results indicate that the Kv7/M-channel may have a role in touch sensation. Cells that contained the Kv/M-channel of which the Kv7.2 subunit makes up a component have been shown to regulate arterial barometric discharges (Wladyka et al., 2008). The question of whether the channel is involved in the transduction of other sensory modalities could be explored further but regardless the presence of the channel within the soma of some nociceptive neurons agrees with studies where a role for the channel in the initiation and transduction of nociceptive stimuli has been reported in *in vivo* and in vitro experiments on skin nerve terminals from (Linley et al., 2008;Passmore et al., 2012).

Immunoreactivity to Kv7.2 within peripheral nerve terminals allows what is known about the regulation of the Kv7/M-channel from somatic recordings within sensory neurons to be extended. In agreement with the staining obtained in the DRG, some (but not all) of the peripheral nerve endings stained for the Kv7.2 subunit, these included myelinated and non-myelinated fibres and TRPV1

positive nociceptive fibres. The myelinated fibres stained with Kv7.2 maybe of the thermosensitive Aδ type whose discharges due to noxious thermal stimuli were reduced by local application and retigabine and initiated by local application of XE991 (Passmore et al., 2012) these effects were extended to *in vivo* studies in the same publication where intraplantar injection of XE991 led to increased responses to thermal stimuli in deep dorsal horn neurons of the Aδ type. Alteration of nociceptive responses in peripheral terminals of unmyelinated fibres directly due to Kv7/M-channel modulation has been difficult to demonstrate but increased nocifensive responses (Linley et al., 2008) and increased mechanically evoked responses (Passmore et al., 2012) observed with intraplantar injection of XE991 into rat paw infers that it is the modulation of the channel at peripheral terminals that likely to be responsible for the effects observed in these studies.

The Kv7.2 staining in the skin may reflect the Kv7/M-channels presence in other fibre types as the source of fibres that did not co-stain with neuronal markers is unknown. Some of the other fibres may be sympathetic nerve endings as demonstrated by tyrosine hydroxylase co-immunoreactivity with Kv7.2 in some of the peripheral nerve fibres. The staining of sympathetic nerve fibres with Kv7.2 concurs with evidence of functional Kv7/M-channels within in sympathetic nerve endings and processes (Lechner et al., 2003;Hernandez et al., 2008;Zaika et al., 2011b) and these results should be considered when Kv7/M-channel modulators are utilised as pharmaceutical treatments.

Kv7.2 is known to localise with sodium channels at the nodes of Ranvier in myelinated peripheral neurons where the Kv7/M-channel can control ectopic excitability (Devaux et al., 2004;Schwarz et al., 2006). Apart from the experiments examining the effects of Kv7/M-channel modulators on the excitability of the human sural nerve by (Lang et al., 2008) there is limited information regarding the functional role of Kv7/M-channels along unmyelinated axons. The experiments described in this thesis revealed clear immunoreactivity for Kv7.2 in unmyelinated fibres within the vagus nerve and a

reproducible XE991 sensitive hyperpolarisation by retigabine which is primarily due to unmyelinated fibres as these comprise a vast proportion of vagal fibres (80%). The vagus nerve conveys sensory information from fibres whose endings terminate in the viscera, including aortic chemoreceptors and baroreceptors and also fibres that pass to and through the nodose ganglion. The fibres immunoreactive to Kv7.2 could source from one of these visceral sources as the Kv7.2 subunit has been identified in baroreceptors (Wladyka et al., 2008) and in nodose ganglion (Wladyka and Kunze, 2006).

The presence of the Kv7/M-channels along nociceptive unmyelinated fibres raises some questions. Firstly, is the Kv7/M-channel present along the length of nociceptive fibres not just at the peripheral endings and soma? Kv7/M-channel presence along the nociceptive axons is suggested by observations from the following studies. Rivera-Arconada and Lopez-Garcia, (2006) found that application retigabine induced a hyperpolarisation in rat dorsal spinal roots from sensory neurons, (Roza et al., 2011) found in mice that local application of retigabine inhibited discharges from peripheral sensory neuromas and (Rose et al., 2011) found that in rats thermal hyperalgesia, measured by hind paw withdrawal latency to heat, was reduced by local application of retigabine.

Another question raised by the presence of Kv7/M-channels on unmyelinated peripheral fibres is what effect they have on the conduction of nerve impulses? (Lang et al., 2008) demonstrated that the threshold of action potentiation spike generation can be affected by modulating the M-current, an effect which has been demonstrated in unmyelinated central neurons (Shah et al., 2008) therefore the channel may affect the conduction of repetitive activity, but this remains to be conclusively determined as the conducting distance used in the present study (<5 mm) meant that it was not possible to accurately determine if there was a significant change in conduction velocity.

Peripheral unmyelinated fibres express an assortment of neurotransmitter receptors including members of the G-protein coupled receptor family (GPCR): 5-hydroxytriptamine 4 receptor (5HT-4) (Costa et al., 2003), the purinoceptor 1 (P2Y1) (Lang et al., 2002) and the receptor for substance P neurokinin-1 (NK1) (Zhang et al., 2008)) and also members of the ligand gated receptor family: Nicotinic receptor (Lang et al., 2003;Freysoldt et al., 2009;Dehkordi et al., 2009), GABA receptor (Brown and Marsh, 1978), 5HT-3 receptor (Lang et al., 2006;Yu et al., 2008) and TRPV1 (Marsh et al., 1987;Lang and Grafe, 2007). Compounds can be released from nearby glial cells, tissue or blood which can activates these receptors e.g. Schwann cells around that sciatic nerve have been shown release ATP following stimulation with UTP a P2Y agonist (Liu et al., 2005). This can lead to G-protein activation and a subsequent change in PIP2 levels and/or to changes in intracellular calcium (which can also be modulated by voltage gated calcium channels present along unmyelinated nerve fibres (Elliott et al., 1989). Changes in PIP2 levels or intracellular calcium can modulate the Kv7/M-channel. It would therefore be interesting to see if activation of GPCR and ligand gated channels known to be expressed along unmyelinated fibres above are capable of regulating the C-fibre M-channel response.

Results in this thesis demonstrating immunoreactivity to Kv7.2, mRNA to Kv7 subunits, the modulation of current and membrane potential of keratinocytes by retigabine and XE991 and the retigabine enhanced TRPV3 induced ATP release, (of which the mechanism in not yet clear) suggest that functional Kv7/M-channels are present in keratinocytes. These results were unexpected and potentially important as keratinocytes express many of the same sensory transduction channels and mechanisms of nociceptors and are capable of releasing various chemicals following stimulation or injury including; serotonin, ATP, histamine, prostaglandins, leukocytes, and cytokines (Denda et al., 2007). In theory, paracrine signalling due to the release of these chemicals could activate receptors on nearby nerve endings which could lead to the generation of action potentials within the nerve terminals. There has been accumulating

evidence for the active participation of epidermal keratinocytes in cutaneous sensory and pain transmission (Koizumi et al., 2004;Chung et al., 2004b;Huang et al., 2008;Mandadi et al., 2009;Tsutsumi et al., 2011). In particular the observations of (Mandadi et al., 2009) with co-cultures of keratinocytes and sensory neurons show that thermally induced ATP release from keratinocytes was sufficient to activate adjacent sensory neurons. Therefore the initial response in the keratinocytes might be contributing to the sensory neuron response suggesting a role for keratinocytes in the generation of the thermal nociception.

In neurons retigabine and Kv7/M-channel opening is known to lead to a hyperpolarisation of the membrane which diminishes rather than enhances thermal nociception as was reported with Aδ fibres thermal responses by (Passmore et al., 2012). As the results from this thesis suggest that retigabine may increase ATP release from keratinocytes which in theory would be stimulatory to thermal nociception this excludes a possible role for ATP release from keratinocytes in the results obtained from the isolated skin nerve recordings. It is possible however that if an alternative physiological stimulus than the application of carvacrol, for example heat or mechanical stimulation was used to induce ATP release a different effect of M-channel on this release may be observed.

The enhanced TRPV3 induced ATP release seen in cultured keratinocytes could be calcium dependent as hyperpolarisation of the membrane by retigabine could increase in the driving force for calcium. This remains to be clearly determined. The measurements of carvacrol-induced Ca^{2+} increases in individual cultured keratinocytes produced a small enhancement Ca^{2+} signal with retigabine. But as the results from this experiment were very variable further experimentation is required to confirm this effect.

There are many other roles that the Kv7/M-channel may have in keratinocytes if the channel is involved in crosstalk with the TRPV3 channel. Interestingly,

TRPV3 stimulation of keratinocytes can also releases prostaglandin E(2) (PGE2) (Huang et al., 2008). PGE2 is an inflammatory mediator which can contribute to pain (Ma and Quirion, 2008) it would be interesting to see whether the Kv7/M-channel had an effect on this release as PGE2 could contribute to pain transduction by binding to the PGE2 receptor on a nearby nociceptor. Loss of TRPV3 has been shown to impair behavioural responses to heat (Moqrich et al., 2005) this is likely to be due to loss of TRPV3 in keratinocytes as TRPV3 is not known to be expressed in DRGs (Peier et al., 2002) and also the expression of the TRPV3 channel was not detected in mouse neuronal tissue via northern analysis (Asakawa et al., 2006). If the Kv7/M-channel is capable of modulating the activity of the TRPV3 channel in keratinocytes this could be important in other signalling pathways within the epidermis involved in the growth and differentiation of keratinocytes the control of which underlies many disease states including psoriasis and skin cancer. Recently Cheng et al. (2010) demonstrated that TRPV3 in keratinocytes around the hair shaft form a molecular complex with the epidermal growth factor receptor (EGFR) and this appears to be involved in hair morphology, TRPV3 knockouts (KO) were shown to have a curly hair phenotype compared to wild type littermates and in a keratinocytes specific knockout of TRPV3 the epidermis exhibited a >2-fold increase in the thickness in the outer keratin positive layer for the epidermis. Regardless of TRPV3 crosstalk changes in membrane potential are also involved in differentiation and cell division in non-excitable cells e.g. somatic cells and glia (Sundelacruz et al., 2009). As the Kv7/M-channel is capable of modulating the keratinocyte membrane potential the channel may have an effect on mitosis and differentiation of keratinocytes especially as recent results by (Zhou et al., 2011) report that Kv7/M-channel opening decreased the survival of cultured hippocampal neurons.

CONCLUSIONS

The work described in this thesis has provided new neuroanatomical information regarding the localisation of a primary M-channel subunit that is both helpful to the interpretation of functional studies on the role of M-channels in regulating peripheral nociception, and also raises additional possibilities regarding their role in other forms of sensory perception. The functional studies also expand the repertoire of potential roles for M-channels to the regulation of C-fibre activity and to aspects of keratinocyte function. As with the associated work on peripheral nociception by Passmore et al (2012) these results also raise the question of how far the effects of retigabine (and other M-channel enhancers) stem from peripheral actions, as opposed to those on the central nervous system.

FUTURE EXPERIMENTS

The results from this thesis leave some unanswered questions and directions that future experiments based on the results described in this thesis could take. Firstly the question of which of the Kv7/M-channel subunits is the dominant subunit in the fibres and their associated peripheral endings needs to be clarified. This could be answered by immunostaining with the other subunits of the Kv7/M-channel. The staining of the vagus nerve revealed that the Kv7/M-channel is present along unmyelinated fibres it would be worth investigating whether these are nociceptive unmyelinated axons by immunostaining with a specific nociceptive markers e.g. TRPV1. To determine what might be the function of these channels and how they might effect conduction velocity and the frequency of conduction down the fibre the measurement of the effects on the C-fibre M-channel response due to activators of different neurotransmitters receptors expressed in unmyelinated C-fibres by either by the methods described in this thesis or by using a threshold tracking experiment set up as described by (Lang and Grafe, 2007) could be completed.

Further experiments are required to address the role of Kv7/M-channel in keratinocytes and whether the channel crosstalks with TRPV3. To address whether there is a crosstalk confirmation that TRPV3 and Kv7/M-channel are in the same cells could be completed by co-immunofluorescent staining of skin and keratinocytes for the different Kv7 subunits and TRPV3. To address whether calcium influx may be a possible mechanism for the induced ATP release seen in cultured keratinocytes further experimentation is also required to confirm whether the small enhancement of carvacrol-induced Ca^{2+} increases with retigabine observed are significant. As the Kv7/M-channel blocker alone did not induce a significant change in the carvacrol-induced ATP release from keratinocytes the effect of other modalities of physiological stimulation e.g. heat, pressure on ATP release with the Kv7/M-channel modulators could be investigated in cultured keratinocytes. It cannot be ruled out entirely that the

thermally evoked changed in excitability seen with the Kv7/M-channel modulators in the isolated skin saphenous nerve preparation is due to a substance being release from the keratinocytes. In order to test whether this is the case the isolated skin nerve experiments could be repeated with a global ATP receptor (P2) antagonist such as Suramin or an ATPase such as Apyrase (adenosine diphosphatase). Also, since TRPV3 activation induces PGE2 release it would be interesting to see if the Kv7/M-channel modulators affected this. Tests could be undertaken in cultured keratinocyte using the methods for the measurement of PGE2 release as those described in (Huang et al., 2008). A role for Kv7/M-channel and TRPV3 activation in keratinocyte proliferation would be interesting to investigate as the control of proliferation is important in many disease states. This could be studied via a BrdU cell proliferation assay with cultured keratinocytes incubated with the Kv7/M-channel modulators.

APPENDIX 1

Figure	Sample	Luminometer reading (LR)	[ATP] in reaction mixture (LR/ 1.56) (nM)	[ATP] in the bath fluid (nM)	Amount of ATP in dish (pmol)
7.1	control	76.00	48.82	97.64	48.82
7.1	control	54.16	34.79	69.58	34.79
7.1	control	50.10	32.18	64.36	32.18
7.1	control	39.23	25.20	50.40	25.20
7.1	control	33.46	21.49	42.99	21.49
7.1	control	73.86	47.44	94.89	47.44
7.1	4% NaOH	756.20	485.74	971.48	485.74
7.1	4% NaOH	857.40	550.75	1101.49	550.75
7.1	4% NaOH	520.50	334.34	668.68	334.34
7.1	4% NaOH	386.50	248.27	496.53	248.27
7.1	4% NaOH	569.40	365.75	731.50	365.75
7.1	4% NaOH	828.00	531.86	1063.72	531.86
7.11	control	91.50	58.77	117.55	58.77
7.11	control	61.84	39.72	79.45	39.72
7.11	control	65.40	42.01	84.02	42.01
7.11	camp 3mM	56.72	36.43	72.87	36.43
7.11	camp 3mM	72.27	46.42	92.84	46.42
7.11	camp 3mM	89.66	57.59	115.18	57.59
7.11	camp 10 mM	107.00	68.73	137.46	68.73
7.11	camp 10 mM	15.33	9.85	19.69	9.85
7.11	camp 10 mM	29.75	19.11	38.22	19.11
7.12	control	48.60	31.22	62.44	31.22

7.12	control	58.20	37.38	74.77	37.38
7.12	control	32.40	20.81	41.62	20.81
7.12	control	49.82	32.00	64.00	32.00
7.12	2- APB 100 µM	53.79	34.55	69.10	34.55
7.12	2- APB 100 µM	52.01	33.41	66.82	33.41
7.12	2- APB 100 µM	49.41	31.74	63.48	31.74
7.12	2- APB 100 µM	58.67	37.69	75.37	37.69
7.12	Carvacrol 1 mM	131.00	84.15	168.29	84.15
7.12	Carvacrol 1 mM	82.60	53.06	106.12	53.06
7.12	Carvacrol 1 mM	117.10	75.22	150.44	75.22
7.12	Carvacrol 1 mM	110.70	71.11	142.21	71.11
7.13 (A)	control	7.96	5.11	10.23	5.11
7.13 (A)	control	4.87	3.13	6.26	3.13
7.13 (A)	control	13.29	8.54	17.07	8.54
7.13 (A)	control	10.29	6.61	13.22	6.61
7.13 (A)	control	8.58	5.51	11.02	5.51
7.13 (A)	control	3.58	2.30	4.60	2.30
7.13 (A)	Carvacrol 1 mM	363.00	233.17	466.34	233.17
7.13 (A)	Carvacrol 1 mM	281.50	180.82	361.64	180.82
7.13 (A)	Carvacrol 1 mM	427.00	274.28	548.56	274.28
7.13 (A)	Carvacrol 1 mM	293.40	188.46	376.93	188.46
7.13 (A)	Carvacrol 1 mM	300.90	193.28	386.56	193.28
7.13 (A)	Carvacrol 1 mM	115.60	74.25	148.51	74.25
7.13 (A)	Carvacrol 1 mM + Retigabine 3 µM	1423.00	914.05	1828.11	914.05
7.13 (A)	Carvacrol 1 mM + Retigabine 3 µM	1011.00	649.41	1298.82	649.41
7.13 (A)	Carvacrol 1 mM + Retigabine 3 µM	1228.00	788.80	1577.60	788.80
7.13 (A)	Carvacrol 1 mM +	484.20	311.02	622.05	311.02

	Retigabine 3 µM				
7.13 (A)	Carvacrol 1 mM + Retigabine 3 µM	645.30	414.50	829.01	414.50
7.13 (B)	Control	33.83	21.73	43.46	21.73
7.13 (B)	Control	10.84	6.96	13.93	6.96
7.13 (B)	Control	22.70	14.58	29.16	14.58
7.13 (B)	Control	16.26	10.44	20.89	10.44
7.13 (B)	Control	43.99	28.26	56.51	28.26
7.13 (B)	Carvacrol 1 mM	174.00	111.77	223.54	111.77
7.13 (B)	Carvacrol 1 mM	161.30	103.61	207.22	103.61
7.13 (B)	Carvacrol 1 mM	113.60	72.97	145.94	72.97
7.13 (B)	Carvacrol 1 mM	172.30	110.68	221.35	110.68
7.13 (B)	Carvacrol 1 mM	172.00	110.48	220.97	110.48
7.13 (B)	Carvacrol 1 mM + Retigabine 3 µM	428.00	274.92	549.85	274.92
7.13 (B)	Carvacrol 1 mM + Retigabine 3 µM	332.70	213.71	427.42	213.71
7.13 (B)	Carvacrol 1 mM + Retigabine 3 µM	330.80	212.49	424.97	212.49
7.13 (B)	Carvacrol 1 mM + Retigabine 3 µM	343.30	220.52	441.03	220.52
7.13 (B)	Carvacrol 1 mM + Retigabine 3 µM	393.10	252.51	505.01	252.51
7.13 (B)	Carvacrol + XE991 10 µM	282.10	181.21	362.41	181.21
7.13 (B)	Carvacrol + XE991 10 µM	115.60	74.25	148.51	74.25
7.13 (B)	Carvacrol + XE991 10 µM	347.60	223.28	446.56	223.28
7.13 (B)	Carvacrol +	417.60	268.24	536.49	268.24

	XE991 10 µM				
7.13 (B)	Carvacrol 1 mM + XE991 10 µM	240.20	154.29	308.58	154.29
7.14	Carvacrol 1 mM	42.73	27.45	54.89	27.45
7.14	Carvacrol 1 mM	65.49	42.07	84.13	42.07
7.14	Carvacrol 1 mM	43.23	27.77	55.54	27.77
7.14	Carvacrol 1 mM	74.09	47.59	95.18	47.59
7.14	Carvacrol 1 mM + Retigabine 10 µM	254.70	163.60	327.21	163.60
7.14	Carvacrol 1 mM + Retigabine 10 µM	208.50	133.93	267.86	133.93
7.14	Carvacrol 1 mM + Retigabine 10 µM	180.40	115.88	231.76	115.88
7.14	Carvacrol 1 mM + Retigabine 10 µM	275.70	177.09	354.19	177.09
7.14	XE 991 10 µM + Carvacrol 1 mM + Retigabine 10 µM	49.54	31.82	63.64	31.82
7.14	XE 991 10 µM + Carvacrol 1 mM + Retigabine 10 µM	30.50	19.59	39.18	19.59
7.14	XE 991 10 µM + Carvacrol 1 mM + Retigabine 10 µM	29.66	19.05	38.10	19.05

REFERENCE LIST

Alexander,J.E., Hunt,D.F., Lee,M.K., Shabanowitz,J., Michel,H., Berlin,S.C., MacDonald,T.L., Sundberg,R.J., Rebhun,L.I., and Frankfurter,A. (1991). Characterization of posttranslational modifications in neuron-specific class III beta-tubulin by mass spectrometry. Proc. Natl. Acad. Sci. U. S. A *88*, 4685-4689.

Alloui,A., Zimmermann,K., Mamet,J., Duprat,F., Noel,J., Chemin,J., Guy,N., Blondeau,N., Voilley,N., Rubat-Coudert,C., Borsotto,M., Romey,G., Heurteaux,C., Reeh,P., Eschalier,A., and Lazdunski,M. (2006). TREK-1, a K+ channel involved in polymodal pain perception. EMBO J. *25*, 2368-2376.

Anderson,K., Anderson,L.E., and Glanze,W.D. (1998). Mosby's medical dictionary. *5th ed*.

Asakawa,M., Yoshioka,T., Matsutani,T., Hikita,I., Suzuki,M., Oshima,I., Tsukahara,K., Arimura,A., Horikawa,T., Hirasawa,T., and Sakata,T. (2006). Association of a mutation in TRPV3 with defective hair growth in rodents. J Invest Dermatol *126*, 2664-2672.

Bal,M., Zaika,O., Martin,P., and Shapiro,M.S. (2008a). Calmodulin binding to M-type K+ channels assayed by TIRF/FRET in living cells. J. Physiol *586*, 2307-2320.

Bal,M., Zhang,J., Zaika,O., Hernandez,C.C., and Shapiro,M.S. (2008b). Homomeric and heteromeric assembly of KCNQ (Kv7) K+ channels assayed by total internal reflection fluorescence/fluorescence resonance energy transfer and patch clamp analysis. J. Biol Chem *283*, 30668-30676.

Basbaum,A.I., Bautista,D.M., Scherrer,G.g., and Julius,D. (2009). Cellular and Molecular Mechanisms of Pain. Cell *139*, 267-284.

Bentzen,B.H., Schmitt,N., Calloe,K., Dalby Brown,W., Grunnet,M., and Olesen,S.P. (2006). The acrylamide (S)-1 differentially affects Kv7 (KCNQ) potassium channels. Neuropharmacology *51*, 1068-1077.

Biervert,C., Schroeder,B.r.C., Kubisch,C., Berkovic,S.F., Propping,P., Jentsch,T.J., and Steinlein,O.K. (1998). A Potassium Channel Mutation in Neonatal Human Epilepsy. Science *279*, 403-406.

Blackburn-Munro,G., and Jensen,B.S. (2003). The anticonvulsant retigabine attenuates nociceptive behaviours in rat models of persistent and neuropathic pain. European Journal of Pharmacology *460*, 109-116.

Blahd,W.H. First-Degree Burn: Superficial Burn. Blahd, William H. Healthwise.org . 2011. Healthwise.org.
Ref Type: Electronic Citation

Brouard,M., Casado,M., Djelidi,S., Barrandon,Y., and Farman,N. (1999). Epithelial sodium channel in human epidermal keratinocytes: expression of its subunits and relation to sodium transport and differentiation. J. Cell Sci. *112 (Pt 19)*, 3343-3352.

Brown,B.S., and Yu,S.P. (2000). Modulation and genetic identification of the M channel. Progress in Biophysics and Molecular Biology *73*, 135-166.

Brown,D.A., and Adams,P.R. (1980). Muscarinic suppression of a novel voltage-sensitive K+ current in a vertebrate neurone. Nature *283*, 673-676.

Brown,D.A., and Marsh,S. (1978). Axonal GABA-receptors in mammalian peripheral nerve trunks. Brain Res. *156*, 187-191.

Brown,D.A., and Passmore,G.M. (2009). Neural KCNQ (Kv7) channels. Br. J. Pharmacol. *156*, 1185-1195.

Brumovsky,P., Shi,T.S., Landry,M., Villar,M.J., and Hokfelt,T. (2007). Neuropeptide tyrosine and pain. Trends Pharmacol. Sci. *28*, 93-102.

Burrell,H.E., Wlodarski,B., Foster,B.J., Buckley,K.A., Sharpe,G.R., Quayle,J.M., Simpson,A.W., and Gallagher,J.A. (2005). Human keratinocytes release ATP and utilize three mechanisms for nucleotide interconversion at the cell surface. J. Biol. Chem. *280*, 29667-29676.

Cadaveira-Mosquera,A., P+¬rez,M., Reboreda,A., Rivas-Ram+¡rez,P., Fern+índez-Fern+índez,D., and Lamas,J. (2012). Expression of K2P Channels in Sensory and Motor Neurons of the Autonomic Nervous System. Journal of Molecular Neuroscience *48*, 86-96.

Caterina,M.J., Schumacher,M.A., Tominaga,M., Rosen,T.A., Levine,J.D., and Julius,D. (1997). The capsaicin receptor: a heat-activated ion channel in the pain pathway. Nature *389*, 816-824.

Caulfield,M.P., Jones,S., Vallis,Y., Buckley,N.J., Kim,G.D., Milligan,G., and Brown,D.A. (1994). Muscarinic M-current inhibition via G alpha q/11 and alpha-adrenoceptor inhibition of Ca2+ current via G alpha o in rat sympathetic neurones. The Journal of Physiology *477*, 415-422.

Chung,M.K., Lee,H., Mizuno,A., Suzuki,M., and Caterina,M.J. (2004a). 2-aminoethoxydiphenyl borate activates and sensitizes the heat-gated ion channel TRPV3. J. Neurosci. *24*, 5177-5182.

Chung,M.K., Lee,H., Mizuno,A., Suzuki,M., and Caterina,M.J. (2004b). TRPV3 and TRPV4 mediate warmth-evoked currents in primary mouse keratinocytes. J. Biol. Chem. *279*, 21569-21575.

Colton,C.K., and Zhu,M.X. (2007). 2-Aminoethoxydiphenyl Borate as a Common Activator of TRPV1, TRPV2, and TRPV3 Channels
Transient Receptor Potential (TRP) Channels. V. Flockerzi, and B. Nilius, eds. Springer Berlin Heidelberg), pp. 173-187.

Constanti,A., and Brown,D.A. (1981). M-Currents in voltage-clamped mammalian sympathetic neurones. Neurosci Lett. *24*, 289-294.

Cooper,E.C., Aldape,K.D., Abosch,A., Barbaro,N.M., Berger,M.S., Peacock,W.S., Jan,Y.N., and Jan,L.Y. (2000). Colocalization and coassembly of two human brain M-type potassium channel subunits that are mutated in epilepsy. Proc. Natl. Acad. Sci. U. S. A *97*, 4914-4919.

Cooper,E.C., Harrington,E., Jan,Y.N., and Jan,L.Y. (2001). M Channel KCNQ2 Subunits Are Localized to Key Sites for Control of Neuronal Network Oscillations and Synchronization in Mouse Brain. The Journal of Neuroscience *21*, 9529-9540.

Costa,S.K., Brain,S.D., Antunes,E., De,N.G., and Docherty,R.J. (2003). Phoneutria nigriventer spider venom activates 5-HT4 receptors in rat-isolated vagus nerve. Br J Pharmacol. *139*, 59-64.

Costigan,M., and Woolf,C.J. (2000). Pain: Molecular mechanisms. The Journal of Pain *1*, 35-44.

Crozier,R.A., Ajit,S.K., Kaftan,E.J., and Pausch,M.H. (2007). MrgD activation inhibits KCNQ/M-currents and contributes to enhanced neuronal excitability. J. Neurosci *27*, 4492-4496.

De Schepper,H.U., De Winter,B.Y., Van,N.L., Timmermans,J.P., Herman,A.G., Pelckmans,P.A., and De Man,J.G. (2008). TRPV1 receptors on unmyelinated C-fibres mediate colitis-induced sensitization of pelvic afferent nerve fibres in rats. J. Physiol *586*, 5247-5258.

Dedek,K., Kunath,B., Kananura,C., Reuner,U., Jentsch,T.J., and Steinlein,O.K. (2001). Myokymia and neonatal epilepsy caused by a mutation in the voltage sensor of the KCNQ2 K+ channel. Proceedings of the National Academy of Sciences *98*, 12272-12277.

Dehkordi,O., Rose,J.E., Balan,K.V., Kc,P., Millis,R.M., and Jayam-Trouth,A. (2009). Neuroanatomical relationships of substance P-immunoreactive intrapulmonary C-fibers and nicotinic cholinergic receptors. J Neurosci Res *87*, 1670-1678.

Delmas,P., and Brown,D.A. (2005). Pathways modulating neural KCNQ/M (Kv7) potassium channels. Nat Rev. Neurosci *6*, 850-862.

Delmas,P., Hao,J., and Rodat-Despoix,L. (2011). Molecular mechanisms of mechanotransduction in mammalian sensory neurons. Nat Rev Neurosci *12*, 139-153.

Delmas,P., Wanaverbecq,N., Abogadie,F.C., Mistry,M., and Brown,D.A. (2002). Signaling microdomains define the specificity of receptor-mediated InsP(3) pathways in neurons. Neuron *34*, 209-220.

Demolombe,S., Franco,D., de Boer,P., Kuperschmidt,S., Roden,D., Pereon,Y., Jarry,A., Moorman,A.F.M., and Escande,D. (2001). Differential expression of KvLQT1 and its regulator IsK in mouse epithelia. American Journal of Physiology - Cell Physiology *280*, C359-C372.

Denda,M., Ashida,Y., Inoue,K., and Kumazawa,N. (2001). Skin surface electric potential induced by ion-flux through epidermal cell layers. Biochem. Biophys. Res. Commun. *284*, 112-117.

Denda,M., Nakatani,M., Ikeyama,K., Tsutsumi,M., and Denda,S. (2007). Epidermal keratinocytes as the forefront of the sensory system. Exp Dermatol *16*, 157-161.

Devaux,J.J., Kleopa,K.A., Cooper,E.C., and Scherer,S.S. (2004). KCNQ2 is a nodal K+ channel. J. Neurosci *24*, 1236-1244.

Dixon,C.J., Bowler,W.B., Littlewood-Evans,A., Dillon,J.P., Bilbe,G., Sharpe,G.R., and Gallagher,J.A. (1999). Regulation of epidermal homeostasis through P2Y2 receptors. Br. J. Pharmacol. *127*, 1680-1686.

Dlugosz,A.A., Glick,A.B., Tennenbaum,T., Weinberg,W.C., and Yuspa,S.H. (1995). Isolation and utilization of epidermal keratinocytes for oncogene research. Methods Enzymol. *254*, 3-20.

Dobler,T., Springauf,A., Tovornik,S., Weber,M., Schmitt,A., Sedlmeier,R., Wischmeyer,E., and D+¦ring,F. (2007). TRESK two-pore-domain K+ channels constitute a significant component of background potassium currents in murine dorsal root ganglion neurones. The Journal of Physiology *585*, 867-879.

Doerner,J.F., Hatt,H., and Ramsey,I.S. (2011). Voltage- and temperature-dependent activation of TRPV3 channels is potentiated by receptor-mediated PI(4,5)P2 hydrolysis. The Journal of General Physiology *137*, 271-288.

Elliott,P., Marsh,S.J., and Brown,D.A. (1989). Inhibition of Ca-spikes in rat preganglionic cervical sympathetic nerves by sympathomimetic amines. Br J Pharmacol. *96*, 65-76.

Fang,X., Djouhri,L., McMullan,S., Berry,C., Waxman,S.G., Okuse,K., and Lawson,S.N. (2006). Intense isolectin-B4 binding in rat dorsal root ganglion neurons distinguishes C-fiber nociceptors with broad action potentials and high Nav1.9 expression. J. Neurosci *26*, 7281-7292.

Fillingim,R. American Pain Society . 2012. 6-9-0012.
Ref Type: Electronic Citation

Fornaro,M., Lee,J.M., Raimondo,S., Nicolino,S., Geuna,S., and Giacobini-Robecchi,M. (2008). Neuronal intermediate filament expression in rat dorsal root ganglia sensory neurons: An in vivo and in vitro study. Neuroscience *153*, 1153-1163.

Freysoldt,A., Fleckenstein,J., Lang,P.M., Irnich,D., Grafe,P., and Carr,R.W. (2009). Low concentrations of amitriptyline inhibit nicotinic receptors in unmyelinated axons of human peripheral nerve. Br J Pharmacol. *158*, 797-805.

Gamper,N., Reznikov,V., Yamada,Y., Yang,J., and Shapiro,M.S. (2004). Phosphatidylinositol [correction] 4,5-bisphosphate signals underlie receptor-specific Gq/11-mediated modulation of N-type Ca2+ channels. J Neurosci *24*, 10980-10992.

Gamper,N., and Shapiro,M.S. (2003). Calmodulin mediates Ca2+-dependent modulation of M-type K+ channels. J. Gen. Physiol *122*, 17-31.

Gamper,N., and Shapiro,M.S. (2007). Regulation of ion transport proteins by membrane phosphoinositides. Nat Rev Neurosci *8*, 921-934.

Green,N.M. (1990). Avidin and streptavidin. Methods Enzymol. *184*, 51-67.

Greenwood,I.A., and Ohya,S. (2009). New tricks for old dogs: KCNQ expression and role in smooth muscle. Br J Pharmacol. *156*, 1196-1203.

Grynkiewicz,G., Poenie,M., and Tsien,R.Y. (1985). A new generation of Ca2+ indicators with greatly improved fluorescence properties. J. Biol Chem *260*, 3440-3450.

Hadley,J.K., Noda,M., Selyanko,A.A., Wood,I.C., Abogadie,F.C., and Brown,D.A. (2000). Differential tetraethylammonium sensitivity of KCNQ1ΓÇô4 potassium channels. British Journal of Pharmacology *129*, 413-415.

Hadley,J.K., Passmore,G.M., Tatulian,L., Al-Qatari,M., Ye,F., Wickenden,A.D., and Brown,D.A. (2003). Stoichiometry of expressed KCNQ2/KCNQ3 potassium channels and subunit composition of native ganglionic M channels deduced from block by tetraethylammonium. J. Neurosci. *23*, 5012-5019.

Harper,A.A., and Lawson,S.N. (1985). Conduction velocity is related to morphological cell type in rat dorsal root ganglion neurones. J. Physiol *359*, 31-46.

Heidenreich,M., Lechner,S.G., Vardanyan,V., Wetzel,C., Cremers,C.W., De Leenheer,E.M., Aranguez,G., Moreno-Pelayo,M.A., Jentsch,T.J., and Lewin,G.R. (2012). KCNQ4 K+ channels tune mechanoreceptors for normal touch sensation in mouse and man. Nat Neurosci *15*, 138-145.

Hennings,H., Michael,D., Cheng,C., Steinert,P., Holbrook,K., and Yuspa,S.H. (1980). Calcium regulation of growth and differentiation of mouse epidermal cells in culture. Cell *19*, 245-254.

Hernandez,C.C., Zaika,O., Tolstykh,G.P., and Shapiro,M.S. (2008). Regulation of neural KCNQ channels: signalling pathways, structural motifs and functional implications. The Journal of Physiology *586*, 1811-1821.

Higashida,H., Hoshi,N., Zhang,J.S., Yokoyama,S., Hashii,M., Jin,D., Noda,M., and Robbins,J. (2005). Protein kinase C bound with A-kinase anchoring protein is involved in muscarinic receptor-activated modulation of M-type KCNQ potassium channels. Neuroscience Research *51*, 231-234.

Hu,H.Z., Gu,Q., Wang,C., Colton,C.K., Tang,J., Kinoshita-Kawada,M., Lee,L.Y., Wood,J.D., and Zhu,M.X. (2004). 2-aminoethoxydiphenyl borate is a common activator of TRPV1, TRPV2, and TRPV3. J. Biol. Chem. *279*, 35741-35748.

Huang,S.M., Lee,H., Chung,M.K., Park,U., Yu,Y.Y., Bradshaw,H.B., Coulombe,P.A., Walker,J.M., and Caterina,M.J. (2008). Overexpressed transient receptor potential vanilloid 3 ion channels in skin keratinocytes modulate pain sensitivity via prostaglandin E2. J Neurosci *28*, 13727-13737.

Hughes,S., Marsh,S.J., Tinker,A., and Brown,D.A. (2007). PIP(2)-dependent inhibition of M-type (Kv7.2/7.3) potassium channels: direct on-line assessment of PIP(2) depletion by Gq-coupled receptors in single living neurons. Pflugers Arch. *455*, 115-124.

Inoue,K., Koizumi,S., Fuziwara,S., Denda,S., Inoue,K., and Denda,M. (2002). Functional vanilloid receptors in cultured normal human epidermal keratinocytes. Biochem. Biophys. Res. Commun. *291*, 124-129.

Jankowski MP,K.HR. (2010). Neurotrophic Factors and Nociceptor Sensitization. In Translational Pain Research: From Mouse to Man, L.A. Kruger L, ed. (Boca Raton, FL: CRC Press).

Jentsch,T.J. (2000). Neuronal KCNQ potassium channels: physiology and role in disease. Nat Rev. Neurosci *1*, 21-30.

Julius,D., and Basbaum,A.I. (2001). Molecular mechanisms of nociception. Nature *413*, 203-210.

Kang,D., and Kim,D. (2006). TREK-2 (K2P10.1) and TRESK (K2P18.1) are major background K+ channels in dorsal root ganglion neurons. American Journal of Physiology - Cell Physiology *291*, C138-C146.

Kharkovets,T., Hardelin,J.P., Safieddine,S., Schweizer,M., El-Amraoui,A., Petit,C., and Jentsch,T.J. (2000). KCNQ4, a K+ channel mutated in a form of dominant deafness, is expressed in the inner ear and the central auditory pathway. Proc. Natl. Acad. Sci. U. S. A *97*, 4333-4338.

King,C.H., and Scherer,S.S. (2012). Kv7.5 is the primary Kv7 subunit expressed in C-fibers. J. Comp Neurol. *520*, 1940-1950.

Koizumi,S., Fujishita,K., Inoue,K., Shigemoto-Mogami,Y., Tsuda,M., and Inoue,K. (2004). Ca2+ waves in keratinocytes are transmitted to sensory neurons: the involvement of extracellular ATP and P2Y2 receptor activation. Biochem. J. *380*, 329-338.

Kolly,C., Suter,M.M., and Muller,E.J. (2005). Proliferation, cell cycle exit, and onset of terminal differentiation in cultured keratinocytes: pre-programmed pathways in control of C-Myc and Notch1 prevail over extracellular calcium signals. J. Invest Dermatol. *124*, 1014-1025.

Kubisch,C., Schroeder,B.C., Friedrich,T., Lutjohann,B., El-Amraoui,A., Marlin,S., Petit,C., and Jentsch,T.J. (1999). KCNQ4, a novel potassium channel expressed in sensory outer hair cells, is mutated in dominant deafness. Cell *96*, 437-446.

Lang,P.M., Burgstahler,R., Sippel,W., Irnich,D., Schlotter-Weigel,B., and Grafe,P. (2003). Characterization of neuronal nicotinic acetylcholine receptors in the membrane of unmyelinated human C-fiber axons by in vitro studies. J Neurophysiol. *90*, 3295-3303.

Lang,P.M., Fleckenstein,J., Passmore,G.M., Brown,D.A., and Grafe,P. (2008). Retigabine reduces the excitability of unmyelinated peripheral human axons. Neuropharmacology *54*, 1271-1278.

Lang,P.M., and Grafe,P. (2007). Chemosensitivity of unmyelinated axons in isolated human gastric vagus nerve. Auton. Neurosci *136*, 100-104.

Lang,P.M., Moalem-Taylor,G., Tracey,D.J., Bostock,H., and Grafe,P. (2006). Activity-dependent modulation of axonal excitability in unmyelinated peripheral rat nerve fibers by the 5-HT(3) serotonin receptor. J Neurophysiol. *96*, 2963-2971.

Lang,P.M., Tracey,D.J., Irnich,D., Sippel,W., and Grafe,P. (2002). Activation of adenosine and P2Y receptors by ATP in human peripheral nerve. Naunyn Schmiedebergs Arch Pharmacol. *366*, 449-457.

Lechner,S.G., Mayer,M., and Boehm,S. (2003). Activation of M1 muscarinic receptors triggers transmitter release from rat sympathetic neurons through an inhibition of M-type K+ channels. The Journal of Physiology *553*, 789-802.

Lehninger,A.L. (1975). Biochemistry
the molecular basis of cell structure and function. *2nd ed*.

Lerche,C., Scherer,C.R., Seebohm,G., Derst,C., Wei,A.D., Busch,A.E., and Steinmeyer,K. (2000). Molecular Cloning and Functional Expression of KCNQ5, a Potassium Channel Subunit That May Contribute to Neuronal M-current Diversity. Journal of Biological Chemistry *275*, 22395-22400.

Linley,J.E., Pettinger,L., Huang,D., and Gamper,N. (2012). M channel enhancers and physiological M channel block. J. Physiol *590*, 793-807.

Linley,J.E., Rose,K., Patil,M., Robertson,B., Akopian,A.N., and Gamper,N. (2008). Inhibition of M current in sensory neurons by exogenous proteases: a signaling pathway mediating inflammatory nociception. J. Neurosci *28*, 11240-11249.

Lippens,S., Denecker,G., Ovaere,P., Vandenabeele,P., and Declercq,W. (2005). Death penalty for keratinocytes: apoptosis versus cornification. Cell Death Differ *12 Suppl 2*, 1497-1508.

Liu,B., Linley,J.E., Du,X., Zhang,X., Ooi,L., Zhang,H., and Gamper,N. (2010). The acute nociceptive signals induced by bradykinin in rat sensory neurons are mediated by inhibition of M-type K+ channels and activation of Ca2+-activated Cl- channels. J. Clin Invest *120*, 1240-1252.

Liu,C.N., Michaelis,M., Amir,R., and Devor,M. (2000). Spinal nerve injury enhances subthreshold membrane potential oscillations in DRG neurons: relation to neuropathic pain. J. Neurophysiol. *84*, 205-215.

Liu,G.J., Werry,E.L., and Bennett,M.R. (2005). Secretion of ATP from Schwann cells in response to uridine triphosphate. European Journal of Neuroscience *21*, 151-160.

Loeser,J.D. IASP Taxonomy. International Association for the Study of Pain . 1994.
Ref Type: Electronic Citation

Ma,W., and Quirion,R.+. (2008). Does COX2-dependent PGE2 play a role in neuropathic pain? Neuroscience Letters *437*, 165-169.

Main,M.J., Cryan,J.E., Dupere,J.R.B., Cox,B., Clare,J.J., and Burbidge,S.A. (2000). Modulation of KCNQ2/3 Potassium Channels by the Novel Anticonvulsant Retigabine. Molecular Pharmacology *58*, 253-262.

Mandadi,S., Sokabe,T., Shibasaki,K., Katanosaka,K., Mizuno,A., Moqrich,A., Patapoutian,A., Fukumi-Tominaga,T., Mizumura,K., and Tominaga,M. (2009). TRPV3 in keratinocytes transmits temperature information to sensory neurons via ATP. Pflugers Arch. *458*, 1093-1102.

Marsh,B., Acosta,C., Djouhri,L., and Lawson,S.N. (2012). Leak K(+) channel mRNAs in dorsal root ganglia: relation to inflammation and spontaneous pain behaviour. Mol. Cell Neurosci *49*, 375-386.

Marsh,S.J. (1982). Conductance measurements in mammalian unmyelinated nerves. The Journal of Physiology *325*, 5P-6P.

Marsh,S.J., Stansfeld,C.E., Brown,D.A., Davey,R., and McCarthy,D. (1987). The mechanism of action of capsaicin on sensory C-type neurons and their axons in vitro. Neuroscience *23*, 275-289.

Martire,M., Castaldo,P., D'Amico,M., Preziosi,P., Annunziato,L., and Taglialatela,M. (2004). M Channels Containing KCNQ2 Subunits Modulate Norepinephrine, Aspartate, and GABA Release from Hippocampal Nerve Terminals. The Journal of Neuroscience *24*, 592-597.

McGarth,J.A., Eady,R.A.J., and Pope,F.M. (2012). Anatomy and Organization of Human skin. In Rook's Textbook of Dermatology, Eighth Edition, T. Burns, S. Breathnach, N. Cox, and C. Griffiths, eds. Blackwell Publishing Ltd), p. 3.1-3.15.

Melzack,R., and Wall,P.D. (1965). Pain mechanisms: a new theory. Science *150*, 971-979.

Mizumoto,N., Mummert,M.E., Shalhevet,D., and Takashima,A. (2003). Keratinocyte ATP release assay for testing skin-irritating potentials of structurally diverse chemicals. J. Invest Dermatol. *121*, 1066-1072.

Momin,A., and Wood,J.N. (2008). Sensory neuron voltage-gated sodium channels as analgesic drug targets. Current Opinion in Neurobiology *18*, 383-388.

Moqrich,A., Hwang,S.W., Earley,T.J., Petrus,M.J., Murray,A.N., Spencer,K.S.R., Andahazy,M., Story,G.M., and Patapoutian,A. (2005). Impaired Thermosensation in Mice Lacking TRPV3, a Heat and Camphor Sensor in the Skin. Science *307*, 1468-1472.

Mucha,M., Ooi,L., Linley,J.E., Mordaka,P., Dalle,C., Robertson,B., Gamper,N., and Wood,I.C. (2010). Transcriptional Control of KCNQ Channel Genes and the Regulation of Neuronal Excitability. The Journal of Neuroscience *30*, 13235-13245.

Nilius,B. (2007). TRP channels in disease. Biochim. Biophys. Acta *1772*, 805-812.

Nuwer,M.O., Picchione,K.E., and Bhattacharjee,A. (2010). PKA-induced internalization of slack KNa channels produces dorsal root ganglion neuron hyperexcitability. J. Neurosci *30*, 14165-14172.

Owen,D.G., Marsh,S.J., and Brown,D.A. (1990). M-current noise and putative M-channels in cultured rat sympathetic ganglion cells. J Physiol *431*, 269-290.

Padilla,K., Wickenden,A.D., Gerlach,A.C., and McCormack,K. (2009). The KCNQ2/3 selective channel opener ICA-27243 binds to a novel voltage-sensor domain site. Neuroscience Letters *465*, 138-142.

Passmore,G.M., Selyanko,A.A., Mistry,M., Al-Qatari,M., Marsh,S.J., Matthews,E.A., Dickenson,A.H., Brown,T.A., Burbidge,S.A., Main,M., and Brown,D.A. (2003). KCNQ/M currents in sensory neurons: significance for pain therapy. J. Neurosci. *23*, 7227-7236.

Passmore,G.M., Reilly,J.M., Thakur,M., Keasberry,V.N., Marsh,S.J., Dickenson,A.H., and Brown,D.A. (2012). Functional significance of M-type potassium channels in nociceptive cutaneous sensory endings. Frontiers in Molecular Neuroscience *5*.

Patapoutian,A., Peier,A.M., Story,G.M., and Viswanath,V. (2003). ThermoTRP channels and beyond: mechanisms of temperature sensation. Nat Rev Neurosci *4*, 529-539.

Peier,A.M., Reeve,A.J., Andersson,D.A., Moqrich,A., Earley,T.J., Hergarden,A.C., Story,G.M., Colley,S., Hogenesch,J.B., McIntyre,P., Bevan,S., and Patapoutian,A. (2002). A heat-sensitive TRP channel expressed in keratinocytes. Science *296*, 2046-2049.

Perl,E.R. (2007). Ideas about pain, a historical view. Nat Rev Neurosci *8*, 71-80.

Pfeiffer-Guglielmi,B., Coles,J.A., Francke,M., Reichenbach,A., Fleckenstein,B., Jung,G.+., Nicaise,G., and Hamprecht,B. (2006). Immunocytochemical analysis of rat vagus nerve by antibodies against glycogen phosphorylase isozymes. Brain Research *1110*, 23-29.

Plant,L.D. (2012). A role for K2P channels in the operation of somatosensory nociceptors. Frontiers in Molecular Neuroscience *5*.

Ramsey,I.S., Delling,M., and Clapham,D.E. (2006). An introduction to TRP channels. Annu. Rev Physiol *68*, 619-647.

Rang,H.P., and Ritchie,J.M. (1968). On the electrogenic sodium pump in mammalian non-myelinated nerve fibres and its activation by various external cations. The Journal of Physiology *196*, 183-221.

Rasmussen,H.B., Frokjaer-Jensen,C., Jensen,C.S., Jensen,H.S., Jorgensen,N.K., Misonou,H., Trimmer,J.S., Olesen,S.P., and Schmitt,N. (2007). Requirement of subunit co-assembly and ankyrin-G for M-channel localization at the axon initial segment. J. Cell Sci. *120*, 953-963.

Rivera-Arconada,I., and Lopez-Garcia,J.A. (2006). Retigabine-induced population primary afferent hyperpolarisation in vitro. Neuropharmacology *51*, 756-763.

Robbins,J. (2001). KCNQ potassium channels: physiology, pathophysiology, and pharmacology. Pharmacology & Therapeutics *90*, 1-19.

Rose,K., Ooi,L., Dalle,C., Robertson,B., Wood,I.C., and Gamper,N. (2011). Transcriptional repression of the M channel subunit Kv7.2 in chronic nerve injury. Pain *152*, 742-754.

Roza,C., Castillejo,S., and Lopez-Garcia,J. (2011). Accumulation of Kv7.2 channels in putative ectopic transduction zones of mice nerve-end neuromas. Molecular Pain *7*, 58.

Rundfeldt,C., and Netzer,R. (2000a). The novel anticonvulsant retigabine activates M-currents in Chinese hamster ovary-cells tranfected with human KCNQ2/3 subunits. Neurosci Lett. *282*, 73-76.

Rundfeldt,C. (1997). The new anticonvulsant retigabine (D-23129) acts as an opener of K+ channels in neuronal cells. European Journal of Pharmacology *336*, 243-249.

Rundfeldt,C., and Netzer,R. (2000b). Investigations into the Mechanism of Action of the New Anticonvulsant Retigabine - Interaction with GABAergic and glutamatergic neurotransmission and with voltage gated ion channels. Arzneimittelforschung *50*, 1063-1070.

Ruscheweyh,R., Forsthuber,L., Schoffnegger,D., and Sandkuhler,J. (2007). Modification of classical neurochemical markers in identified primary afferent neurons with Abeta-, Adelta-, and C-fibers after chronic constriction injury in mice. J. Comp Neurol. *502*, 325-336.

Sabirov,R.Z. (2005). ATP release via anion channels. Purinergic signalling *1*, 311.

Schalow,G. (2005). Tapering of human nerve fibres. Gen. Physiol Biophys. *24*, 427-448.

Schmidt,R., Schmelz,M., Forster,C., Ringkamp,M., Torebjork,E., and Handwerker,H. (1995). Novel classes of responsive and unresponsive C nociceptors in human skin. The Journal of Neuroscience *15*, 333-341.

Schroder,R.L., Jespersen,T., Christophersen,P., Str++b+ªk,D., Jensen,B.S., and Olesen,S.P. (2001). KCNQ4 channel activation by BMS-204352 and retigabine. Neuropharmacology *40*, 888-898.

Schroeder,B.C., Hechenberger,M., Weinreich,F., Kubisch,C., and Jentsch,T.J. (2000). KCNQ5, a novel potassium channel broadly expressed in brain, mediates M-type currents. J. Biol. Chem. *275*, 24089-24095.

Schroeder,B.C., Kubisch,C., Stein,V., and Jentsch,T.J. (1998). Moderate loss of function of cyclic-AMP-modulated KCNQ2/KCNQ3 K+ channels causes epilepsy. Nature *396*, 687-690.

Schwake,M., Jentsch,T.J., and Friedrich,T. (2003). A carboxy-terminal domain determines the subunit specificity of KCNQ K+ channel assembly. EMBO Rep *4*, 76-81.

Schwarz,J.R., Glassmeier,G., Cooper,E.C., Kao,T.C., Nodera,H., Tabuena,D., Kaji,R., and Bostock,H. (2006). KCNQ channels mediate IKs, a slow K+ current regulating excitability in the rat node of Ranvier. J. Physiol *573*, 17-34.

Shah,M.M., Migliore,M., Valencia,I., Cooper,E.C., and Brown,D.A. (2008). Functional significance of axonal Kv7 channels in hippocampal pyramidal neurons. Proc. Natl. Acad Sci U. S. A *105*, 7869-7874.

Shah,M.M., Mistry,M., Marsh,S.J., Brown,D.A., and Delmas,P. (2002c). Molecular correlates of the M-current in cultured rat hippocampal neurons. J. Physiol *544*, 29-37.

Singh,N.A., Charlier,C., Stauffer,D., DuPont,B.R., Leach,R.J., Melis,R., Ronen,G.M., Bjerre,I., Quattlebaum,T., Murphy,J.V., McHarg,M.L., Gagnon,D., Rosales,T.O., Peiffer,A., Anderson,V.E., and Leppert,M. (1998). A novel potassium channel gene, KCNQ2, is mutated in an inherited epilepsy of newborns. Nat Genet. *18*, 25-29.

Sittl,R., Carr,R.W., Schwarz,J.R., and Grafe,P. (2010). The Kv7 potassium channel activator flupirtine affects clinical excitability parameters of myelinated axons in isolated rat sural nerve. Journal of the Peripheral Nervous System *15*, 63-72.

Soltanpour,N., and Santer,R.M. (1996). Preservation of the cervical vagus nerve in aged rats: morphometric and enzyme histochemical evidence. J. Auton. Nerv. Syst. *60*, 93-101.

Sundelacruz,S., Levin,M., and Kaplan,D.L. (2009). Role of membrane potential in the regulation of cell proliferation and differentiation. Stem Cell Rev. *5*, 231-246.

Tamsett,T.J., Picchione,K.E., and Bhattacharjee,A. (2009). NAD+ activates KNa channels in dorsal root ganglion neurons. J. Neurosci *29*, 5127-5134.

Tatulian,L., Delmas,P., Abogadie,F.C., and Brown,D.A. (2001). Activation of expressed KCNQ potassium currents and native neuronal M-type potassium currents by the anti-convulsant drug retigabine. J. Neurosci *21*, 5535-5545.

Telezhkin,V., Brown,D.A., and Gibb,A.J. (2012). Distinct subunit contributions to the activation of M-type potassium channels by PI(4,5)P2. The Journal of General Physiology.

Tsutsumi,M., Goto,M., Denda,S., and Denda,M. (2011). Morphological and functional differences in coculture system of keratinocytes and dorsal-root-ganglion-derived cells depending on time of seeding. Experimental Dermatology *20*, 464-467.

Turner,P.C. (2005). Molecular biology. *3rd ed*.

Wang,H.S., Pan,Z., Shi,W., Brown,B.S., Wymore,R.S., Cohen,I.S., Dixon,J.E., and McKinnon,D. (1998). KCNQ2 and KCNQ3 potassium channel subunits: molecular correlates of the M-channel. Science *282*, 1890-1893.

Wang,Q., Curran,M.E., Splawski,I., Burn,T.C., Millholland,J.M., VanRaay,T.J., Shen,J., Timothy,K.W., Vincent,G.M., de,J.T., Schwartz,P.J., Toubin,J.A., Moss,A.J., Atkinson,D.L., Landes,G.M., Connors,T.D., and Keating,M.T. (1996). Positional cloning of a novel potassium channel gene: KVLQT1 mutations cause cardiac arrhythmias. Nat Genet. *12*, 17-23.

Watt,F.M. (1989). Terminal differentiation of epidermal keratinocytes. Curr. Opin. Cell Biol. *1*, 1107-1115.

Wickenden,A.D., and McNaughton-Smith,G. (2009). Kv7 channels as targets for the treatment of pain. Curr. Pharm. Des *15*, 1773-1798.

Wickenden,A.D., Zou,A., Wagoner,P.K., and Jegla,T. (2001). Characterization of KCNQ5/Q3 potassium channels expressed in mammalian cells. Br. J. Pharmacol. *132*, 381-384.

Wickenden,A.D., Yu,W., Zou,A., Jegla,T., and Wagoner,P.K. (2000). Retigabine, A Novel Anti-Convulsant, Enhances Activation of KCNQ2/Q3 Potassium Channels. Molecular Pharmacology *58*, 591-600.

Williams,T.K., Yeo,C.J., and Brody,J. (2008). Does this band make sense? Limits to expression based cancer studies. Cancer Letters *271*, 81-84.

Winks,J. Agonist-induced inhibition of the M-current: involvement of the phosphoinositide cycle. 1-220. 2004. London, University College London.
Ref Type: Thesis/Dissertation

Winks,J.S., Hughes,S., Filippov,A.K., Tatulian,L., Abogadie,F.C., Brown,D.A., and Marsh,S.J. (2005). Relationship between membrane phosphatidylinositol-4,5-bisphosphate and receptor-mediated inhibition of native neuronal M channels. J. Neurosci *25*, 3400-3413.

Wladyka,C.L., and Kunze,D.L. (2006). KCNQ/M-currents contribute to the resting membrane potential in rat visceral sensory neurons. J. Physiol *575*, 175-189.

Wladyka,C.L., Feng,B., Glazebrook,P.A., Schild,J.H., and Kunze,D.L. (2008). The KCNQ/M-current modulates arterial baroreceptor function at the sensory terminal in rats. The Journal of Physiology *586*, 795-802.

Wolfensohn,S., and Lloyd,M. (2003). Handbook of laboratory animal management and welfare. *3rd ed*.

Woolf,C.J., and Ma,Q. (2007). Nociceptors--noxious stimulus detectors. Neuron *55*, 353-364.

Wuttke,T.V., Seebohm,G., Bail,S., Maljevic,S., and Lerche,H. (2005). The New Anticonvulsant Retigabine Favors Voltage-Dependent Opening of the Kv7.2 (KCNQ2) Channel by Binding to Its Activation Gate. Molecular Pharmacology *67*, 1009-1017.

Xiong,Q., Sun,H., and Li,M. (2007). Zinc pyrithione-mediated activation of voltage-gated KCNQ potassium channels rescues epileptogenic mutants. Nat Chem Biol *3*, 287-296.

Xu,H., Delling,M., Jun,J.C., and Clapham,D.E. (2006). Oregano, thyme and clove-derived flavors and skin sensitizers activate specific TRP channels. Nat Neurosci *9*, 628-635.

Yang,W.P., Levesque,P.C., Little,W.A., Conder,M.L., Ramakrishnan,P., Neubauer,M.G., and Blanar,M.A. (1998). Functional expression of two KvLQT1-related potassium channels responsible for an inherited idiopathic epilepsy. J. Biol. Chem. *273*, 19419-19423.

Yeung,S.Y., and Greenwood,I.A. (2005). Electrophysiological and functional effects of the KCNQ channel blocker XE991 on murine portal vein smooth muscle cells. British Journal of Pharmacology *146*, 585-595.

Yu,S., Ru,F., Ouyang,A., and Kollarik,M. (2008). 5-Hydroxytryptamine selectively activates the vagal nodose C-fibre subtype in the guinea-pig oesophagus. Neurogastroenterol. Motil. *20*, 1042-1050.

Zaika,O., Zhang,J., and Shapiro,M.S. (2011a). Combined phosphoinositide and Ca2+ signals mediating receptor specificity toward neuronal Ca2+ channels. J. Biol Chem *286*, 830-841.

Zaika,O., Lara,L.S., Gamper,N., Hilgemann,D.W., Jaffe,D.B., and Shapiro,M.S. (2006). Angiotensin II regulates neuronal excitability via phosphatidylinositol 4,5-bisphosphate-dependent modulation of Kv7 (M-type) K+ channels. The Journal of Physiology *575*, 49-67.

Zaika,O., Zhang,J., and Shapiro,M.S. (2011b). Functional role of M-type (KCNQ) K+ channels in adrenergic control of cardiomyocyte contraction rate by sympathetic neurons. The Journal of Physiology *589*, 2559-2568.

Zhang,S.H., Sun,Q.X., Seltzer,Z., Cao,D.Y., Wang,H.S., Chen,Z., and Zhao,Y. (2008). Paracrine-like excitation of low-threshold mechanoceptive C-fibers innervating rat hairy skin is mediated by substance P via NK-1 receptors. Brain Res Bull. *75*, 138-145.

Zhang,X.F., Han,P., Neelands,T.R., McGaraughty,S., Honore,P., Surowy,C.S., and Zhang,D. (2011). Coexpression and activation of TRPV1 suppress the activity of the KCNQ2/3 channel. J. Gen. Physiol *138*, 341-352.

Zhou,X., Wei,J., Song,M., Francis,K., and Yu,S.P. (2011). Novel role of KCNQ2/3 channels in regulating neuronal cell viability. Cell Death Differ *18*, 493-505.